CHEMITHERMOMECHANICAL PULPING CHARACTERISTICS OF BUDWORM-KILLED TREES

Zoltan Koran
Professor

and

Kibi Nlombi
Graduate Student

Université du Québec à Trois-Rivières, C.P. 500
Trois-Rivières (Québec) Canada G9A 5H7

(Received September 1993)

ABSTRACT

Chemithermomechanical pulps (CTMP) were produced from balsam-fir trees [*Abies balsamea* (L.) Mill] that were harvested one and three years after they were killed by spruce budworm beetles. Laboratory tests revealed that the spruce budworm produced significant reductions in wood density (30%), fiber length (19%), long fiber fraction (36%), brightness (4%), tensile strength (25%), and burst strength (24%), but most significantly in the tear strength of paper (51%). However, these negative effects were accompanied by some positive results, e.g., a 15% decrease in the energy of refining, a 73% reduction in pulp rejects, coupled with a 108% increase in the fine content of the pulp and by a 5% increase in the opacity of paper. In order to profit from the above advantages and to prevent any further reduction in the quality of paper, the dead trees must be harvested within three years of their defoliation—the sooner, the better.

Keywords: Chemithermomechanical pulp, balsam-fir, spruce budworm, dead trees, paper strength, optical properties, burst index, breaking length, tear index, Canadian Standard Freeness, NaOH solubility.

INTRODUCTION

The spruce budworm, *Choristoneura fumiferana,* is the most widely distributed and the most destructive defoliator of the spruce-balsam-fir forests of the northeastern part of North America. Since 1909, there have been at least two major waves of budworm outbreaks, the latest of which occurred in the early seventies. Although balsam-fir is the preferred host of the spruce budworm beetle, other coniferous trees are also affected, including white, red and black spruce, tamarack, white pine, and occasionally eastern hemlock.

Once the forest is attacked by the spruce budworm, the infested trees become progressively defoliated. The damage first appears on the top part of the tree, and then spreads towards the lower branches. As a result of infestation, the translocation of nutrients and water is disrupted, causing the terminal leader to die. As the attack continues, the infested trees are progressively defoliated until they die, usually 6–8 years after the attack.

Choristoneura fumiferana has been responsible for initiating the destruction of hundreds of million cords of balsam-fir and spruce pulpwood, as well as timber. Economic losses include significant reductions in tree growth, coupled with important reductions in the quantity and quality of wood harvested from the budworm-infested forest. In Québec alone, 94,000,000 m^3 of timber was attacked by the budworm beetle during 1984 (Atack et al. 1985). Because of this epidemic, the losses are considerable. During the epidemic (Koran 1989), there was a 4% decrease in the harvested volume of balsam-fir.

Wood and Fiber Science, 26(4), 1994, pp. 489–495

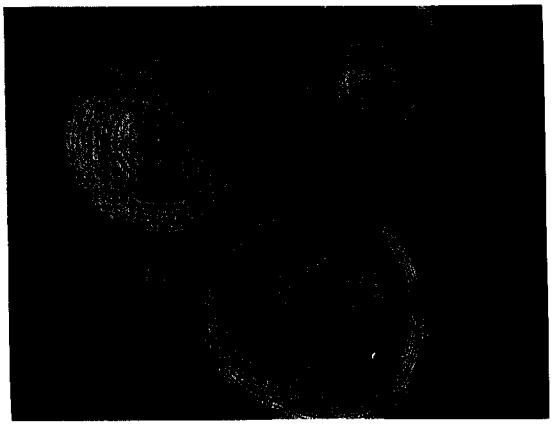

FIG. 1. Discs of balsam-fir trees which were harvested one (1) and three (3) years after they were killed by the spruce budworm insect. Sample zero (0) is a disc of a healthy tree.

Once the trees die, the timber becomes susceptible to attack by beetles, wasps, microorganisms, and fungi, which in turn leads to the development of sap stain and sap rot. Within a few years after the death of the tree, the decay enters the sapwood and progresses from the periphery of the tree towards the heartwood. This decay produces a visible discoloration in the wood, coupled with a significant decrease in its density and a corresponding increase in its solubility in 1% NaOH.

During the past 3 decades, numerous studies have been carried out concerning the salvage and utilization of the timber affected by the spruce budworm beetle. The damaged wood was converted into stone groundwood (SGW; Robitaille 1985), pressurized groundwood (PGW; Atack et al. 1985), refiner mechanical pulp (RMP; Robitaille 1985), thermomechanical pulp (TMP; Fereshtehkhou et al. 1985, Imada et al. 1983), and into chemimechanical pulp (CMP; Tombler and Dines 1985). To our knowledge, the characteristics of chemithermomechanical pulps (CTMP) produced from the spruce budworm-damaged wood have not yet been investigated, in spite of the widespread application of this process in the industry. Consequently, the specific objective of this study was to evaluate the quality of CTMP from the spruce budworm-infested forest as a function of time since the death of the trees.

MATERIALS AND METHODS

The material used in this study was prepared from balsam-fir (*Abies balsamea* (L.) Mill) harvested in the Montmorency forest near Québec City. Well identified trees were felled after one year (1) and three years (3) of their death, along with some healthy trees (0) for the sake of comparison (Fig. 1). The debarked trees were transformed into chips, which were then converted into chemithermomechanical pulp (CTMP) in a Sunds pilot plant described elsewhere (Koran et al. 1985).

First, the chips were screened, washed, presteamed for 10 min at atmospheric pressure; then they were impregnated with a 6% sodium sulfite liquor (Na_2SO_3), followed by a 5-min cooking in a vertical steaming vessel at 135 C (367 kPa). The first-stage refining was carried out under 367 kPa pressure at a feed consistency of 10%, followed by a second-stage refining under atmospheric conditions at 6 specific energy levels. The pulp samples possessing different levels of CSF were then washed, subjected to a 30-min latency treatment at 85 C, and evaluated by the standard methods of CPPA/TAPPI. The weighted average fiber length was determined by the Bauer-McNett fiber classification technique (Tasman 1972).

RESULTS AND DISCUSSION

The experimental results are summarized in Table 1 and are plotted in Figs. 2 to 9. These data reveal that the spruce budworm infestation significantly affects the quality of wood, the specific energy of refining, the fiber characteristics of the pulp, the optical properties of the handsheets, and the strength behavior of paper.

Wood quality

Reduced growth rate resulting from severe defoliation over a number of years is a characteristic feature of the budworm-killed tree, which is particularly pronounced in sample 3 (Fig. 1). A visible discoloration of the wood

TABLE 1. *Chemithermomechanical pulp (CTMP) properties produced at a constant specific energy (9 MJ/kg) from healthy balsam-fir trees (0) and from trees which were harvested one (1) and three (3) years after the trees were killed by the spruce budworm. The percent (%) reductions (−), or increases (+) are based on the values obtained for healthy trees (0).*

	Years since death					
	0		1		3	
	Values	%	Values	%	Values	%
Wood density, g/cm^3	0.37	0	0.32	−13	0.26	−30
NaOH solubility, %	14.1	0	16.71	+18	19.6	+39
CSF, ml	290	0	195	−33	150	−48
Rejects, %	0.3	0	0.26	−13	0.08	−73
Average fiber length, mm	1.7	0	1.58	−7	1.38	−19
Fraction <28 + 48>, %	53	0	40.8	−23	34	−36
Fines, %	16	0	25	+56	33.2	+108
Sheet density, g/cm^3	0.36	0	0.36	0	0.36	0
Breaking length, km	5.3	0	5	−6	4	−25
Burst index, kPa·m^2/g	3.3	0	3.1	−6	2.5	−24
Tear index, mN·m^2/g	9	0	7.8	−13	4.4	−51
Stretch, %	2.2	0	2.4	+9	2.2	0
Scatt. coeff., cm^2/g	405	0	405	0	445	+10
Brightness, %	67.5	0	65.8	−3	64.5	−4
Opacity, %	91	0	94	+3	95.5	+5

can also be observed due to the presence of sap stain and sap rot. The latter is confirmed by a significant reduction (30%) in the density of the affected wood three years after the death of the tree (Table 1). A progressive decay in the budworm-killed tree is also indicated by a significant increase (39%) in the solubility of wood in 1% NaOH 3 years after the death of the tree (Table 1). According to Atack et al. (1985), all of the principal constituents of wood, including lignin, cellulose, and the hemicelluloses, are attacked by the decay to almost identical degrees.

Energy consumption in refining

Figure 2 shows that the budworm-killed trees consume 15% less energy than healthy trees. Almost similar energy savings (20%) were obtained in the TMP process (Imada et al. 1983; Fereshtehkhou 1982). These reductions may be attributed to the partial delignification of the dead wood caused by the fungi (Atack et al. 1985). It is interesting to note that the fracture at high temperature occurs in the lignin-rich compound middle lamella region (Koran 1968, 1970). Consequently, even a small reduction in lignin content would tend to facilitate the defibration process and thus account for the reduction in specific energy.

Fiber characteristics

Table 1 shows that the reject content in the pulp decreased by 73% 3 years after the death

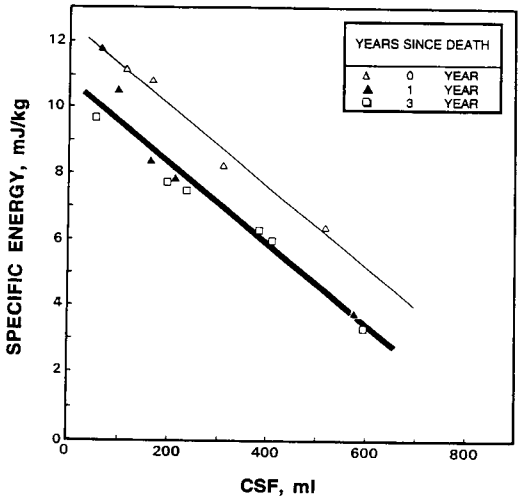

FIG. 2. Specific energy versus Canadian Standard Freeness for chemithermomechanical pulp (CTMP) of balsam-fir trees harvested one (1) and three (3) years after they were killed by the spruce budworm infestation. Sample zero (0) is a healthy tree.

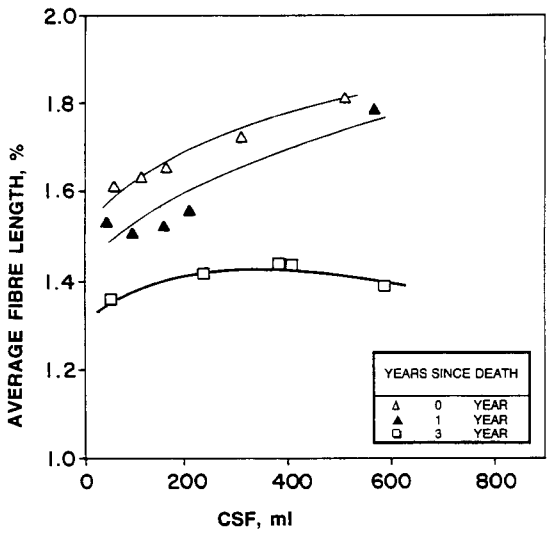

FIG. 3. Average fiber length versus Canadian Standard Freeness for CTMP. Symbols are same as in Fig. 2.

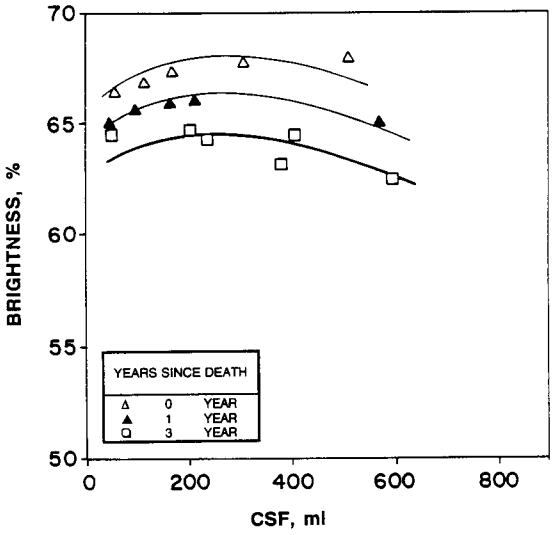

FIG. 5. The brightness of paper versus Canadian Standard Freeness for CTMP. Symbols are same as in Fig. 2.

of the tree. This implies that the defibering process is facilitated by the partial decay of wood. As a result, there is a more complete defibration, thus leaving fewer fiber bundles in the pulp.

However, this positive effect was accompanied by a significant reduction (19%) in fiber length at all levels of CSF (Fig. 3). This is a 19% decrease after 3 years (Table 1), which is due to a reduction in the intrinsic tensile strength of fibers caused by the attack of fungi.

The reduction in fiber length corresponds to a significant decrease in the long fiber fraction (28 + 48) of the Bauer-McNett fiber classification, e.g., 23% after 1 year and 36% after 3 years (Table 1). These reductions are accompanied by the production of high quantities of fines in the pulp: 56% after 1 year and 108% after 3 years. An increase in fine content, in turn, is known to affect both the optical and strength properties of paper.

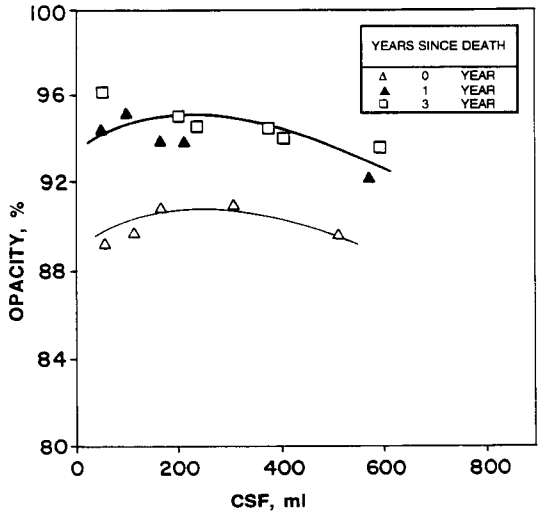

FIG. 4. Opacity of paper versus Canadian Standard Freeness for CTMP. Symbols are same as in Fig. 2.

Optical properties of paper

The scattering coefficient, for example, increased by 10%, which was accompanied by a 5% increase in the opacity of paper after 3 years (Fig. 4 and Table 1). These increases can be attributed to the 108% increase in the fines content of the pulp (Table 1). Even a 5% increase in opacity results in an important improvement in the printing quality of paper.

Unlike opacity, the brightness of paper was reduced by 4% (Fig. 5 and Table 1). However, this is an important reduction in paper quality, which is caused by a visible discoloration of wood during decay (Fig. 1). An additional stage

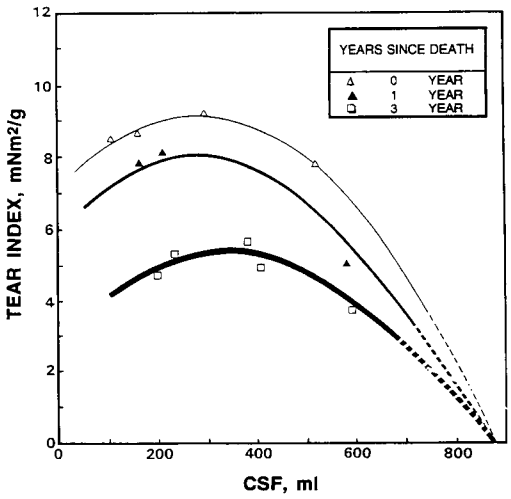

FIG. 6. The tear strength of paper versus Canadian Standard Freeness of handsheet prepared from the CTMP of budworm-killed balsam-fir trees harvested one (1) and three (3) years after they were killed by the budworm insect. Sample zero (0) is a healthy tree.

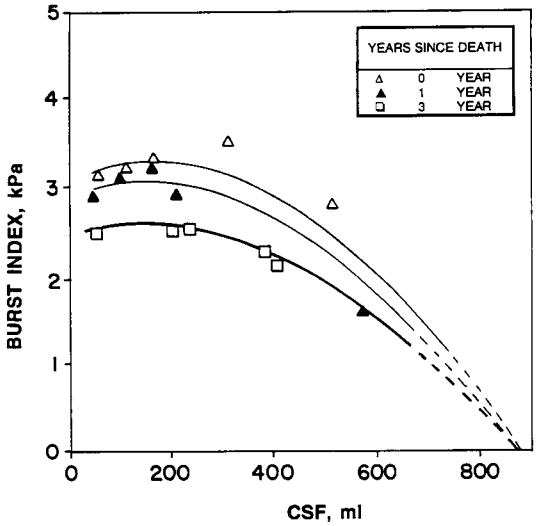

FIG. 7. The burst index of paper versus Canadian Standard Freeness for CTMP. Symbols are same as in Fig. 6.

of bleaching may be necessary in order to achieve brightness of paper equal to that made of soundwood.

Strength properties of paper

Figure 6 shows a 51% loss in the tear strength of paper that was produced from the budworm-killed trees 3 years after their death (Table 1). The latter is similar to the 47% decrease obtained for TMP (Fereshtehkhou 1982; Imada et al. 1983), but higher than the values reported for RMP (32%; Robitaille 1985), PGW (31%; Atack et al. 1985), and for SGW (24%; Robitaille 1985). These differences are most likely due to the effect of the sodium sulfite treatment and to the various differences in the defibering conditions. On the other hand, the decrease in tear strength (Fig. 6) can be attributed mostly to a significant reduction in fiber length, as observed in Fig. 3 and Table 1.

In contrast to tear, the tensile strength of paper was reduced only by 25% after 3 years. The corresponding reductions were 22% for SGW (Robitaille 1985), 19% for TMP (Fereshtehkhou 1982; Imada et al. 1983), 17% for PGW (Atack et al. 1985) and 15% for RMP (Robitaille 1985). These reductions are illustrated in Fig. 9 where the CTMP shows the steepest slope (25%), followed by SGW (22%), TMP (19%), PGW (17%), and RMP (15%) at the lowest end of the scale. Thus, the relative slope of each line is a measure of the effect of the spruce budworm infestation on the tensile strength of paper.

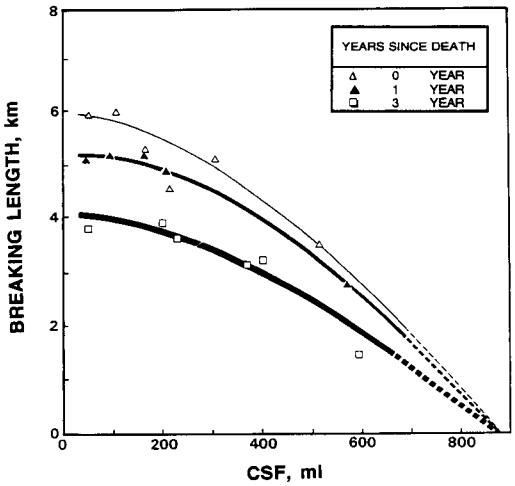

FIG. 8. The breaking length of paper versus Canadian Standard Freeness for CTMP. Symbols are same as in Fig. 6.

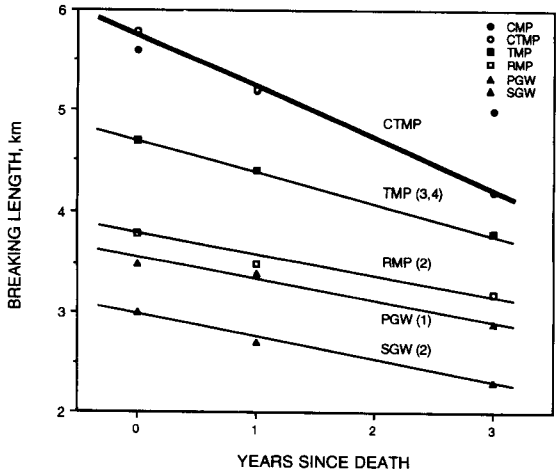

FIG. 9. Breaking length of handsheets made from trees that were harvested one (1) and three (3) years after they were killed by the spruce budworm in chemithermomechanical pulping (CTMP: present study), in thermomechanical (TMP) pulping (Fereshtehkhou 1982; Imada et al. 1983), in refiner mechanical (RMP) pulping (Robitaille 1985), in pressurized (PGW) groundwood (Atack et al. 1985), and in the conventional stone groundwood (SGW) process (Robitaille 1985). Sample zero (0) represents a healthy tree.

It is evident that the reduction in the BL (25%) is only half of the value (51%) obtained for the tear strength of CTMP. Although the reduction in fiber length (Fig. 3 and Table 1) is an important cause for the decrease in breaking length, it was partially compensated by a significant increase (108%) in the fines content of the pulp. The presence of fines is known to improve fiber-to-fiber bonding in paper, thus accounting for the smaller separations between the curves of Figs. 7 and 8, in comparison with those of Fig. 6.

Since in practice the spruce budworm-killed wood is always used in some blends along with soundwood, the reduction in the strength properties of paper is directly proportional to the relative proportions of each type of wood in a chip furnish. Thus, in a 75/25 blend of soundwood/budworm-killed wood, for example, the burst strength is reduced by only 6%, instead of 24%; but at the same time the advantages are also reduced by 75% of their initial values.

Time of harvest of the budworm-killed trees

Table 1 shows that if the trees are harvested only 1 year after their death, the tear strength of paper is little affected, but 2 additional years of exposure to the elements produce a fourfold (51%) reduction in the same property. A fourth year of exposure of the dead tree would be expected to reduce the tear strength by 75% and other properties by proportionally similar degrees.

However, if the trees are harvested 2 years after their death, the various pulp and paper properties would be affected to considerably lesser degrees, but still more than within 1 year. Thus, the economic outcome of the spruce budworm damage hinges around an efficient program of salvage of the budworm-killed trees—the sooner, the better.

CONCLUSIONS

The budworm-killed trees produced important changes in wood quality, as well as in the physical properties of pulp and paper. Already 3 years after death, the wood density was reduced by 30%, along with a significant reduction (39%) in the 1% NaOH solubility of wood. Among the various pulp properties, the fines content was doubled (108%), which was accompanied by significant increases in scattering coefficient (10%) and in opacity (5%). On the other hand, significant reductions were obtained in pulp rejects (73%), long fiber fraction (36%), fiber length (19%), brightness (4%), tear index (51%), breaking length (25%), and in the burst index (24%).

The positive results include increases in fines, scattering coefficient and in opacity, coupled with significant decreases in pulp rejects and in the specific energy of refining. All of the other changes represent negative effects on the final properties of pulp and paper.

ACKNOWLEDGMENT

The authors wish to express their thanks for the research grant provided by the Ministry of Forestry of the Québec Government via the

Multiregional Forestry Research Center of the University of Québec.

REFERENCES

ATACK, D., J. FONTEBASSO, AND M. I. STATIONWALA. 1985.The characterization and grinding of budworm-killed balsam-fir. Pulp Paper Sci. 11(1):1–7.

FERESHTEHKHOU, S. 1982. The properties of pulp and paper from spruce budworm-killed balsam-fir. M.Sc. thesis, Department of Forest Products, University of Minnesota, St. Paul, MN.

———, R. D. NEUMAN, AND S. A. SINCLAIR. 1985. Thermomechanical pulp properties of spruce budworm-killed balsam-fir. Pulp Paper Can. 86(4):43–45.

IMADA, S. E., D. G. MCVEY, AND D. A. HOLDER. 1983. Utilization of budworm balsam-fir in TMP. Conference on the utilization of spruce and fir. University of Maine, Orono, ME.

KORAN, Z. 1968. Electron microscopy of tangential tracheid surfaces of black spruce produced by tensile failure at various temperatures. Svensk Papperstidn. 71(17): 567–576.

———. 1970. Surface structure of TMP fibers studied by electron microscopy. Wood Fiber 2(3):247–258.

———. 1989. Different processes can be used to enhance hardwood pulping quality. Pulp Paper Can. 90(2):18–20.

———, A. PICHÉ, AND R. BOUCHARD. 1985. White birch TMP in newsprint manufacture. Pulp Paper Can. 86(10): 49–51.

ROBITAILLE, J. M. 1985. Influence of dead wood in paper mill. Technical Report. Consolidated-Bathurst Newsprint, Port-Alfred, Québec, Canada.

SAMUELSON, L., P. J. MJOBERG, N. HARTLER, L. VALLANDER, AND K. E. ERIKSSON. 1980. Influence of fungal treatment on the strength versus energy relationship in mechanical pulping. Svensk Papperstidn. 83(8):221–225.

TASMAN, J. E. 1972. The fiber length of Bauer-McNett screen fractions. Tappi 55(1):136–138.

TOMBLER, G., AND R. E. DINES. 1985. Mechanical and chemimechanical pulping of budworm-killed balsam-fir for the manufacture of newsprint. Symposium on the economic utilization of dead trees. Fredericton, New Brunswick, Can. For. Serv., Ottawa, Ontario, Canada.

FUNDAMENTAL ASPECTS OF WOOD DEFORMATION PERTAINING TO MANUFACTURE OF WOOD-BASED COMPOSITES

Michael P. Wolcott

Assistant Professor
Wood Science
Division of Forestry
West Virginia University
Morgantown, WV 26506

Frederick A. Kamke

Associate Professor
Department of Wood Science and Forest Products
Virginia Polytechnic Institute and State University
Blacksburg, VA 24061

and

David A. Dillard

Associate Professor
Department of Engineering Science and Mechanics
Virginia Polytechnic Institute and State University
Blacksburg, VA 24061

(Received February 1994)

ABSTRACT

During processing, wood-based composites are pressed using extreme heat and pressure for varying lengths of time. Evidence exists that the environmental conditions under which the wood densifies can alter the properties of both the solid wood and the composite product. Given the larger number and extreme nature of variables that exist during composite manufacture, it is imperative that the deformation process be understood from a fundamental standpoint. The objective of this research was to determine the applicability of basic materials engineering theory to the viscoelastic deformation of wood in transverse compression under a variety of temperatures and moisture contents.

Theories of cellular solids were used to model the nonlinear compression behavior of small wood elements. For low-density woods, it was determined that cellular collapse can result from elastic buckling of the cell wall. The dependence of inelastic behavior of the gross wood on the elastic properties of the cell wall allows the time, temperature, and moisture dependence to be modeled with classical linear viscoelastic theory of amorphous polymers. Time-temperature-moisture superposition was shown to be applicable to stress relaxation data collected for temperatures between 39 and 99 C and moisture contents between 3 and 16%. The shift factors derived were described using free volume and entropy-based equations. This research demonstrates that wood behaves similarly under those conditions to the general class of cellular amorphous polymers. This conclusion opens many possibilities for experimentally and mathematically modeling the pressing of wood-based composites.

Keywords: Viscoelasticity, cellular metering, free volume, composites pressing.

---

[1] 1990 Wood Award Paper (2nd place).

Wood and Fiber Science, 26(4), 1994, pp. 496–511

INTRODUCTION

One advantage of composites over traditional materials is the ability to tailor the material properties to meet structural design requirements. The properties of the composite will be a function of the raw material properties in situ and the geometry in which the components are arranged. Scientists and engineers have been more successful in designing synthetic fiber-reinforced composites than wood-based composites, mainly because of the microstructural complexity and variability of the latter. However, proficiency in designing wood-based composites is necessary if these products are to compete with other materials in future markets. The research presented here is aimed at improving our fundamental understanding of material behavior during the processing of wood-based composites. This improvement can be accomplished through mathematical and experimental modeling of the pressing cycle. These models can be useful as a tool to understand complex behavior that is not immediately intuitive.

For many non-veneered wood-based composites, the focal point of manufacturing is a highly automated process in which wood and adhesive components are flat-pressed, using extreme heat and pressure. During pressing, a simultaneous heat and mass transfer results in transient temperature and humidity gradients in the mat (Suchsland 1962; Humphrey 1979; Kamke and Casey 1988a). When force is applied to consolidate the mat, the wood components deform in bending and compression. The densification resulting from compression alters the physical and mechanical properties of the wood component. Changes in the strength, stiffness, sorption, and swelling of wood were found to be strongly influenced by the environment in which the densification occurred (Casey 1987; Geimer et al. 1985; Price 1976; Koch 1964; Kunesh 1961; Seborg and Stamm 1941). Environmental conditions also significantly influence the degree of damage to cell walls (Geimer et al. 1985). Significant evidence exists that these changes in wood properties can be manifested in the composite product (Hsu 1987; Geimer et al. 1985; Hujanen 1973; Heebink and Hefty 1969; Suchsland and Enlow 1968).

Clearly, the interaction of time, temperature, and moisture with nonlinear mechanical properties presents tremendous complexities to this problem. Empirical research for wood-based composites will be determined by our ability to simultaneously control the vast array of interacting variables, many of which are governed by inflexible laws of nature. Eventually, a thorough understanding of this complex system will depend on theories founded on fundamental principles. The necessity to develop theories will arise from two distinct needs: (1) a means to eliminate and narrow the focus of parameters in experiments, and (2) a framework to interpret experimental results. The objective of this research is to demonstrate the applicability of materials engineering theory to wood deformation, as it pertains to the pressing of wood-based composites. Demonstrating that wood behavior is governed by the same physical laws as other less complex materials will allow a significant step forward in the engineering design of wood-based composites.

In general, wood can be classified as a polymeric cellular material. The properties of cellular materials are governed by the cellular geometry and properties of the solid cell wall. Temperature and moisture are not likely to significantly alter the cellular structure; therefore, the influence of these factors must be primarily restricted to the cell-wall material. For polymers, the dependence of mechanical properties on time, temperature, and moisture is unified through the viscoelastic properties. The primary thesis of this paper is that the interaction of time, temperature, and moisture on the nonlinear mechanical properties of wood in transverse compression can be described using fundamental theories of cellular materials and viscoelasticity of polymers. An underlying assumption of this approach is two-part: (1) nonlinear behavior arises solely from collapse of the wood cellular structure, and (2) the ma-

terial behavior of the cell-wall material can be described using linear viscoelastic theory. These assumptions are also used by Gibson and Ashby (1988) in deriving the linear viscoelastic behavior of honeycomb structures.

Theories of cellular materials

A characteristic mechanical response for cellular materials in compression is shown in Fig. 1. The material begins deforming in a linear elastic manner. A yield point is exhibited at the onset of cellular collapse. The material continues to deform at nearly a constant stress level. When a majority of the cells have collapsed, densification begins. During densification, stress rapidly increases as the collapsed cell walls consolidate.

Many micromechanics models have been developed to predict linear elastic and yielding properties of cellular materials from cell geometry and mechanical properties of the cell-wall material (Warren and Kraynik 1987; Gibson et al. 1982; Gibson and Ashby 1982; Meinecke and Clark 1973; Leaderman 1971; Whittaker 1971; Chan and Nakamura 1969; Ko 1965; Gent and Thomas 1959). Recently, Gibson and Ashby have produced a comprehensive set of theories that address the linear, nonlinear, and failure properties for elastic, plastic, and brittle cellular materials (Gibson and Ashby 1988; Gibson et al. 1982, 1988; Gibson and Ashby 1982; Ashby 1983; Maiti et al. 1984). The primary difference between Gibson and Ashby's original work and that of their predecessors is that they correctly assumed that cell-wall bending rather than extension governed deformation. These theories have been applied to a number of natural materials including wood (Ashby et al. 1985; Maiti et al. 1984; Easterling et al. 1982), cork (Gibson et al. 1981), bone (Gibson and Ashby 1988), and the iris leaf (Gibson et al. 1988).

The major shortcoming of utilizing the current applications of Gibson and Ashby's theories to wood is that nonlinear behavior is assumed to be a function of plastic yielding or fracture of the cell wall. These failure-oriented cell-wall properties are difficult to measure and will most certainly vary tremendously with environmental conditions. The variable nature of cell-wall collapse is evidenced in Fig. 2.

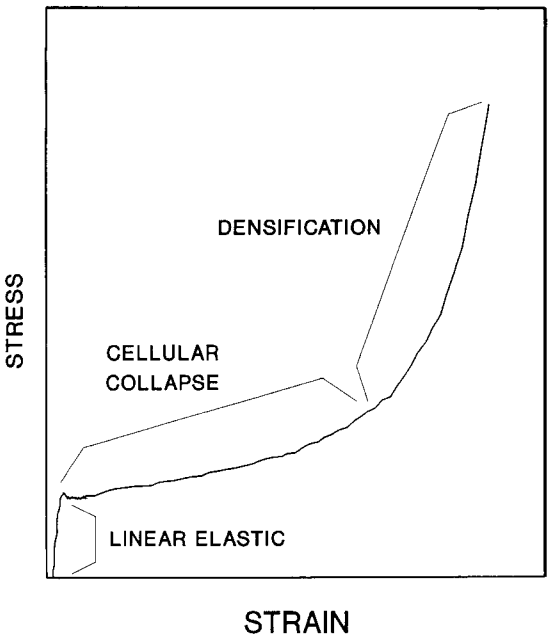

FIG. 1. A characteristic stress-strain diagram for a cellular material in compression.

Viscoelastic behavior of amorphous polymers

Amorphous polymers are termed viscoelastic because they can exhibit a range of properties from viscous fluids to linear elastic solids depending on the time scale, temperature, diluent concentration (i.e., moisture content) of the test (Fig. 3) (Ward 1983). In relative terms, at short times, low temperatures, and low diluent concentrations, the polymer exhibits glassy behavior, which can be characterized as stiff and brittle. At long times, high temperatures, and high diluent concentrations, the polymer exhibits rubbery behavior that is characterized as compliant and elastic. Between these two distinct regions is termed the transition phase; the temperature associated with the phase change is typically called the glass transition temperature (T_g). At extremely high times, temperatures, and diluent concen-

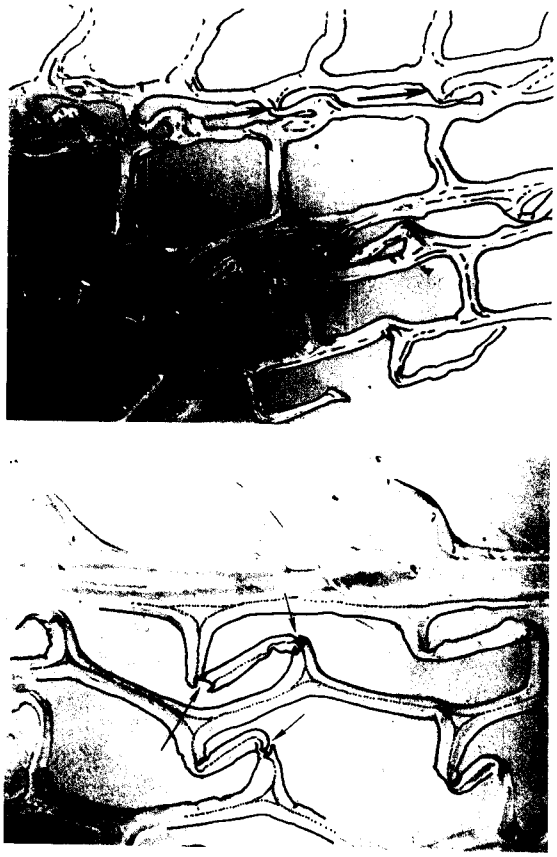

FIG. 2. Cross-sectional views of Douglas-fir flakes recovered from a pressed panel showing (a) elastic collapse and (b) fractures in the cell walls.

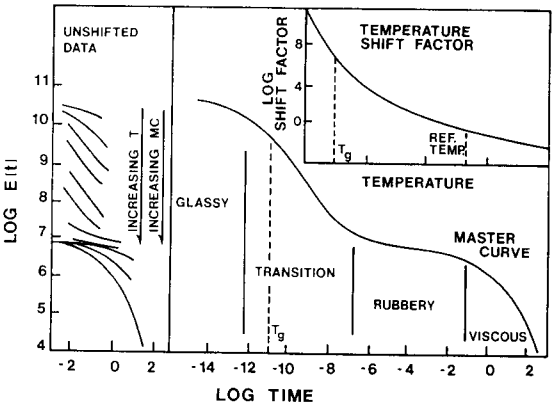

FIG. 3. Typical variation of relaxation modulus [E(t)] for an amorphous polymer with time, temperature, and diluent concentration. The master curve denotes the specific viscoelastic regions of polymer behavior.

trations, some polymers (i.e., thermoplastics) exhibit viscous flow. However, unmodified wood undergoes thermal degradation before this phase is reached.

The analogous behavior of polymers with different loading time, temperatures, and diluent concentrations is exhibited best in thermorheologically simple systems (Christensen 1982). In these polymer systems, the time-dependent mechanical responses at different temperatures and diluent concentrations are related by a change in the time scale only. From this equivalence, the long-term behavior of mechanical properties can be derived using time-temperature superposition. With this technique, the time-dependent [illegible]

tests at different temperatures as shown on the left in Fig. 3. These curves are then shifted along the log time axis to form a smooth, contiguous curve similar to that shown on the right in Fig. 3. The horizontal shift needed at each temperature is recorded as the shift factor shown in the upper right of Fig. 3. Once the time-dependent response of a polymer is determined over a large range of times (termed a master curve), the effect of a temperature change is equivalent to a horizontal shift of the master curve via a time multiplier (the shift factor) (Fig. 3). This relation is expressed mathematically as reduced time (t′) by the relation:

$$t' = \int_0^t \frac{d\xi}{a[T]} \qquad (1)$$

where:

t' = reduced time
t = time
$a[T]$ = temperature shift factor

At a constant temperature and diluent concentration, Eq. [1] will reduce to: $t' = t/a(T,M)$, where $a(T,M)$ is the shift factor for temperature and moisture content.

The power of this analytical tool [illegible]

but also in the ramifications of the behavior as defined by the Williams-Landel-Ferry (WLF) equation (Ferry 1980). The WLF equation indicates that for temperatures above T_g, the shift factor for time-temperature superposition is similar for all amorphous polymers. Although this observation was originally empirical, a fundamental basis for the equation has been provided using free volume theories. Free volume can be defined as the difference between the occupied volume and specific volume of a polymer (Billmeyer 1984). Occupied volume is defined as the volume occupied by the actual mass of molecule plus any volume it occupies from thermal vibrations that exclude other molecules from its domain (Adamson 1980). The influence of temperature on the viscoelastic properties of polymers results from the linear increase of free volume with temperature above T_g. Simply stated, viscoelasticity can be viewed as a self-diffusion of polymer molecules in response to a mechanical perturbation. Therefore, the mobility of polymer molecules is related to the amount of free volume at any given condition (Ferry 1980). This leads to the conclusion that increased states of free volume result in an increase in the rate of deformation. A thorough mathematical derivation of these concepts is beyond the scope of this paper but is presented elsewhere (LeFebvre et al. 1989; Knauss and Emri 1981; Ferry 1980).

The WLF equation has been shown to hold for temperatures in the range of T_g to T_g + 100 C for most amorphous polymers (Ward 1983). Salmen (1984) showed that shift factors determined for water-saturated wood are consistent with the WLF equation for temperatures in the range of T_g to T_g + 55 C. Kelley et al. (1987) determined that the WLF equation is valid between T_g and T_g + 85 C for wood plasticized with formamide. These agreements with the WLF equation lend credibility to the concept that the viscoelastic behavior of wood is a direct function of the viscoelastic response of the amorphous constituent polymers (i.e., lignin, hemicelluloses, and amorphous cellulose).

Objectives

In an effort to provide a fundamental basis for understanding the deformation processes of wood during hot-pressing, the specific objectives of this work are:

1. To formulate a methodology for describing the nonlinear transverse compression behavior of wood using theories of cellular materials in a manner that can be integrated with the viscoelastic response of cell-wall polymers.
2. To describe the interaction of time, temperature, and moisture with the mechanical properties of the cell wall using viscoelasticity theories of amorphous polymers.

EXPERIMENTAL METHODS

The experimental portion of this research involved determining the nonlinear compression and viscoelastic properties of wood in the transverse directions under a variety of temperature and moisture conditions. These experiments were intended to provide data for the analysis of theories presented above, not to provide a comprehensive description of the behavior of wood at these conditions.

Specimen preparation

Green yellow-poplar (*Liriodendron tulipifera*) blocks were split into large sections to aid in grain orientation. In preparing compression samples, the sections were conditioned to a nominal 8% moisture content, planed to 20 mm thick, and then cut to 20- × 20- mm square cross section. In addition to cubes, wood flakes were produced with a tangential face on a laboratory scale disk flaker from green blocks. The flakes were approximately 0.9 mm thick with a 20- × 20- mm square cross section. For stress relaxation tests, prismatic tension specimens were machined from the large sections. The parallel-sided tension specimens measured 20 × 8 mm in cross section and were 155 mm long. The radial direction was ori-

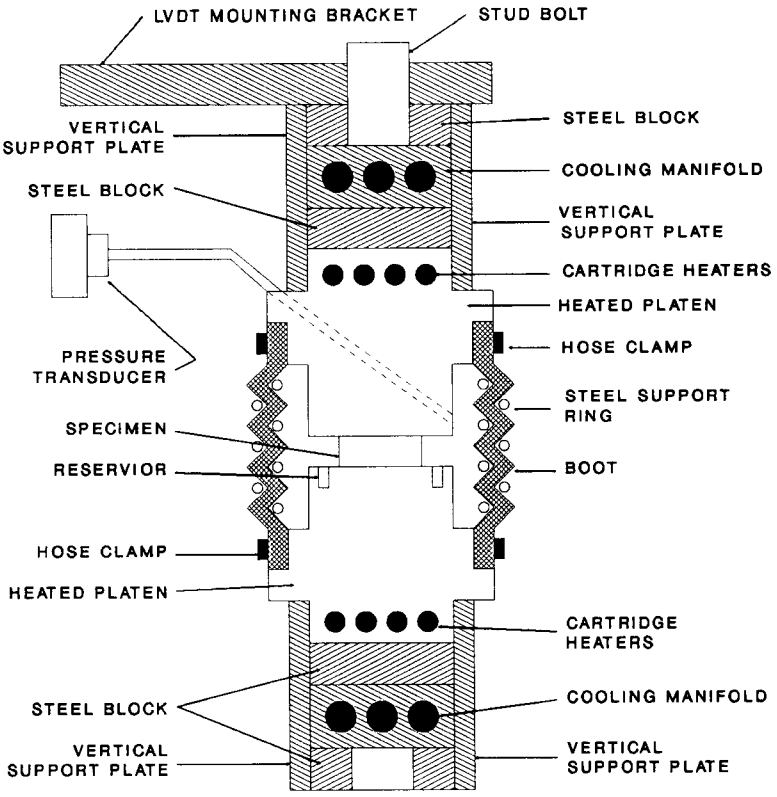

FIG. 4. Assembled test apparatus for the nonlinear compression tests.

ented with the long axis of the specimen. All specimens were loaded in the radial direction.

Nonlinear compression tests

Specimens were compressed at 6% strain per minute on a universal hydraulic testing machine equipped with heated platens rigidly attached to the crosshead and base (Fig. 4). Both aluminum loading blocks were machined flat and parallel to 0.25 mm. Each block was heated with four cartridge heaters that were inserted near the block surface remote to the specimen. A thermocouple was placed near each loading surface to provide feedback for a temperature controller. A steel block separated the loading block from the cooling manifold. Water was passed through the cooling manifold to maintain an acceptance temperature at the load cell and base. Deflection was measured with the linear variable displacement transformer (LVDT) attached to the crosshead with a stiff aluminum arm. The load-deflection relationship of the test apparatus was measured and compensated for in the test data. Both load and deflection were acquired in real time by computer and immediately converted into stress and strain.

Moisture content and temperature conditions below 100 C were maintained during the test by sealing the specimens prior to heating and compressing. The 20-mm cubes were heat-sealed in poly(vinylidene chloride) (SARAN Wrap 560, 0.15-mm-thick) envelopes. Flakes were sealed in three layers of aluminum foil (0.05 mm thick) because the deformation of the polymer film was significant compared to the deformation of the wood specimen. Pressures exceeding one atmosphere were needed

to maintain saturated conditions at 120 C and 140 C. For these conditions, the compression apparatus was fit with a bellows-style reinforced rubber boot that was clamped around the cylindrical loading blocks (Fig. 4). A channel machined near the perimeter of the lower platen was filled with water. The temperature of the blocks was increased after sealing the apparatus with the test specimen inside. Gas pressure inside the sealed apparatus was monitored using an electronic pressure transducer to assure that a saturated environment was achieved.

Stress relaxation tests

Relaxation modulus was determined using a single specimen tested at a series of different temperatures and moisture contents with a universal servohydraulic testing machine equipped with an environmental chamber. The test specimen was held at each end between two serrated steel plates that were bolted together. The gripped length of the specimen was 40 mm at each end. The total gage length between the grips was 75 mm. The plates were fastened to the test machine by steel pins. This gripping arrangement allowed the specimen to be unfastened from the test machine at the pinned ends without removing the specimen from the grips.

The stress relaxation tests were conducted by imposing a step increase in strain of 0.005 and maintaining this strain for approximately 600 seconds. The specimen was then returned to zero strain for an equal recovery period. Strain was measured using an extensometer (25.4-mm gage length) attached to the specimen with metallic coil springs. The load and strain data were acquired in real time by a computer.

Each group of stress relaxation tests was conducted at a constant nominal moisture content between 3% and 16% in a single day. In general, tests were conducted at temperatures between 39 C and 99 C at 3 C intervals. The actual temperatures deviated from this range at low and high moisture contents because of equipment limitations. The actual moisture content and temperatures are listed in Table 1. The relative humidity needed to achieve a target moisture content at each temperature was calculated using an inverted form of the one-hydrate Hailwood-Horobin equation as presented by Simpson (1973). The moisture content of the test specimen was estimated using control samples that remained in the test chamber at all times except during weighing. The moisture content of the control samples was measured at the beginning and end of each day's tests. Moisture content was found to vary less than 1.5% between the beginning and end of the day; however, the variation between these times is unknown.

TABLE 1. *Environment conditions used in stress relaxation tests to construct relaxation modulus master curves. Tests were conducted at 3 C intervals.*

Moisture content (%)		Temperature range (deg C)	
Nominal	Actual	Low	High
3	3.1	57	99
6	5.6	39	99
10	9.3	39	99
12	12.0	39	90
16	16.6	39	75

RESULTS AND DISCUSSION

Nonlinear compression behavior

Elastic versus plastic collapse mechanisms.—It has been shown that micromechanical models developed for honeycomb and closed cell foams can be applied to wood (Maiti et al. 1984; Easterling et al. 1982). These researchers assume that the nonlinear mechanical response of wood results from the plastic yielding and fracture of the cell walls. Without doubt, the cell walls of wood are damaged during transverse compression to large strains. However, the question arises whether the elastic buckling of cell walls contributes to the collapse mechanisms and can be used to adequately model the nonlinear mechanical behavior. To answer this question, experimental evidence is evaluated using the theories developed by Gibson and Ashby (1988).

The Young's modulus (E) of a closed cellular solid can be written as:

$$E = C_2 E_w \delta^3 \quad (2)$$

where:

C_2 = constant
E_w = cell wall modulus
δ = relative density (ratio of the cellular density to the cell wall density)

This equation is derived from classical plate theory and applies to elastomeric and rigid plastic cellular materials.

The yield stress (σ_y) of cellular materials is influenced by the collapse mechanism of the cell wall. Yielding in elastomeric foams results from elastic buckling of the cell walls. The yield point can be calculated by:

$$\sigma_y = C_3 E_w \delta^3 \quad (3)$$

where:

C_3 = constant

For rigid plastic cell-wall materials that exhibit a yield point, yielding in the cellular solid results from the formation of plastic hinges. Yield stress in the cellular material can be determined from the fully plastic moment in the cell wall:

$$\sigma_r = C_4 \sigma_{yw} \delta^2 \quad (4)$$

where:

C_4 = constant
σ_{yw} = cell wall yield stress

Given Hooke's Law ($E = \sigma/\epsilon$), C_3 in Eq. [3] is equivalent to the yield strain (ϵ_y). Therefore, ϵ_y should be independent of density for cellular materials that deform nonlinearly from elastic buckling of the cell wall. However, it can be shown from Eqs. [2] and [4] that this relation does not hold for rigid plastic foams. Inspection of data presented by Easterling et al. (1982) showed that ϵ_y did not vary significantly for balsa (*Ochroma lagopus*) with density ranging from 0.078 to 0.218 g/cm^3. Mechanical tests conducted by Kasal (1989), using balsa, yellow-poplar, and maple (*Acer rubrum*) at a range of moisture contents and temperatures, showed that ϵ_y consistently equalled approximately 0.015. This agrees closely with the value of 0.014 determined by Maiti et al. (1984) and 0.012 from Easterling et al. (1982). These results can be reconciled if elastic buckling occurred prior to developing a fully plastic moment in the cell wall. The cell wall could then be damaged after collapse. This concept is proposed by Gibson and Ashby (1988) to explain the shape of failure envelopes for multiaxial loading.

To illustrate the argument presented above, ϵ_y and σ_y were calculated for wood, assuming both elastic and plastic collapse. The results are presented in Figs. 5 and 6. Because E_w and σ_{yw} are unknown, they were calculated from the measured modulus and σ_y using Eqs. [2] and [4] respectively. For 20-mm cubes conditioned to 8% moisture content and 30 C, E_w = 12 GPa and σ_{yw} = 49 MPa.

For low relative densities, the difference between the predicted values of σ_y assuming elastic and plastic collapse mechanisms is small. However, large differences exist between the predicted values of ϵ_y. For higher relative densities when plastic collapse may actually occur, the error introduced to the predicted σ_y by assuming elastic collapse is not serious for relative densities less than 0.35. Comparing these results with those observed experimentally, it seems likely that the cell walls collapse from elastic buckling at low relative densities. It is important to realize that this conclusion does not exclude the possibility that the cell walls yield or fracture after collapse has occurred.

Modeling the structural nonlinearity of the cell wall.—Clearly, the characteristic shape of the stress-strain diagram is a direct result of the geometric nonlinearity resulting from the response of the cellular structure. Rusch (1969) first proposed the separation of the structural and cell-wall material response through a modification of Hooke's Law:

$$\sigma = E\epsilon\phi(\epsilon) \quad (5)$$

The nonlinear strain function, $\phi(\epsilon)$, is a function of the applied strain that governs the geo-

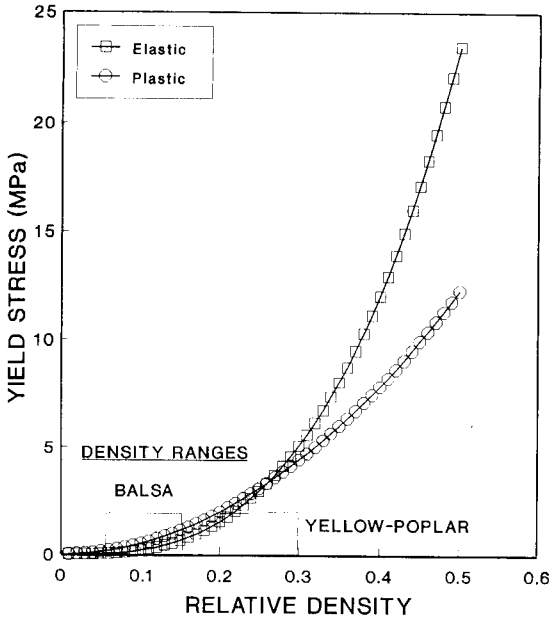

FIG. 5. Yield stress as a function of relative density calculated assuming elastic and plastic collapse mechanisms.

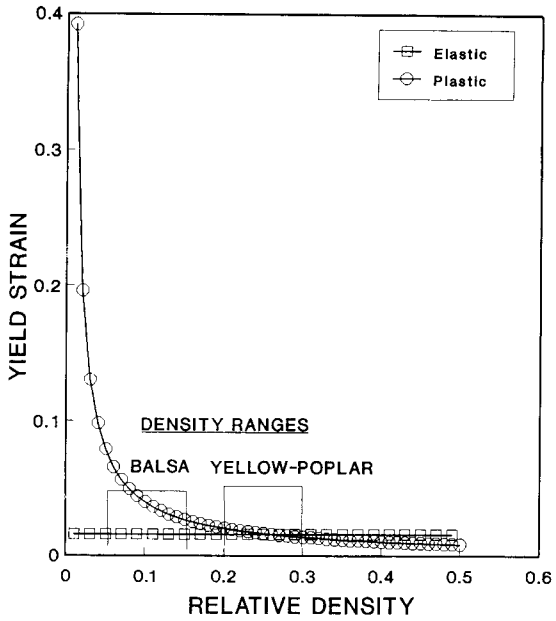

FIG. 6. Yield strain as a function of relative density calculated assuming elastic and plastic collapse mechanisms.

metric nonlinearities. It can be derived experimentally from the observed plastic strain in the stress-strain diagram (Rusch 1969). Maiti et al. (1984) derived a relation to describe the plateau and densification region of the stress-strain diagram. The longest cell walls were assumed to buckle first, resulting in the yield point. They then postulated that the length of the cell walls that will buckle with increasing compression strain could be described as a function of the longest cell-wall length and the increasing elative density with strain ($\delta(\epsilon)$). These equations can be rewritten allowing $\phi(\epsilon)$ to be described for strains greater than ϵ_y (Wolcott et al. 1989a):

$$\phi(\epsilon) = \frac{\epsilon_y}{\epsilon}\left[\frac{1 - \delta}{1 - \delta(\epsilon)^{1/3}}\right]^3 \qquad (6)$$

For strains less than ϵ_y, $\phi(\epsilon)$ is equal to unity. If $\delta(\epsilon)$ is calculated from the plastic strain, then $\phi(\epsilon)$ is equal to unity when $\epsilon = \epsilon_y$.

Dilatation (volume change) results from cellular collapse even in uniaxial loading. Therefore, $\delta(\epsilon)$ is a monitor of the cellular collapse. Little or no lateral expansion occurs in an elastomeric foam specimen within the nonlinear region of the stress-strain relationship. For this case, $\delta(\epsilon) = \delta/(1 - \epsilon)$. However, lateral expansion has been noted for wood (Wolcott et al. 1989a). When the loaded surfaces are restrained from frictional forces, the specimen exhibits barrelling and $\delta(\epsilon)$ can be determined by (Kasal 1989):

$$\delta(\epsilon) = \delta\left[1 - \epsilon_p + \frac{2}{3}\mu\epsilon_p - \mu\epsilon_p^2\right]^{-1} \qquad (7)$$

where: ϵ_p = plastic strain = $\epsilon - \epsilon_y$

The expansion coefficient (μ) is defined as the ratio of the lateral strain to compressive strain in the nonlinear stress-strain region. This parameter is influenced by specimen height because the surfaces are restrained by frictional forces between the test samples and compression platens. Characteristic values of μ for yellow-poplar at 30 C and 12% moisture content were between 0.1 and 0.15 for 20-mm cubes and approximately 0.05 for 0.9-mm-thick

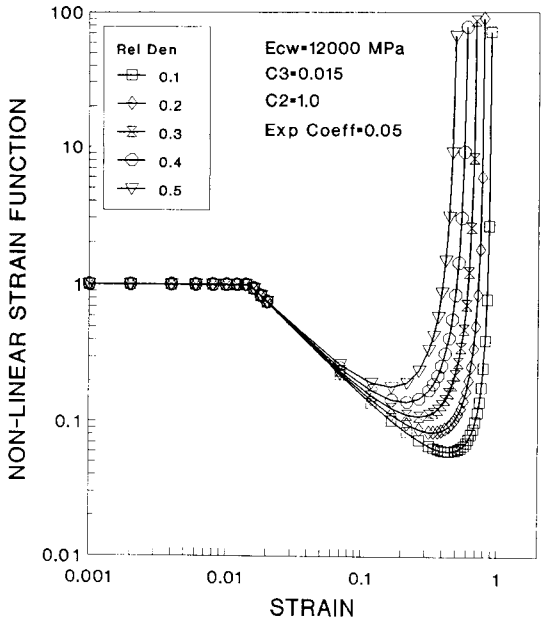

FIG. 7. Predicted nonlinear strain function ($\phi(\epsilon)$) by relative density.

flakes. A thorough discussion of this is presented elsewhere (Kasal 1989).

Whereas ϵ_y was found to be relatively invariant with material variables such as species, density, moisture content, and temperature, it has been found to be affected significantly by specimen geometry (Wolcott et al. 1989b; Menges and Knipschild 1982; Kunesh 1968; Bodig 1963). It has been found that the apparent E increases nonlinearly with specimen height, while ϵ_y varies with the reciprocal of E. A conclusive explanation of this behavior is lacking. However, the phenomenon has been related experimentally (Menges and Knipschild 1982) and theoretically (Wolcott et al. 1989b) to the excessive deformation of the loaded surfaces. Wolcott et al. (1989a) showed that surface asperities as small as 0.25 mm could significantly influence the measured E in wood. The relationship described above can be modeled through C_2 in Eq. [2] and should be viewed purely as a specimen effect (Wolcott et al. 1989a).

Experimental results.—The primary focus

whether the nonlinear response of wood in transverse compression can be modeled using theories of cellular materials assuming elastic collapse mechanisms. To remove the variability introduced by the unknown cell-wall modulus, Young's modulus and ϵ_y for the radial direction were determined for every specimen. These values, along with the measured density, were used in Eqs. [5], [6], and [7] to calculate the predicted nonlinear response.

A comparison of experimental and predicted behavior for the plateau and densification regions was made using two distinct points: ϵ_{den}, ϵ_u. These points were chosen as a measure to test the theoretical behavior with experimental results because they can be easily identified both mathematically and visually through the nonlinear strain function: $\phi(\epsilon)$ (Fig. 7). The ϵ_{den} is defined here as the beginning of the densification region, which is denoted by a minimum in $\phi(\epsilon)$. The point where $\phi(\epsilon)$ equals unity after reaching ϵ_{den} is defined here as ϵ_u.

Experimental and predicted values for the stress and strain at ϵ_{den} and ϵ_u were used to quantitatively determine how well $\phi(\epsilon)$ predicted the collapse and densification regions of the stress-strain relation for flakes. Typical predicted and experimental curves are presented in Fig. 8. On average, predicted values of ϵ_{den} and ϵ_u are less than those measured experimentally. The mean errors in predicting ϵ_{den} are 11.1% for stress and 8.2% for strain. For predicting ϵ_u, the mean errors were 9.5% for stress and 9.9% for strain. Given these results, the theories regarding the nonlinear behavior of cellular materials presented here appear to represent wood in transverse compression.

Interaction of time, temperature, and moisture

Analytical development.—An important aspect of classical viscoelasticity theory in polymers is time-temperature equivalence. Originally, time-temperature superposition was used

to shorten the time required to determine time

the advent of free volume theories and their relation to the WLF equation. Ferry (1980) notes that criteria other than the smooth shifting of curves should be used to substantiate the validity of experimentally determined shift factors. Theory such as the WLF equation can be used to substantiate validity of the time-temperature equivalence when prior experience does not exist for shifting. Successful application of these theories also indicates that a material behaves viscoelastically, like other amorphous polymers. For wood, this conclusion has important implications both theoretically and experimentally.

This research involves the interaction of both temperature and moisture with time-dependent properties of wood. An equivalent approach to time-temperature superposition has been used with moisture (Maksimov et al. 1975, 1976). In time-temperature-moisture superposition, time-dependent properties are determined at different temperatures and moisture contents. These curves are then shifted along the log time axis to form the master curve in a manner analogous to time-temperature superposition. The shift factor for temperature and moisture (a[T,M]) is then defined using reduced time:

$$t' = \int_0^t \frac{d\xi}{a[T, M]} \qquad (8)$$

Knauss and Emri (1981) proposed a free volume theory that accounts for changes in temperature, diluent concentration, and hydrostatic stress to predict nonlinear viscoelastic properties. Their model assumes that a change in free volume of a polymer depends on the dilatation from these three variables. The free volume of a polymer can then be expressed as:

$$f = f_o + \alpha(T - T_o) + \beta(C - C_o) + \delta\sigma \qquad (9)$$

where:

f = fractional free volume
T = temperature
C = diluent concentration
σ = hydrostatic stress

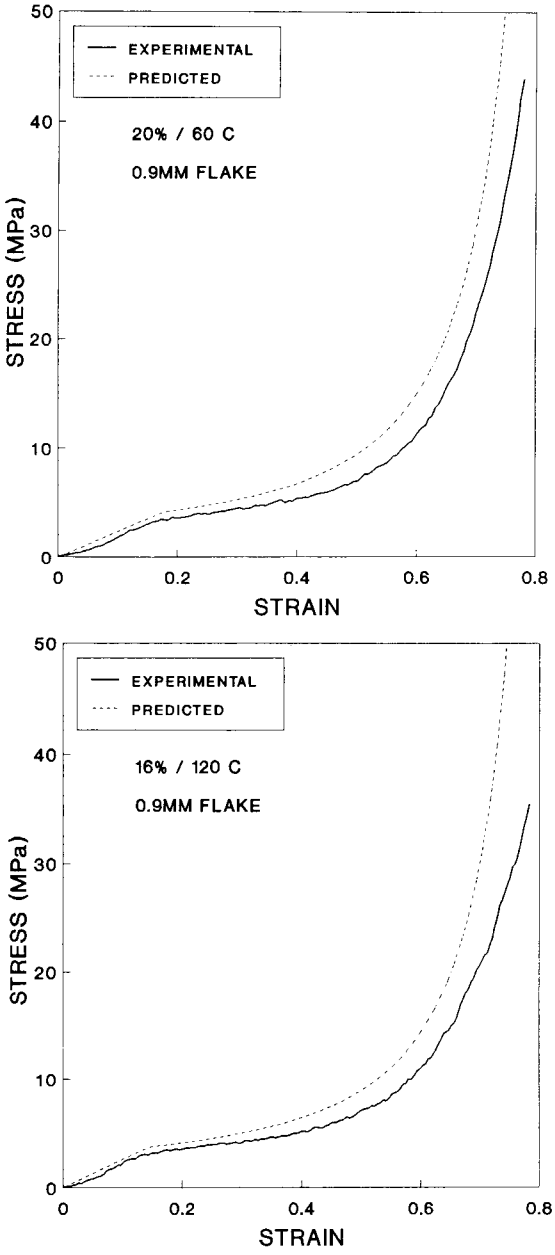

FIG. 8. Experimental and predicted stress-strain diagrams for 0.9-mm flakes.

α, β, δ are free volume expansion coefficients. Subscript o refers to the reference condition

The shift factor can be defined in terms of fractional free volume through the Dolittle equation (Ferry 1980):

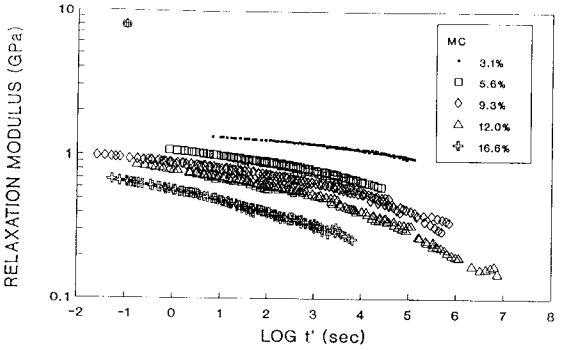

FIG. 9. Temperature-compensated relaxation modulus (E(t')) plotted against reduced time (t' = t/a[T,M]). The temperature-compensated curves are shifted to a reference temperature of 60 C.

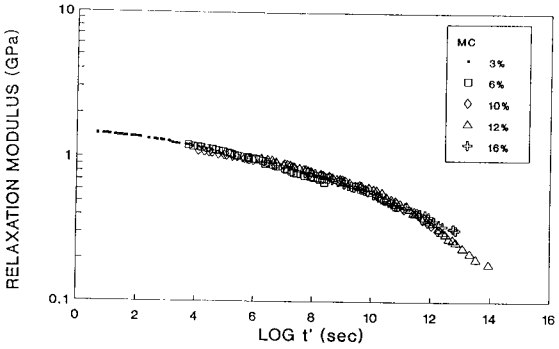

FIG. 10. Relaxation modulus (E(t')) plotted against reduced time (t' = t/a[T,M]). The master curve was developed by shifting the temperature-compensated curves in Fig. 9 to a reference moisture content of 3.1%.

$$\log a = \frac{B}{2.303}\left[\frac{1}{f} - \frac{1}{f_0}\right] \qquad (10)$$

where B = constant.

Combining Eqs. (9) and (10):

$$\log a[T, C, \sigma] = -\frac{B}{2.303}\left[\frac{\alpha(T - T_0) + \beta(C - C_0) + \delta\sigma}{f_0 + \alpha(T - T_0) + \beta(C - C_0) + \delta\sigma}\right] \qquad (11)$$

Equation [11] defines the behavior of the shift factor for amorphous polymers above the glass transition temperature. It is likely that a majority of the stress relaxation tests conducted under the conditions outlined in Table 1 will correspond with the glassy region of lignin. At temperatures below T_g, free volume does not expand in a linear manner. In the glassy region, the shift factor can be described using an Arrhenius-type equation [10], which is derived from entropy-based arguments (LeFebvre et al. 1989). Substituting this temperature dependence while neglecting stress effects that are difficult to evaluate on a cell-wall level, temperature and moisture dependence can be described through the shift factor as:

$$\log a[T, M] = \frac{\Delta H_a}{2.303RT} - \left[\frac{(B/2.303f_0)(C - C_0)}{(f_0/\beta) + (C - C_0)}\right] \qquad (12)$$

where:

ΔH_a = apparent activation energy
R = universal gas constant

Experimental results

The relaxation modulus (E[t]) determined for different temperatures at a common moisture content was shifted along the log time axis to a reference temperature of 60 C (Fig. 9). The temperature-compensated curves were then shifted along the time axis to construct a master curve for both temperature and moisture content (Fig. 10). This shifting process resulted in a smooth curve possessing a shape consistent with those displayed by amorphous polymers. The recorded shift factors were then evaluated using Eq. [12]. To solve for the four unknowns (ΔH_g, B, f_o, β), a two-step procedure was utilized. First, the temperature dependence of the relation was determined by differentiating Eq. [12] with respect to 1/T:

$$\frac{d(\log a[T, M])}{d(1/T)} = \frac{\Delta H_a}{2.303R} \qquad (13)$$

Using Eq. [13], a linear regression of d(log a[T,M]) versus d(1/T) will yield a slope value equal to $\Delta H_a/2.303R$. The differential values of log a[T,M] and 1/T are calculated from a

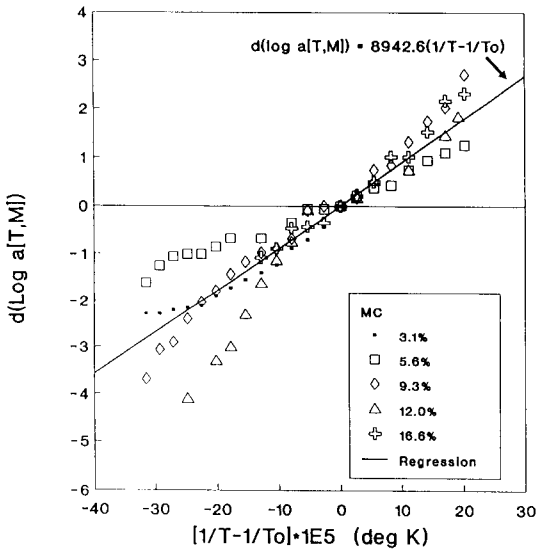

FIG. 11. Linear regression results of d(log a[T,M]) versus (1/T − 1/To). The reference temperature (To) equals 333.15 K. The $r^2 = 0.83$ for the regression analysis.

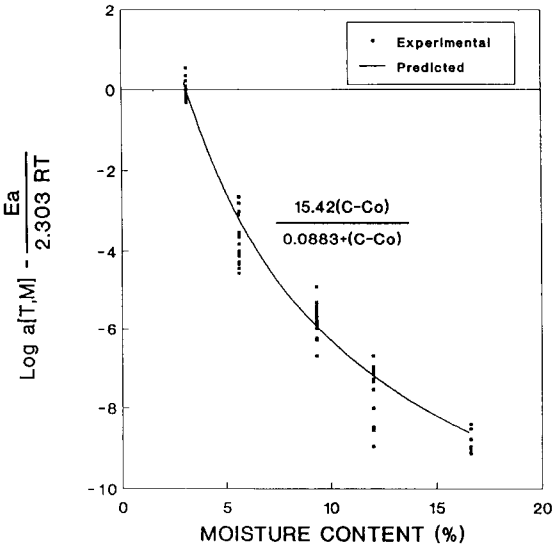

FIG. 12. Nonlinear regression results to determine moisture dependence at a[T,M].

reference value of 60 C (333 K). In the second step, the values of $(B/2.303f_0)$ and (f_0/β) were determined using a nonlinear regression technique. The model used was:

$$\log a[T, M] - \frac{\Delta H_a}{2.303RT} = -\left[\frac{(B/2.303f_0)(C - C_0)}{(f_0/\beta) + (C - C_0)}\right] \quad (14)$$

The results of this two-stage procedure are presented graphically in Figs. 11 and 12.

The linear regression analysis used to solve for the temperature dependence of the shift factor yielded the slope shown in Fig. 11. The intercept was not significant at the 0.05 level. This result is expected because the shift factor will equal zero at the reference temperature. The apparent activation energy calculated from the slope of this regression is found to be 171 kJ/mole. This value is nearly identical to the 172 kJ/mole determined by Caulfield (1984) for the viscoelastically dominated rate of loading and duration of loading effects for strength properties of wood. Van de Put (1987) determined an activation energy for short-term relaxation properties of wood as 209 kJ/mole. As Caulfield recognized, these apparent activation energies are approximately equivalent to that required to break nine hydrogen bonds. Nissan (1977) has developed a theory for creep of hydrogen-bonded materials that involves the simultaneous breaking of hydrogen bonds.

The results of the nonlinear regression analysis are shown in Fig. 12. To evaluate the meaning of these coefficients, they must be reduced to the fundamental variables of f_o and β. The constant B from the Dolittle equation is typically assumed to equal unity from previous experimental results (Ferry 1980). With this relation, the identity for $(B/2.303f_0) = 15.4$ and $(f_o/\beta) = 0.083$ can be solved simultaneously to yield $f_o = 0.028$ and $\beta = 0.33$.

The universal value for f_o is 0.025 at T_g (Ferry 1980). This value is remarkably consistent with 0.023 determined by Salmen (1984) and 0.0245 by Kelley et al. (1987) at T_g. Fractional free volume can be viewed as the fraction of micro-voids in the cell wall that is often referred to in the wood/moisture literature (Skaar 1972; Stamm 1964). Stamm (1964) calculated that the fraction of micro-voids in mercerized cellulose was equal to 0.023 using the differ-

ence between swelling volume and the volume of water adsorbed. This same technique was used independently by Adamson (1987) in determining a fractional free volume of 0.025 for neat epoxy. Certainly, the agreement of the results presented here with that of various researchers lends credibility to the general nature of free volume concepts.

Little experimental evidence is available to evaluate the expansion coefficient β. However, a mathematical relation is given for the fractional free volume of polymer/diluent systems by McKenna (1989):

$$f = v_p f_p + v_d f_d - k v_p v_d \qquad (15)$$

where:

f = fractional free volume
v = volume fraction
k = interaction parameter (ca. 10^{-2})
subscripts p and d denote polymer and diluent, respectively

The free volume expansion coefficient, β, is equivalent to the first derivative of Eq. [15] with respect to C. Because of the difficulty in converting from weight fraction (C) to volume fraction, this differential was evaluated numerically. For moisture contents ranging from 3% to 16%, the average value for df/dC = 0.33 for a $f_d = 0.28$. This value is within the range of 0.1 to 0.3 given for small-molecule diluents far above T_g (McKenna 1989). Given these agreements, the parameters determined for Eq. [12] are certainly within the range predicted by theory and determined experimentally for the general class of amorphous polymers.

CONCLUSIONS

Theories of mechanical properties of cellular materials and viscoelastic properties of amorphous polymers were presented and compared to the experimental behavior of wood. The objective of this research was to evaluate the conformity of wood behavior to these theories to provide a fundamental basis for understanding the deformation processes of wood during the pressing cycle of wood-based composites.

Wood was observed to display a stress-strain relationship in transverse compression that is characteristic of cellular materials. Comparison was made between the theoretical and experimental yield points assuming both plastic and elastic collapse mechanisms. It was concluded the cell walls in low density species of wood are likely to undergo elastic collapse. Only small errors are introduced by assuming elastic collapse for high density woods. An analysis of the collapse and densification regions of the stress-strain relationship for yellow-poplar flakes was found to be adequately predicted by theory assuming elastic collapse mechanisms.

The viscoelastic behavior of wood was compared to free volume theories for amorphous polymers. Specifically, the interactions of temperature and moisture content with the transverse relaxation modulus of wood were studied through time-temperature-diluent concentration superposition. Shift factors were evaluated using a modified version of the free volume theory presented by Knauss and Emri (1981). The analysis showed that temperature dependence is controlled by an Arrhenius-type behavior with an apparent activation energy of 171 kJ/mole. This value is consistent with findings by other researchers with wood. Moisture dependence was found to be controlled by changes in free volume with moisture content. The fractional free volume for the glassy region was determined to be 0.028. This value is remarkably consistent with the "universal" figure of 0.025 for amorphous polymers. The free volume expansion coefficient for moisture changes was calculated to be 0.33. This value is within the range predicted by theory.

There is a certain appeal to the fundamental materials engineering models, presented here, which can unify the interactions of time, temperature, and moisture with the nonlinear response of wood in compression. The polymers and cellular structure that dictate responses under these conditions are common to all species of wood. In addition, fiber and flake-based mats of wood-based composites can also be viewed as a cellular material. The conformity of wood with these general materials theories

opens many avenues for research aimed at fully engineered wood-based composites. For instance, the predictive nature of these theories can be used to understand wood behavior under environmental conditions indicative of the pressing cycle that are extremely difficult to control experimentally. Also, wood mats can be experimentally modeled using mats composed of synthetic polymer fibers and films. These systems could provide stepping stones in our understanding of more complicated wood-based systems by eliminating experimental parameters such as moisture and natural variability. Finally, the demonstration that wood behavior can be studied as a function of the governing polymer behavior, coupled with the structural geometry of the cellular anatomy, has implications far beyond the scope of this particular problem.

ACKNOWLEDGMENTS

The authors would like to acknowledge the McIntire-Stennis program (Project No. WVA00062) for partial funding of this research. This manuscript is published as Scientific Article no. 2246 of the West Virginia Agriculture and Forestry Experiment Station.

REFERENCES

ADAMSON, M. J. 1980. Thermal expansion and swelling of cured epoxy resin used in graphite/epoxy composites materials. J. Mater. Sci. 15:1736–1745.

———. 1987. Some free volume concepts of the effects of adsorbed moisture in graphite/epoxy composite laminates. In: H. Brinson, J. P. Wightman, and T. C. Ward, eds. Adhesion Science Review, Proc. 5th Ann. Prog. Rev., Vir. Tech. Adh. Sci. VPI&SU, Blacksburg, VA.

ASHBY, M. F. 1983. The mechanical properties of cellular solids. Mettal. Trans. A. 14A:1755–1769.

———, K. E. EASTERLING, R. HARRYSSON, AND S. K. MAITI. 1985. The fracture and toughness of woods. Proc. Royal Soc. London A398:261–280.

BILLMEYER, F. W. 1984. Textbook of polymer science, 3rd ed. John Wiley and Sons, New York, NY.

BODIG, J. 1963. The peculiarity of compression of conifers in the radial direction. Forest Prod. J. 13(10):438.

CASEY, L. J. 1987. Changes in wood-flake properties in relation to heat, moisture, and pressure during flakeboard manufacture. Master's thesis, VPI&SU, Blacksburg, VA.

———, E. A. SOKHOLOV, AND V. P. MOCHALOV. 1975. Effect of temperature and moisture on the creep of polymeric materials. Polymer Mech. 11(3):334–339.

CAULFIELD, D. F. 1984. A chemical kinetics approach to the duration-of-load problem in wood. Wood Fiber Sci. 17(4):504–521.

CHAN, R., AND M. NAKAMURA. 1969. Mechanical properties of plastic foams: The dependence of yield stress and modulus on the structural variables of closed-cell and open-celled foams. J. Cell. Plast. 5:112–118.

CHRISTENSEN, R. M. 1982. Theory of viscoelasticity: An introduction, 2nd ed. Academic Press Inc., New York, NY.

EASTERLING, K. E., R. HARRYSSON, L. J. GIBSON, AND M. F. ASHBY. 1982. On the mechanics of balsa and other woods. Proc. Royal Soc. London, A383:31–41.

FERRY, J. D. 1980. Viscoelastic properties of polymers, 3rd ed. John Wiley and Sons, New York, NY.

GEIMER, R. L., R. J. MAHONEY, S. P. LOEHNERTZ, AND R. W. MEYER. 1985. Influence of processing-induced damage on strength of flakes and flakeboards. Res. Paper 463. USDA Forest Prod. Lab., Madison, WI.

GENT, A. N., AND A. G. THOMAS. 1959. The deformation of foamed elastic materials. J. Appl. Polymer Sci. 1(1): 107–113.

GIBSON, L. J., AND M. F. ASHBY. 1982. THE MECHANICS OF THREE-DIMENSIONAL CELLULAR MATERIALS. PROC. ROYAL SOC. LONDON A382:43–59.

———, AND ———. 1988. Cellular solids: Structure and properties. Pergamon Press, New York, NY.

———, ———, AND K. E. EASTERLING. 1988. Structure and mechanics of the iris leaf. J. Mater. Sci. 23:3041–3048.

———, ———, G. S. SCHAJER, AND C. ROBERTSON. 1982. The mechanics of two-dimensional cellular materials. Proc. Royal Soc. London A382:25–42.

———, K. E. EASTERLING, AND M. F. ASHBY. 1981. The structure and mechanics of cork. Proc. Royal Soc. London A377:99–117.

HEEBINK, B. G., AND F. V. HEFTY. 1969. Treatments to reduce thickness swelling of phenolic-bonded particleboard. Forest Prod. J. 11:17–26.

HSU, W. E. 1987. A process for stabilizing waferboard/OSB. Proc. of the WSU Particleboard Symposium, Washington State Univ., Pullman, WA.

HUJANEN, D. R. 1973. Comparison of three methods for dimensionally stabilizing wafer-type particleboard. Forest Prod. J. 6:29–30.

HUMPHREY, P. E. 1979. Fundamental aspects of wood particleboard manufacture. Ph.D. dissertation, Univ. of Wales, Bangor, Wales, UK.

KAMKE, F. A., AND L. J. CASEY. 1988a. Gas pressure and temperature in the mat during flakeboard manufacture. Forest Prod. J. 38(3):41–43.

———, AND ———. 1988b. Fundamentals of flakeboard manufacture: Internal-mat conditions. Forest Prod. J. 38[6]:38–44.

KASAL, B. 1989. Behavior of wood under transverse compression. Master's thesis, VPI&SU, Blacksburg, VA.

KELLEY, S. S., T. G. RIALS, AND W. G. GLASSER. 1987. Relaxation behaviour of the amorphous components of wood. J. Mater. Sci. 22:617–624.

KNAUSS, W. G., AND I. J. EMRI. 1981. Nonlinear viscoelasticity based on free volume considerations. Computers and Structures 13:123–128.

KO, W. L. 1965. Deformations of foamed elastomers. J. Cell. Plast. 1:45–50.

KOCH, C. B. 1964. The recovery of wood after subjection to high compressive strains perpendicular to the grain. Ph.D. dissertation, Univ. of Michigan, Ann Arbor, MI.

KUNESH, R. H. 1961. The inelastic behavior of wood: A new concept in improved panel forming processes. Forest Prod. J. 9:395–406.

———. 1968. Strength and elastic properties of wood in transverse compression. Forest Prod. J. 18(1):65–72.

LEADERMAN, J. M. 1971. The prediction of the tensile properties of flexible foams. J. Appl. Polymer Sci. 15(3): 693–703.

LEFEBRVE, D. R., D. A. DILLARD, AND T. C. WARD. 1989. A model for the diffusion of moisture in adhesive joints, Part 1: Equations governing diffusion. J. Adhesion 27: 1–18.

MAITI, S. K., L. J. GIBSON, AND M. F. ASHBY. 1984. Deformation and energy absorption diagrams for cellular solids. Acta Metal. 32(11):1963–1975.

MAKSIMOV, R. D., V. P. MOCHALOV, AND E. A. SOKHOLOV. 1976. Influence of temperature and humidity on the creep of polymeric materials. Polymer Mech. 12(6):859–864.

———, E. A. SOKHOLOV, AND V. P. MOCHALOV. 1975. Effect of temperature and moisture on the creep of polymeric materials. Polymer Mech. 11(3):334–339.

MCKENNA, G. B. 1989. Glass formation and glassy behavior. *In* C. Booth and C. Price, eds. Comprehensive polymer science, vol. 2, Polymer properties. Pergamon Press, New York, NY.

MEINECKE, E. A., AND R. C. CLARK. 1973. Mechanical properties of polymeric foams. Technomic, Westport, CT.

MENGES, G., AND F. KNIPSCHILD. 1982. Stiffness and strength: Rigid plastic foams. *In* N. C. Hilyard, ed. Mechanics of cellular plastics. MacMillan Publishing Co., New York, NY.

NISSAN, A. 1977. Lectures in fiber science no. 4, Pulp and Paper Technology Series. Tappi-C.P.P.A., Joint Textbook Committee of the Paper Industry, Canada.

PRICE, E. W. 1976. Determining tensile properties of sweetgum veneer flakes. Forest Prod. J. 26(10):50–53.

RUSCH, K. C. 1969. Load-compression behavior of flexible foams. J. Appl. Polymer Sci. 13:2297–2311.

SALMEN, N. L. 1984. Viscoelastic properties of in situ lignin under water-saturated conditions. J. Mater. Sci. 19:3090–3096.

SEBORG, R. M., AND A. J. STAMM. 1941. The compression of wood. Research Report R1258. USDA Forest Prod. Lab.

SIMPSON, W. T. 1973. Predicting equilibrium moisture content of wood by mathematical models. Wood Fiber 5(1):41–49.

SKAAR, C. 1972. Water in wood. Syracuse Univ. Press, Syracuse, NY.

STAMM, A. J. 1964. Wood and cellulose science. The Ronald Press Co., New York, NY.

SUCHSLAND, O. 1962. The density distribution in flakeboard. Quart. Bull., Michigan Agric. Exp. Sta., Michigan State Univ. 45(1):104–121.

———, AND R. C. ENLOW. 1968. Heat treatment of exterior particleboard. Forest Prod. J. 8:24–28.

VAN DE PUT, T.A.C.M. 1987. Derivation of a general rheologic model based on the theory of molecular deformation kinetics. Report No. 25-87-56/22-HA-37, Delft Univ. Technology, Stevin Laboratory, Delft, Netherlands.

WARD, I. M. 1983. Mechanical properties of solid polymers, 2nd ed. Wiley-Interscience, New York, NY.

WARREN, W. E., AND A. M. KRAYNIK. 1987. Foam mechanics: The linear elastic response of two-dimensional spatially periodic cellular materials. Mech. Mater. 6:27–37.

WHITTAKER, R. E. 1971. The mechanical behavior of microporous poly-urethane foams. J. Appl. Polymer Sci. 15(5):1205–1218.

WOLCOTT, M. P., B. KASAL, F. A. KAMKE, AND D. A. DILLARD. 1989a. Testing small wood specimens in transverse compression. Wood Fiber Sci. 21(3):320–329.

———, ———, ———, AND ———. 1989b. Modeling wood as a polymeric foam: An application to wood-based composite manufacture. Pages 56–60 *in* Proc. of the 3rd Joint ASCE/ASME Mechanics Conference. Univ. of California at San Diego, LaJolla, CA.

MECHANICAL PROPERTIES IN RELATION TO SPECIFIC GRAVITY IN 342 CHINESE WOODS

Shu-Yin Zhang

Research Fellow
Station de Recherches sur la Qualité des Bois
Centre de Recherches Forestiéres de Nancy, INRA
54280 Champenoux, France

(Received July 1993)

ABSTRACT

Based on 342 Chinese timber species separated into five distinct categories, relationships of various wood mechanical properties (S) with specific gravity (G) were examined at: 1) species rank; 2) generic rank; 3) the category rank as well as in all the softwoods or hardwoods as a whole. The curvilinear equation ($S = \alpha G^{\beta}$) was compared with the linear one ($S = a + bG$) in terms of the goodness at predicting mechanical properties through specific gravity. The results indicate that the mechanical property-specific gravity relationship varies remarkably with the taxonomic rank, the wood category, and wood mechanical property. Further, the goodness of the two equations in terms of the coefficient of determination also varies appreciably with the rank, the wood category, and wood mechanical property. As a whole, however, the curvilinear equation appears to be better than the linear one at predicting most mechanical properties, particularly at species rank and in terms of the regression coefficients.

Keywords: Specific gravity, mechanical properties, wood categories, Chinese woods, regression equations, relationships.

INTRODUCTION

Wood mechanical properties (S) in relation to specific gravity (G) were examined by Newlin and Wilson (1919) based on American woods, and the equation $S = \alpha G^{\beta}$ was first established for describing the relationships between specific gravity and mechanical properties of clear, straight-grained, and defect-free wood. The Wood Handbook (Forest Products Laboratory 1987) gave the regression equations based on the average specific gravity and mechanical property values for the commercially important 43 softwoods and 66 hardwoods grown in the United States. Armstrong et al. (1984) verified the equation with worldwide data on modulus of rupture, modulus of elasticity in static bending, and maximum crushing strength in compression parallel to the grain. The results show that grouping timbers by genera or by gross anatomical categories for developing mechanical property-specific gravity regressions may be preferable to grouping species on a geographical basis. Furthermore, Walton and Armstrong (1986) found significant differences in the mechanical property-specific gravity relationship between most generic groupings and between most pore arrangement groupings. On the other hand, however, it was stated by Liska (1965) and Forest Products Laboratory (1987) that mechanical properties within a species are linearly related to specific gravity, and thus could be better predicted by the linear equation $S = a + bG$. As a matter of fact, this linear equation has been widely used over the years for describing mechanical properties in relation to specific gravity in a species.

When one reviews the relationships between wood mechanical properties and specific gravity, it is natural to ask: 1) Do the relationships of wood mechanical properties with specific gravity change appreciably at different taxonomic ranks (viz. at species, generic and higher ranks)? 2) Between the curvilinear and linear equations, which is better at describing the mechanical property-specific gravity relation-

Wood and Fiber Science, 26(4), 1994, pp. 512–526

ship? Is the linear equation better at species rank, but poorer at generic and higher ranks? 3) How about the regression coefficients of the two equations? Do they also change with the rank? Are they significant statistically? 4) Is the curvilinear equation good at describing various mechanical properties in relation to specific gravity? How about the goodness of the equations at predicting different mechanical properties? The present study aims at answering these questions. Various mechanical properties of major Chinese woods in relation to specific gravity were analyzed in the present study. The data on physico-mechanical properties of major Chinese woods (Anon. 1982) were considered as a unique population able to serve the present study: 1) The population includes a large number of timber species. 2) These species comprise different kinds of softwoods and hardwoods. 3) These species cover tropical, subtropical, and temperate elements. 4) The determination of wood mechanical properties for all the species studied followed one testing standard. 5) Various wood mechanical properties were determined.

MATERIALS AND METHODS

In total, 342 species comprising 74 softwoods and 268 hardwoods were included in the present study. These species include major commercial Chinese woods (Anon. 1982). In consideration of the obvious differences in macroscopic wood structure among the 342 species of softwoods and hardwoods, the following five distinct wood categories were recognized:

1) First softwood category (FSC): the softwoods with gradual transition from earlywood to latewood (e.g., *Abies* and *Picea*);
2) Second softwood category (SSC): the softwoods with abrupt transition from earlywood to latewood (e.g., *Larix* and hard pines);
3) Ring-porous wood category (RPC) (e.g., *Castanopsis* and *Quercus*);
4) Diffuse-porous wood category (DPC) (e.g., *Eucalyptus* and *Populus*);
5) Semi-ring-porous wood category (SPC) (e.g., *Fagus* and *Juglans*).

Among the 342 species studied, 37 species belong to the first softwood category, 37 species to the second softwood category, 58 species to the ring-porous wood category, 136 species to the diffuse-porous wood category, and 74 species to the semi-ring-porous wood category according to Cheng et al. (1979) and Cheng et al. (1992). Descriptive statistics for various mechanical properties of the five distinct wood categories were given by Zhang (1994b).

For those species that were distributed in limited regions or that were commercially less important, only one test was conducted for each of those species based on the trees sampled from one locality. For some important and widely distributed species, however, more than one (up to 16) tests were performed for individual species, and each test was based on the trees sampled from one of a wide range of localities throughout the distribution areas. In total, 557 tests were completed for the 342 species. For each test, normally at least 5 trees were collected from a locality, and at least 30 small clear specimens were prepared and tested for each mechanical property according to the Chinese National Standard (NSB 1980). Mechanical properties tested include:

A. Modulus of rupture in static bending (MOR);
B. Modulus of elasticity in static bending (MOE);
C. Maximum crushing strength in compression parallel to the grain (Cmax);
D. Maximum compression strength perpendicular to the grain (MCS):
   1) MCSp—The loading on the partial surface of the specimen (based on the average of the radial and tangential tests);
   2) MCSe—The loading on the entire surface of the specimen (based on the average of the radial and tangential tests);
E. Maximum shearing strength parallel to the grain (MSS) (based on the average of the radial and tangential tests);

F. Maximum tensile strength parallel to the grain (MTS);
G. Toughness (T);
H. Hardness (H): 1) Hx (transverse); 2) Hrt (based on the average of the radial and tangential tests);

Mechanical property values were adjusted to the air-dry condition, which is considered to be 15% moisture content in China. Wood specific gravity was based on the oven-dry weight/air-dry volume.

The relationships of mechanical properties with specific gravity in this study were explored at the following taxonomic ranks: 1) species rank; 2) generic rank; 3) category rank. In addition, the mechanical property-specific gravity relationship was also examined when all the softwoods or hardwoods studied were considered as a whole. When the relationship was examined at generic or higher rank, the intraspecific variation was not taken into account (viz. based on the average of all tests for individual species). The relationship at species rank, however, was based on the "species-localities" averages or shipment averages (cf. Newlin and Wilson 1919; Liska 1965). In the present study, the relationship at generic rank as well as at species rank was based on two common and important taxa selected from each wood category (except SPC). At generic rank, *Abies* (10 species) and *Picea* (9 species) were selected from FSC, *Larix* (7 species) and *Pinus* (hard pines only, 20 species) from SSC, *Eucalyptus* (11 species) and *Populus* (20 species) from DPC, and *Castanopsis* (15 species) and *Quercus* (12 species) from RPC. At species rank, the "species-localities" averages in a few cases (see Table 3) were from more than one species due to the limited number of the tests for individual species. Regression analysis was performed in the present study. Regression equation was presented for each mechanical property at different ranks and tested by analysis of variance, and the coefficient of determination (R^2) was given for the curvilinear and linear equations as a major index of the ability to predict mechanical properties through specific gravity.

RESULTS

Mechanical property-specific gravity relationship at the category rank as well as in all the softwoods or hardwood as a whole

For most mechanical properties (except MOR, MOE, and MTS) of the first softwood category (FSC), the linear equation ($S = a + bG$) has a slightly higher coefficient of determination (R^2) than the curvilinear one ($S = \alpha G^{\beta}$), as shown in Table 1. It indicates that the linear equation is able to explain a higher percentage of the variation in most mechanical properties except static bending properties and tensile strength. For SSC, however, the reverse holds true: in terms of the coefficient of determination, the curvilinear equation is better than the linear one at predicting most mechanical properties. If all the softwoods studied were considered as a whole (SW), the curvilinear equation is better at predicting most mechanical properties studied. Only the static bending properties are predicted slightly better by the linear equation. As shown in Fig. 1, however, the two prediction equations for MOR ($MOR = 149G^{0.951}$ and $MOR = 3.7 + 148G$) are actually quite close to each other, and the same, to a lesser extent, applies to MOE (Fig. 2). For RPC, the linear equation appears to be more or less better than the curvilinear one at predicting all the mechanical properties (except MTS) in terms of the coefficient of determination (see Table 1). For DPC, however, the curvilinear equation is better at predicting all the mechanical properties (except the static bending properties). For SPC, no remarkable differences in the coefficient of determination can be recognized between the two equations. When all the hardwoods studied were considered as a whole (HW), the curvilinear equation is able to better predict most mechanical properties, as found in the soft-

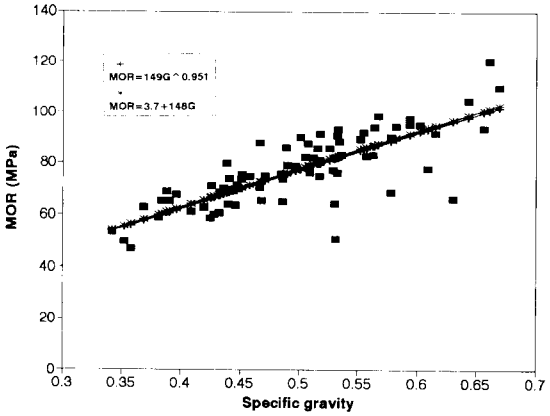

FIG. 1. MOR in relation to specific gravity in the softwoods as a whole (SW) and the comparison of the curvilinear and linear equations.

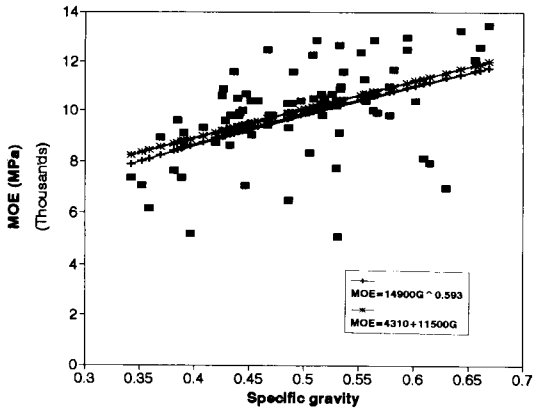

FIG. 2. MOE in relation to specific gravity in the softwoods as a whole (SW) and the comparison of the curvilinear and linear equations.

woods as a whole (SW). Further, the intercept (a) of the linear equation is often not significant statistically, while the two regression coefficients (α and β) of the curvilinear equation are both significant in almost all cases (Table 1). Moreover, the linear relationship using the intercept other than zero has no physical meaning (viz. it predicts a positive or negative property at zero specific gravity), while the curvilinear relationship can degenerate into a linear one when the exponent equals 1. As a whole, therefore, the curvilinear equation appears better than the linear one at predicting mechanical properties at the category or higher rank.

Table 1 also shows that Hrt, MOR, and Cmax in the softwoods as a whole (SW) are most closely related to specific gravity, while MOE and MTS are the least related to specific gravity (also see Figs. 1 and 2 for MOR and MOE as an example). It also holds true in the two softwood categories. But mechanical properties in SSC are generally more closely related to specific gravity than in FSC, and large differences in the relationships of T, MOE, and MTS with specific gravity can be recognized between the two softwood categories. As shown in Table 1, all the mechanical properties studied in SSC are significantly related to specific gravity, while MOE in FSC is not significantly related to specific gravity. In the hardwoods as a whole (HW), as in the softwoods as a whole (SW), H, MOR and Cmax are most closely related to specific gravity (see Fig. 3 for MOR as an example), while T and MTS are the least related to specific gravity. This largely applies to the individual hardwood categories. In general, the mechanical properties in RPC are remarkably less related to specific gravity than in DPC and SPC (Table 1), as demonstrated with MOE in Figs. 4 and 5. All the mechanical properties in RPC, however, are still significantly related to specific gravity, and about half of the variation in the mechanical properties can be explained by specific gravity. For DPC as well as SPC, over half (up to 95%) of the variation can be explained. Compared with the softwoods as a whole, it appears that all the mechanical properties in the hardwoods as a whole (HW) are appreciably more closely related to specific gravity (Table 1). For instance, MOE is poorly related to specific gravity in the softwoods as a whole, but closely related to specific gravity in the hardwoods as a whole (see Figs. 2 and 6). In general, specific gravity in the softwoods as a whole is able to account for about half of the variation in the mechanical properties, while over half, up to

TABLE 1. *The regression coefficients and the coefficient of determination (%) of the curvilinear equation (α, β and R^2—the first row of each mechanical property) and linear equation (a, b, and r^2—the second row) at the category rank (viz. RPC, DPC, SPC, FSC and SSC) as well as in all the softwoods (SW) or hardwoods as a whole (HW).*[1]

	RPC			DPC			SPC		
	α a	β b	R^2 r^2	α a	β b	R^2 r^2	α a	β b	R^2 r^2
MOR	130	0.687	53	150	1.095	80	149	1.037	92
	27.7	107	**58**	−7.9	157	**82**	−1.2	149	**93**
MOE	147	0.586	38	165	0.861	74	169	0.852	87
(×100)	43.1	111	**39**	14.7	153	**75**	16.7	154	87
Cmax	58.5	0.618	45	73.1	1.035	**92**	70.1	0.969	88
	13.8	48.1	**51**	−0.7	73.5	81	2.0	68.4	**89**
MCSp	13.1	1.133	51	16.3	1.633	**80**	16.6	1.674	**90**
	−2.8	17.3	**52**	−4.2	19.4	76	−5.4	21.9	82
MCSe	8.9	1.080	53	11.9	1.718	**78**	11.1	1.597	88
	−2.1	11.7	**55**	−2.9	13.6	74	−2.8	13.5	**89**
MSS	16.1	0.772	47	17.3	1.078	**74**	17.2	1.084	83
	2.2	14.7	**52**	−0.1	17.2	69	−1.0	18.5	**84**
MTS	145	0.570	**32**	158	0.841	**55**	164	0.893	72
	53.0	94.8	29	22.8	136	52	17.1	145	**80**
T	130	1.213	47	124	1.466	**51**	142	1.433	76
	−20.4	1.595	**48**	−31.9	1.612	45	−31.4	1.787	**79**
Hx	96	1.166	64	121	1.633	**85**	115	1.606	91
	−17.2	120	**71**	−42.5	161	84	−35.5	151	91
Hrt	90	1.429	68	115	2.027	**92**	116	2.025	**95**
	−27.0	120	**75**	−56.1	165	88	−48.7	161	93

[1] Underlined R^2 (r^2) and α (a) or/and β (b) indicate that the regression (tested by ANOVA) and the regression coefficient(s) are not significant at the 90% confidence level, respectively; the bold R^2 (or r^2) is relatively larger than the other one; all mechanical properties (except Tougness in N-M/m^2, ×1,000) in MPa (the same applies to Tables 2 and 3).

almost 90%, of the variation can be explained by specific gravity in the hardwoods as a whole.

As shown in Table 1, the regression coefficients α of the curvilinear equations for MOR in most wood categories (except RPC) are close to each other, and the same applies to another regression coefficient (β). It indicates that the prediction curves for most of the different soft-

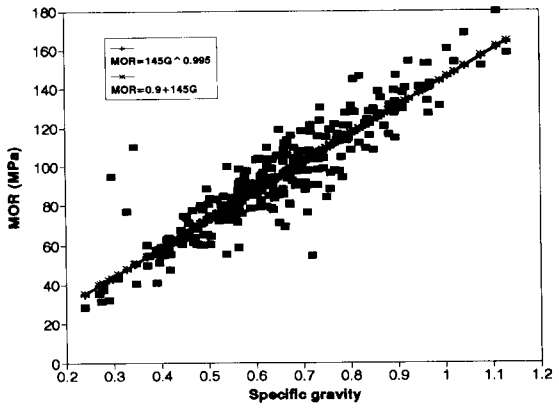

FIG. 3. MOR in relation to specific gravity in the hardwoods as a whole (HW) and the comparison of the curvilinear and linear equations.

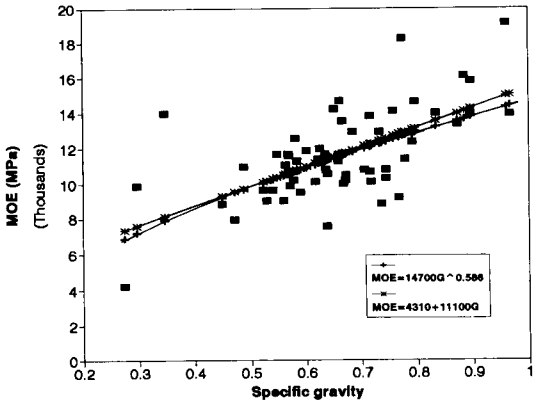

FIG. 4. MOE in relation to specific gravity in the ring-porous wood category (RPC) and the comparison of the curvilinear and linear equations.

TABLE 1. *Extended.*

HW			FSC			SSC			SW		
α a	β b	R^2 r^2	α a	β b	R^2 r^2	α a	β b	R^2 r^2	α a	β b	R^2 r^2
145	0.995	81	146	0.925	**53**	151	0.979	61	149	0.951	61
0.8	145	**82**	8.7	137	52	−0.3	115	**62**	3.7	148	**62**
162	0.802	73	126	0.389	**8**	161	0.692	28	149	0.593	21
20.6	146	73	69.6	56	5	29.4	141	**33**	43.1	115	**23**
68.8	0.932	78	78.3	1.001	52	63.4	0.717	**49**	68.3	0.826	**53**
2.7	67.2	**79**	1.3	76.1	**55**	11.0	55.6	46	7.4	62.7	52
15.8	1.571	**80**	25.7	2.072	51	10.8	1.137	**56**	13.2	1.317	**41**
−4.5	20.0	74	−8.8	31.0	**52**	−0.7	11.4	48	−2.4	15.7	31
11.0	1.562	**80**	14.7	1.905	43	9.1	1.432	**61**	9.7	1.451	**46**
−2.7	13.2	73	−4.3	17.1	**48**	−1.7	10.3	51	−1.9	11.1	41
17.2	1.037	**74**	21.9	1.517	42	15.3	1.068	**65**	17.0	1.209	**50**
−0.2	17.4	73	−3.2	22.1	**43**	0.5	13.5	39	−1.0	16.9	46
158	0.816	**60**	144	0.583	**21**	182	0.969	**45**	161	0.756	**36**
24.7	134	59	45.0	103	18	7.2	174	40	26.5	140	34
127	1.360	**58**	68	0.758	18	99	1.335	**67**	84	1.070	**45**
−28.3	1.636	56	4.7	0.743	**21**	−11.1	1.040	60	−2.8	0.893	42
115	1.552	85	123	1.687	54	69	1.047	**48**	79	1.180	**46**
−35.3	149	85	−26.5	132	**56**	−2.9	74	44	−6.5	85	43
110	1.921	**90**	106	1.991	60	79	1.676	**77**	85	1.740	**68**
−47.4	153	87	−25.4	106	**61**	−17.6	86	70	−18.3	89	65

wood and hardwood categories (except RPC) would be close to each other (see Fig. 7), namely, the predicted MOR values for the different wood categories of the same specific gravity may be comparable (viz. a comparable *weight-strength ratio*). But RPC is appreciably different from the other categories: when specific gravities are within the range of about 0.600,

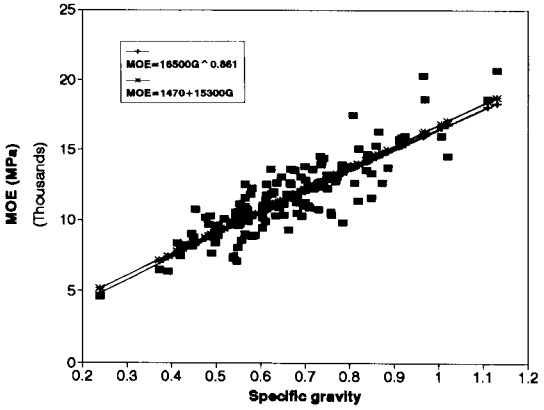

FIG. 5. MOE in relation to specific gravity in the diffuse-porous wood category (DPC) and the comparison of the curvilinear and linear equations.

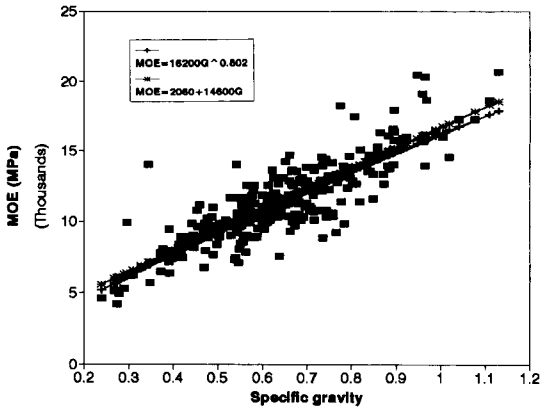

FIG. 6. MOE in relation to specific gravity in the hardwoods as a whole (HW) and the comparison of the curvilinear and linear equations.

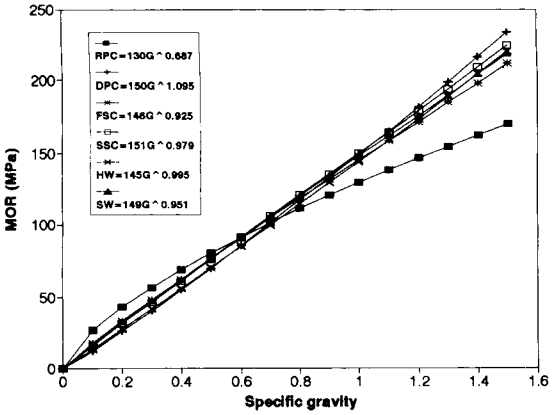

FIG. 7. The predicted MOR for the distinct wood categories.

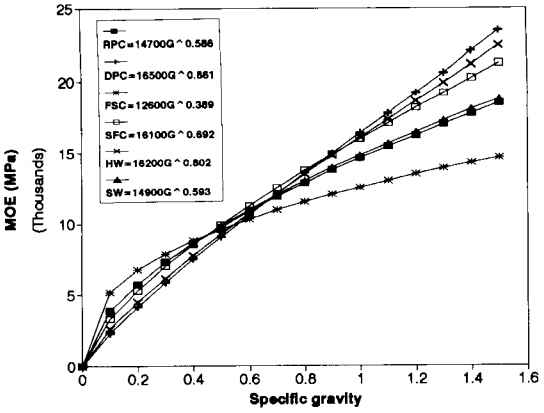

FIG. 8. The predicted MOE for the distinct wood categories.

the predicted MOR value for RPC is generally higher than those for the other categories of the same specific gravity; beyond that range it becomes lower (see Fig. 7). For MOE, the prediction curves for the individual wood categories are appreciably different. As shown in Table 1 and Fig. 8, the prediction equation for the first softwood category (MOE = $12{,}600G^{0.389}$) differs remarkably from SSC (MOE = $16{,}100G^{0.692}$) in both α and β. To a lesser extent, this holds true in two hardwood categories: RPC and DPC. Furthermore, as we noticed in MOR for RPC, the predicted MOE for a category is also related to the range of specific gravity in terms of the comparison with other categories of the same specific gravity. For instance, the predicted MOE for FSC is larger than those for the other categories within the range of 0.6000, but beyond that range MOE for this category does not increase as much as for other categories and thus becomes smaller than for other categories of the same specific gravity. Similar cases were also noticed in other mechanical properties (e.g., Cmax, MTS, MSS, MCSp, and MCSe) (figures not shown), and greater or lesser differences in the prediction curve between the individual wood categories exist. Moreover, the exponent (β) of the curvilinear equation for MOR in all the categories (except the RPC) is very close to 1 (ranging from 0.951 to 1.095), as shown in Table 1. It indicates that MOR at the category rank generally shows an almost linear relation with specific gravity (see Figs. 7 and 9). To a lesser extent, this also applies to MSS and Cmax (see Table 1 and Fig. 9); but H, MCS, and MOE have an appreciable curvilinear relation with specific gravity (see Fig. 9). As shown in Table 1, the exponents (β) of the curvilinear equations for MOE (0.389 to 0.861) and MTS (0.570 to 0.969) in all the wood categories are smaller than 1.000, while those for MCSp (1.133 to 2.072), MCSe (1.080 to 1.905), Hx (1.047 to 1.687), and Hrt (1.429 to 2.027) and T (except in FSC) are larger than 1.000. It implies that the latter mechanical properties may vary with specific gravity at a higher rate than MOE and MTS. In general, H and MCS vary with specific gravity at the highest rate among the various mechanical properties studied, next is T, followed by MSS, MOR, and Cmax, while MOE varies with specific gravity at the lowest rate, as demonstrated in Fig. 9. It should be noticed that both the changing rate and the linearity of a mechanical property with specific gravity in terms of the exponent (β) could be appreciably different between the wood categories, since the exponent (β) of the curvilinear equation for most mechanical properties is more or less different from category to category. Both MOR and Cmax in RPC, for instance, show an obvious curvilinear relation with specific gravity (β = 0.687, 0.618, respectively) although they have near linearity in other cat-

egories, and they vary with specific gravity at a slower rate (see Table 1 and Fig. 7 for MOR as an example). On the contrary, MCSe shows an appreciable curvilinear relation with specific gravity in most categories (β ranges from 1.432 to 1.905), but in RPC it tends to be linearly related to specific gravity (β = 1.080), and varies with specific gravity at a slower rate than in other categories. Table 1 also shows that compared with the two regression coefficients (α and β) of the curvilinear equation, those (a and b) of the linear equation show remarkably larger variation among the wood categories, and the intercept (a) appears to have a relatively wider range than the slope (b).

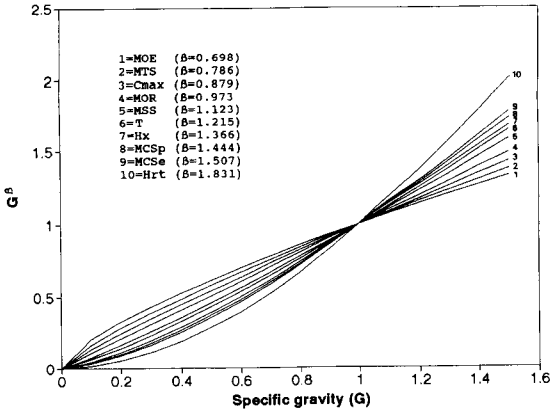

FIG. 9. The comparison of the prediction curves G^{β} (β based on the average of the softwoods and hardwoods) for various mechanical properties showing the changing rate and the linearity of individual mechanical properties with specific gravity.

Mechanical property-specific gravity relationship at generic rank

As in FSC, the linear equation in *Abies,* a genus belonging to FSC (a FSC genus), also has a slightly higher coefficient of determination than the curvilinear one (see Table 2); but it is not the case in *Picea,* another FSC genus where the curvilinear equation is able to explain a higher percentage of the variation in some mechanical properties (viz. MOE, MTS, T, and Hx). In *Larix,* a SSC genus, the curvilinear equation is better at predicting most mechanical properties, as found in SSC; but it does not hold true in *Pinus* (only including hard pines which belong to SSC), as shown in Table 2. The linear equation in the ring-porous genus *Castanopsis,* as in RPC, also has a more or less higher coefficient of determination for most mechanical properties; but it is not the case in the ring-porous genus *Quercus.* In *Eucalyptus,* a DPC genus, the curvilinear equation is able to explain more variation in some mechanical properties. In the diffuse-porous genus *Populus,* however, the linear equation appears to be able to explain more variation in most mechanical properties. If the two genera from each of the four categories studied were considered as a whole, it appears that the curvilinear equation vs. linear equation applied to the generic rank partly follows the case at the category rank. Furthermore, as we noticed at the category rank, the intercept (a) of the linear equation at generic rank is not significant in most cases as well (not shown), and this, to a lesser extent, applies to the regression coefficient b. However, it happens much less frequently to the two regression coefficients of the curvilinear equation, especially to α (see Table 2).

The relationships of mechanical properties with specific gravity at the generic rank, to some extent, vary with the genus under study (Table 2). In the diffuse-porous genus *Eucalyptus,* for instance, all the mechanical properties studied are remarkably more closely related to specific gravity than in the diffuse-porous genus *Populus.* But more often some properties in a genus are remarkably more closely related to specific gravity than in another genus of the same category, as shown in Table 2. If two genera from each category were considered as a whole, the mechanical properties in the SSC genera, unlike at the category rank, do not appear to be more closely related to specific gravity than in the FSC genera, and the mechanical properties in the two DPC genera are not remarkably more closely related to specific gravity than in the two RPC genera, either. But it appears to be true that most mechanical properties in the hardwood genera are slightly more closely related to specific gravity

TABLE 2. *The regression coefficients (α and β) and the coefficient of determination (R^2) of the curvilinear equation and the coefficient of determination (r^2) of the linear equation at generic rank.*

	FSC genus[1]				SSC genus[2]				DPC genus[3]				RPC genus[4]			
	α	β	R^2	r^2	α	β	R^2	r^2	α	β	R^2	r^2	α	β	R^2	r^2
MOR	131	0.762	36	**41**	163	1.107	64	**72**	151	1.413	72	**79**	138	0.830	75	**78**
	225	1.414	83	**85**	126	0.787	32	**34**	86	0.370	15	**18**	138	0.815	**53**	52
MOE	345	1.448	68	**73**	191	0.975	59	**66**	187	1.295	77	**83**	153	0.564	44	**47**
(×100)	306	1.388	**72**	71	126	0.432	5	**9**	149	0.677	**30**	28	160	0.370	7	7
Cmax	87	1.040	72	**75**	78	0.995	64	**69**	71	1.145	65	65	72	0.926	73	**78**
	102	1.278	69	**72**	64	0.788	54	**56**	86	0.370	15	**18**	69	1.129	69	**70**
MCSp	14.6	1.557	73	**75**	8.1	0.648	**39**	38	18.6	2.066	87	**90**	10.8	0.803	30	**35**
	11.0	1.125	35	35	6.5	0.442	12	12	8.0	0.927	23	**28**	17.8	2.375	**58**	51
MCSe	9.9	1.484	60	**62**	5.6	0.596	**14**	12	12.8	2.107	**65**	51	7.4	0.875	46	**54**
	12.2	1.857	29	**40**	4.1	0.290	2	1	4.6	0.628	9	**11**	11.8	2.045	**55**	54
MSS	17.7	1.400	27	**31**	11.7	0.706	**28**	19	15.4	0.811	**64**	62	13.8	0.791	46	**55**
	7.6	0.281	3	**5**	8.9	0.293	3	7	11.3	0.588	**25**	32	16.8	0.964	**42**	40
MTS	146	0.561	6	7	201	1.157	**61**	51	149	1.267	66	**72**	142	0.702	36	**42**
	373	1.715	**82**	78	149	0.683	**16**	15	99	0.202	3	**4**	136	−0.044	0	0
T	106	1.244	35	**37**	69	0.781	**61**	56	164	2.539	**71**	68	162	1.792	66	**73**
	193	2.053	**66**	65	78	1.008	41	**46**	205	1.740	24	**35**	132	0.847	18	**23**
Hx	249	2.454	80	**81**	43	0.287	**5**	2	104	1.361	**76**	72	85	1.100	60	**70**
	95	1.499	**48**	45	67	1.170	**46**	43	47	0.561	14	**19**	114	1.751	69	**70**
Hrt	176	2.644	79	**83**	48	1.038	**29**	26	109	2.000	**88**	87	100	1.877	**91**	89
	39	0.856	15	**16**	79	1.708	**73**	71	45	0.943	20	**26**	106	2.052	**87**	85

[1] The first-row and second-row results of each mechanical property were based on the FSC genera *Abies* and *Picea*, respectively.
[2] The first-row and second-row results were based on the SSC genera *Larix* and *Pinus* (hard pines only), respectively.
[3] The first-row and second-row results were based on the DPC genera *Eucalyptus* and *Populus*, respectively.
[4] The first-row and second-row results were based on the SSC genera *Castanopsis* and *Quercus*, respectively.

than in the softwood genera (Table 2), as we found at the category rank. Comparing Table 2 with Table 1, it appears that the relationships of most mechanical properties with specific gravity in the SSC genera and DPC genera are not as close as those in the respective categories, but it does not apply to other genera. As a whole, H, MOR, and Cmax at generic rank appear most closely related to specific gravity, while MSS at the softwood generic rank and MTS at the hardwood generic rank are the least related to specific gravity.

As shown in Table 2, the two regression coefficients (α and β) of the curvilinear equation for individual wood mechanical properties at generic rank show an appreciably wider range than at the category rank. For instance, the regression coefficients α and β for MOR at generic rank range from 86 to 225, and 0.370 to 1.414, respectively. This indicates that the predicted mechanical property values for the genera of the same specific gravity from different wood categories may be more different than at the category rank. Even for genera of the same category, they may still be appreciably different, as indicated by distinct regression coefficients (Table 2). The exponent (β) of the curvilinear equation for Cmax in most genera studied is still close to 1.000, but this does not apply to MOR and MSS. As shown in Table 2, the exponent (β) for MSS is smaller than 1.000 in most genera, and for MOR it could be smaller than 1.000 in some genera (e.g., *Abies, Castanopsis, Populus,* and *Quercus*), but it could be larger than 1.000 in other genera (e.g., *Eucalyptus* and *Picea*). This case also applies to other mechanical properties studied. Therefore, the relationships of most mechanical properties with specific gravity at generic rank vary in terms of the linearity, depending on the taxon under study.

Mechanical property-specific gravity relationship at species rank

For the species from FSC (FSC species), the linear equation is not better at all even in terms of the coefficient of determination (Table 3). On the contrary, the curvilinear equation is significantly better at predicting most mechanical properties, which is obviously different from the case at the category and generic ranks. The same applies to the SSC species where almost all the mechanical properties are better predicted by the curvilinear equation. At the RPC species rank, unlike at higher ranks, the curvilinear equation also appears to be better at predicting most mechanical properties, and this, to a lesser extent, applies to the DPC species rank. Therefore, at species rank the curvilinear equation is generally better than the linear one at predicting mechanical properties in terms of the coefficient of determination. Furthermore, we also noticed that the intercept (a) of the linear equation at species rank was not significant in most cases as well, and this, to a lesser extent, applies to the regression coefficient b (not shown). It, however, happens appreciably less frequently to the two regression coefficients (α and β) of the curvilinear equation.

As shown in Table 3, the relationships of mechanical properties with specific gravity at species rank also vary with the taxon under study, as noticed at the generic rank. For instance, most mechanical properties in one SSC species (*Cunninghamia lanceolata*) are obviously more closely related to specific gravity than in another SSC species (*Pinus massoniana*). A similar case also exists in the FSC species. As a whole, the mechanical properties at the SSC species rank do not appear to be more related to specific gravity than at the FSC species rank. However, the relationships of mechanical properties with specific gravity at the DPC species rank are appreciably closer than at the RPC species rank, and they are more or less comparable with those at the generic or higher ranks. But the relationships at the RPC species rank are remarkably lower than those at higher ranks. A similar case exists at the softwood species rank where some mechanical properties are poorly related to specific gravity. But it still holds true that the mechanical properties at the hardwood species rank are generally more closely related to specific gravity than at the softwood species rank.

TABLE 3. *Regression coefficients (α and β) and the coefficient of determination (R^2) of the curvilinear equation and the coefficient of determination (r^2) of the linear equation at species rank.*

	FSC species[1]				SSC species[2]				DPC species[3]				RPC species[4]			
	α	β	R^2	r^2	α	β	R^2	r^2	α	β	R^2	r^2	α	β	R^2	r^2
MOR	141	1.027	**38**	33	274	1.467	**49**	47	137	1.098	72	**75**	176	1.318	**65**	64
	223	1.387	**96**	95	106	0.397	**6**	3	155	1.085	**74**	71	131	0.842	**22**	20
MOE	303	1.493	49	**52**	199	0.808	23	**24**	174	1.104	58	**65**	178	0.955	33	**34**
(×100)	331	1.470	**83**	81	179	0.730	**21**	14	210	1.103	**49**	44	160	0.891	13	**18**
Cmax	101	1.390	20	**22**	90	0.947	**51**	48	70	1.022	73	73	69	0.943	21	**27**
	110	1.338	**93**	92	69	0.838	**18**	11	74	1.009	**55**	54	62	0.472	**6**	4
MCSp	4.3	0.085	0	0	11.5	1.244	**41**	38	15.5	1.659	84	**86**	10.7	0.860	11	11
	8.8	0.816	**31**	24	6.9	0.575	7	5	10.2	1.063	**43**	42	14.6	1.316	**10**	6
MCSe	6.3	1.089	21	**24**	15.6	2.009	**34**	31	9.8	1.367	78	**80**	9.9	1.312	24	24
	6.3	0.863	**43**	39	9.3	1.516	**29**	21	10.3	1.123	**50**	48	9.2	0.495	**3**	2
MSS	19.4	1.618	**13**	11	7.5	0.335	2	2	16.6	1.062	**74**	72	10.9	0.398	**5**	4
	7.4	0.218	3	3	12.0	0.621	**23**	18	16.8	1.580	**72**	71	18.3	1.569	54	54
MTS	156	0.716	**20**	17	200	1.017	**50**	49	158	1.192	53	**59**	101	0.257	1	1
	451	1.949	78	78	156	0.784	**16**	8	153	0.720	**34**	29	152	0.262	3	3
T	174	1.988	**51**	48	99	1.385	**28**	25	185	2.163	**42**	36	189	2.223	**38**	37
	191	2.047	**84**	60	84	1.009	**11**	3	284	2.018	**38**	36	59	−2.657	**14**	8
Hx	66	1.302	57	**61**	69	0.963	**35**	32	91	1.024	**71**	67	97	1.489	50	**51**
	90	1.442	**65**	43	52	0.734	**14**	10	61	0.872	**37**	35	105	1.630	**50**	44
Hrt	81	1.948	39	**43**	53	1.214	**52**	50	94	1.701	74	**76**	109	2.064	**75**	74
	43	1.004	**42**	34	45	0.810	**39**	32	92	1.778	**73**	70	106	2.100	**62**	55

[1] The first-row and second-row results of each mechanical property were based on the FSC *Pinus armandi* (a soft pine) and *Picea* species (*P. asperata* and *P. purpurea*), respectively.
[2] The first-row and second-row results were based on the SSC species *Cunninghamia lanceolata* and *Pinus massoniana* (a hard pine), respectively.
[3] The first-row and second-row results were based on the DPC *Eucalyptus* species (*E. globus* and *E. robusta*) and *Populus* species (*P. davidiana* and *P. tomentosa*), respectively.
[4] The first-row and second-row results were based on the SSC *Castanopsis* species (*C. fargesii* and *C. sclerophylla*) and *Quercus* species (*Q. acutissima* and *Q. variabilis*), respectively.

As a whole, H, MOR, and Cmax appear most closely related to specific gravity at the species rank, while MSS at the softwood species rank and MTS at the hardwood species rank are the least related to specific gravity, as we noticed at the generic rank.

Comparing Table 3 with Tables 1 and 2, the two regression coefficients (α and β) of the curvilinear equation for individual mechanical properties at the species rank also show an appreciably wider range than at the category rank, and they are usually (more or less) different from those at the generic rank as well. As shown in Table 3, the differences in the two coefficients of the regression equations for some mechanical properties between some species are quite large. It implies that the predicted *weight-strength ratios* for some species may be quite different. However, the regression coefficients of different species from the same category generally appear closer than those of the species from different categories although the differences in the two regression coefficients of different species from the same category still could be large. Furthermore, the relationships of mechanical properties with specific gravity in terms of the linearity also vary with individual mechanical properties as well as the species under study. For instance, MOR, Cmax, and MOE are almost linearly related to specific gravity only at the DPC species rank, but the linear relationship does not exist in other mechanical properties (e.g., T and Hrt). Moreover, the exponent (β) of the curvilinear equation is appreciably more frequently not significant than the regression coefficient α, as we noticed at the generic rank.

DISCUSSION

The curvilinear equation established by Newlin and Wilson (1919) was based on the results of tests on mixed softwoods and hardwoods. Liska (1965) followed the same treatment, but he found that the curvilinear equation does not differ appreciably in the goodness from the linear one. However, the present study indicates that the differences in the mechanical property-specific gravity relationship among the five wood categories are quite remarkable, and the goodness of the curvilinear and linear equations at describing the relationships in the individual categories is also appreciably different. Therefore, grouping timbers by the wood categories for developing mechanical property-specific gravity regressions appears to be preferable. A similar statement was also made by Armstrong et al. (1984), and they even suggest grouping timbers by genera. This is largely supported by the present study.

The present study clearly indicates that the curvilinear equation is better than the linear one at predicting mechanical properties at species rank in terms of both the coefficient of determination and the regression coefficients. Liska (1965) and Forest Products Laboratory (1987) believed that specific gravity and mechanical properties within a species show a linear relationship rather than a curvilinear one; and a significant linear relationship was reported in many studies (Kellogg and Ifju 1962; Liska 1965; Ifju 1969; Pearson and Gilmore 1971; Manwiller 1972; Bendtsen and Ethington 1972; Schniewind and Gammon 1983; Pearson 1988; Shepard and Shottafer 1992; Zhang and Zhong 1992). But a poor linear relationship between specific gravity and some mechanical properties was also noticed by some authors (McAlister 1976; Leclercq 1980; Schniewind and Gammon 1983; Hunt et al. 1989). In general, very few studies have compared the linear equation with the curvilinear one in terms of the goodness at predicting mechanical properties through specific gravity. Liska (1965) reported that a straight-line relationship between specific gravity and four mechanical properties in Douglas-fir was justified; but a few studies (Biblis 1969a, b; Biblis and Fitzgerald 1970) also found that a curvilinear equation was better than the linear one at describing the relationships of mechanical properties with specific gravity. It should be remembered that the relationships at species rank presented in this study, unlike most studies reported before, were established on the basis of the shipment averages rather than the

results of individual specimens. We thus wonder whether there are appreciable differences in the mechanical property-specific gravity relationship at species rank based on the two different data sources, which will be explored in a subsequent study (Zhang 1994a). In addition, more species should be investigated in order to get a general conclusion on the mechanical property-specific gravity relationship at species rank because the present study indicates that the relationships at species rank, to some extent, vary with the species under study.

It appears difficult to understand a closer mechanical property-specific gravity relationship in the hardwoods as a whole (HW) than in the softwoods (SW) if the more complex structure of hardwoods is considered. However, a remarkably wider range of specific gravities in the hardwoods (roughly ranging from 0.2 to 1.2, see Fig. 3) than in the softwoods (roughly from 0.3 to 0.7, see Fig. 1) may be one contributing factor. In addition, the large variation in the amount of resin among the softwoods studied might be another factor because it, like extractives, adds weight (or specific gravity), but does not modify mechanical strength appreciably (Zhang and Zhong 1992). A closer mechanical property-specific gravity relationship in the diffuse-porous wood category than in the ring-porous wood category appears reasonable in the sense of the more uniform structure in the diffuse-porous woods. However, the appreciable differences in the relationship between the two softwood categories remain to be explored. An appreciably poorer relationship at species rank probably results from the fact that in the present study the mechanical property-specific gravity relationship in individual species was based on the shipment averages, and each test was based on the trees from one of a wide range of the localities throughout the distribution areas. If the study had been based on the results of individual specimens from the same locality, a closer relationship at species rank would have been expected.

CONCLUSIONS

In light of this study on the 342 Chinese woods, it is rational to conclude:

1. The relationships of mechanical properties with specific gravity vary remarkably with the taxonomic rank, the wood category, and wood mechanical property.
   a) In general, most mechanical properties at species rank are appreciably less related to specific gravity than at higher ranks. However, the relationships of mechanical properties with specific gravity at generic rank are partly comparable with those at higher ranks.
   b) Most mechanical properties in the second softwood category appear to be more closely related to specific gravity than in the first softwood category, but this does not hold true at lower ranks. In the ring-porous wood category, they are generally less related to specific gravity than in the diffuse-porous wood category, and this holds true at species rank, but not at generic rank. If the softwoods studied were considered as a whole, mechanical properties in the hardwoods as a whole are generally more closely related to specific gravity, and this applies more or less to the lower ranks as well.
   c) Among various mechanical properties studied, H, MOR, and Cmax at all ranks studied appear most closely related to specific gravity; but MOE and MTS in the softwoods as a whole and T and MTS in the hardwoods as a whole are the least related to specific gravity. This holds true at the category rank, but not at lower ranks where MSS (softwoods) and MTS (hardwoods) appear least related to specific gravity.
2. The goodness of the curvilinear equation and linear equation in terms of the coefficient of determination also varies appreciably with the taxonomic rank, the wood category, and wood mechanical properties. As a whole, however, the curvilinear equa-

tion appears better at predicting most mechanical properties, particularly at species rank.

3. Prediction curves (or the predicted *weight-strength ratios*) for the distinct wood categories are usually (except for MOR) different more or less, and this applies to the lower ranks. Further, the predicted *weight-strength ratio* for a wood category in terms of the comparison with other categories is related to the range of specific gravity (with a turning point at about 0.6000). Moreover, the prediction equation for MOR, MSS, and Cmax at the category or higher rank tends to be linear, but this does not apply to other mechanical properties and lower ranks. In general, H and MCS at the category or higher rank vary with specific gravity at the highest rate among the mechanical properties studied, next is T, followed by MSS, MOR, and Cmax, while MOE varies with specific gravity at the lowest rate. This, however, does not appear to be true at lower ranks. Between the two regression coefficients (α and β), the exponent (β) appears to be more frequently not significant at species and generic ranks, but both of them are remarkably less frequently not significant as compared with those of the linear equation.

ACKNOWLEDGMENTS

The author would like to extend his gratitude to Prof. B. F. Ke, Dr. G. Nepueu, and Prof. Z. Jiang for their encouragement and support for this study. Thanks are due to Dr. J. P. Armstrong and Dr. A. P. Schniewind for their helpful comments on a previous draft of the paper.

REFERENCES

ANONYMOUS. 1982. Physico-mechanical properties of major Chinese woods. Chinese Forestry Press, Beijing, China.

ARMSTRONG, J. P., C. SKAAR, AND C. DEZEEUW. 1984. The effect of specific gravity on some mechanical properties of some world woods. Wood Sci. Technol. 18: 137–146.

BENDTSEN, B. A., AND R. L. ETHINGTON. 1972. Properties of major southern pines. Part II. Structural properties and specific gravity. USDA Forest Serv. Res. Pap. Forest Prod. Lab. 177, Madison, WI.

BIBLIS, E. J. 1969a. Tensile properties of loblolly pine growth zones. Wood Fiber 1(1):18–28.

———. 1969b. Transitional variation and relationships among properties within loblolly pine growth rings. Wood Sci. Technol. 3:14–24.

———, AND J. D. FITZGERALD. 1970. Shear properties of loblolly pine growth zones. Wood Sci. 2:193–202.

CHENG, J. Q., J. J. YANG, P. LIU, AND H. J. LU. 1979. Microscopic structure of Chinese hardwoods. Agricultural Press, Beijing, China.

———, ———, AND ———. 1992. Chinese woods. Chinese Forestry Press, Beijing, China.

FOREST PRODUCTS LABORATORY. 1987. Wood handbook: Wood as an engineering material. Agric. Handb. 72. USDA Forest Service, Washington, DC.

HUNT, M. O., M. H. TRICHE, G. P. MCCABE, AND W. L. HOOVER. 1989. Tensile properties of yellow-poplar veneer strands. Forest Prod. J. 39(9):31–33.

IFJU, G. 1969. Within-growth-ring variation in some physical properties of southern pine wood. Wood Sci. 2:11–19.

KELLOGG, R. M., AND G. IFJU. 1962. Influence of specific gravity and certain other factors on the tensile properties of wood. Forest Prod. J. 12:463–470.

LECLERCQ, A. 1980. Relationships between beechwood anatomy and its physico-mechanical properties. IAWA Bull. n.s. 1(1–2):65–71.

LISKA, J. A. 1965. Research progress on the relationships between density and strength. Pages 89–97 *in* Proceedings of the Symposium on Density: A key to wood quality. USDA Forest Serv. Forest Prod. Lab., Madison, WI.

MANWILLER, F. G. 1972. Characterization of spruce pine. Final Report FS-SO-3201-1.1, USDA Forest Serv., Southern Forest Exp. Sta., Alexandria, LA.

MCALISTER, R. H. 1976. Modulus of elasticity distribution of loblolly pine veneer as related to location within the stem and specific gravity. Forest Prod. J. 26(10): 37–39.

NSB. 1980. National Standard for Testing Wood Physical and Mechanical Properties. GB1927-1943-80, Technical Standard Press, Beijing, China.

NEWLIN, J. A., AND T. R. C. WILSON. 1919. The relation of the shrinkage and strength properties of wood to its specific gravity. Bull. No. 676. USDA Forest Serv., Forest Prod. Lab., Madison, WI.

PEARSON, R. G., AND R. C. GILMORE. 1971. Characterization of the strength of juvenile wood of loblolly pine (*Pinus taeda* L.). Forest Prod. J. 21(1):23–31.

———. 1988. Compressive properties of clear and knotty loblolly pine juvenile wood. Forest Prod. J. 38(7/8): 15–22.

SCHNIEWIND, A. P., AND B. W. GAMMON. 1983. Strength and related properties of knobcone pine. Wood Fiber Sci. 15(1):2–7.

SHEPARD, R. K., AND J. E. SHOTTAFER. 1992. Specific gravity and mechanical property-age relationships in red pine. Forest Prod. J. 42(7/8):60–66.

WALTON, D. R., AND J. P. ARMSTRONG. 1986. Taxonomic and gross anatomic influences on specific gravity-mechanical property relationships. Wood Fiber Sci. 18(3):413–420.

ZHANG, S. Y., AND Y. ZHONG. 1992. Structure-property relationship of wood in East-Liaoning oak. Wood Sci. Technol. 26:139–149.

———. 1994a. Wood mechanical property-specific gravity relationships in individual species selected from distinct wood categories (in preparation).

———. 1994b. General relationships of mechanical properties with specific gravity in 342 Chinese woods (in preparation).

EFFECT OF PRESTEAMING ON DRYING STRESSES OF RED OAK USING A COATING AND BENDING METHOD[1]

Zuoxin Wang
Former Graduate Assistant

Elvin T. Choong
Professor
Louisiana Forest Products Laboratory
School of Forestry, Wildlife, and Fisheries
Louisiana State University Agricultural Center
Baton Rouge, LA 70803

and

Vijaya K. Gopu
Professor
Department of Civil Engineering
Louisiana State University
Baton Rouge, LA 70803

(Received May 1993)

ABSTRACT

This study was initiated to investigate the effect of presteaming on drying stresses of red oak (*Quercus* sp.) using the coating and bending method. Besides the presteaming effect, a directional effect on drying stresses was also tested. Four blocks were randomly selected. Each block was divided into two pairs (four samples). One pair was randomly assigned to steaming while the other was assigned to control. A statistical split-plot model was used to analyze the results. Presteaming increased drying stress by up to 36% and decreased drying time by 23% when red oak was dried at 75% relative humidity and 44 C from average moisture content of 80 to 16%. The maximum drying stress of the steamed samples occurred before that of the unsteamed samples due to faster moisture loss from the sample. This study indicated that the coating and bending method could be used to study drying stresses of red oak. The statistical model revealed the differences between steaming and control and between inner and outer directions. Drying stresses were different in two opposite directions (outward and inward), regardless of whether the wood was steamed or not.

Key Words: Coating and bending method, drying deflection, drying stress, modulus of elasticity, presteaming, slicing method.

INTRODUCTION

Presteaming and steaming of wood have been practiced in Europe since the middle of the 18th century to prepare for drying, to sterilize wood, to darken some species, and to relieve drying stresses (Campbell 1961). They have been in use in Australia for 30 years, but in the United States these processes have not been commercially adopted. One reason is that in this country there is a greater concern for quality than for shorter drying time. Presteaming of wood has been reported to increase the drying rate of heartwood of many wood species

[1] This paper (No. 93-22-7152) is published with the approval of the Director of the Louisiana Experiment Station. The research was supported in part by the McIntire-Stennis Cooperative Forest Research Program. The authors gratefully acknowledge the contribution of Peter J. Fogg, Professor Emeritus of Forestry, during the course of this study.

(Campbell 1961; Simpson 1975; Alexiou et al. 1990a, b). Campbell (1961) reported a reduction in drying time of 20–35% for *Eucalyptus obliqua*. Alexiou et al. (1990a) reported that presteaming increased the drying rate of *Eucalyptus pilularis* by 7–16%.

The reason that presteaming can reduce drying time is not completely clear. Some researchers (Haslett and Kininmonth 1986; Choong and Achmadi 1989) postulated that steaming changes the nature of polyphenolic extractives that line cell walls, lumina, and pit areas. Before steaming, these extractives form a continuous layer. After steaming, the layer appears cracked, blistered, and generally discontinuous; therefore, the cell walls become more accessible to water, and moisture movement is enhanced. Alexiou et al. (1990a) thought that the increase in drying rate is due to the mobilization and partial removal of heartwood extractives, which allow greater access of water molecules to the cell walls. Microscopic investigation (Kubinsky 1971) of steamed northern red oak showed a reduced fiber lumen size, indicating an increased internal swelling that is caused by disruption of the warty layer that lines the lumen walls. The resultant effect is an increase in accessibility of the cell wall to moisture. Transmission electron micrographs of pit membranes of the steamed wood indicate hydrolysis of the membranes, which weakens both the membrane and the bond between the torus and the border, resulting in deaspiration of the pits (Siau 1984). Extraction by hot water and chemical solvents tends to have the same effects on permeability as steaming in softwoods (Fogg 1969) and in tropical woods (Choong and Achmadi 1989).

Drying stresses in wood are closely related to drying rate and they affect drying quality. Several papers (Schniewind 1960, 1963; Kuebler 1960) have described in detail the nature of these stresses. The technique often used to detect the stress in wood is the slicing method (McMillen 1955, 1968; Simpson 1975; Rice 1988), which requires cutting a drying sample into slices. There is a change in dimensions soon after cutting, i.e., an elastic strain in the sample is indicated. This strain causes stress in the wood and results in honeycombs and checks if the stress is greater than the strength of the sample. This phenomenon can also be found if the sample is cut along the neutral plane (Fig. 1).

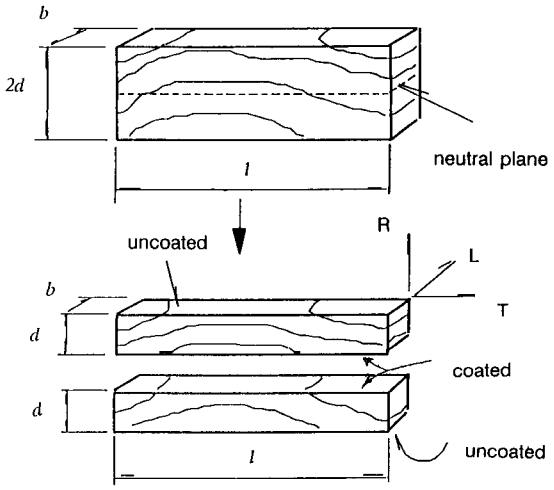

FIG. 1. Sample preparation and dimensions.

The slicing method to analyze drying stress was first used by McMillen (1955). Youngs and Norris (1958, 1959) further refined this method to calculate the internal stress in drying wood. The information derived by their technique gives a clear insight into the stress behavior during drying of wood, although the stress values apply to only one stage of drying of one sample under one set of drying conditions. This method, however, is difficult to use. When wood is sliced, the slices are affected by either a knife or a saw, and by temperature and relative humidity at the slicing site, which cause large variations in the data. Also, attention must be given to the techniques used for gathering data on strain recovery of the slices. McMillen (1968) reported irregular distributions of surface checks in some specimens and this phenomenon discourages any attempt to analyze all of the specimens for actual drying stresses. Rice (1988) reported that because of limitations in the slicing technique, the stresses that occur at the surface cannot be predicted.

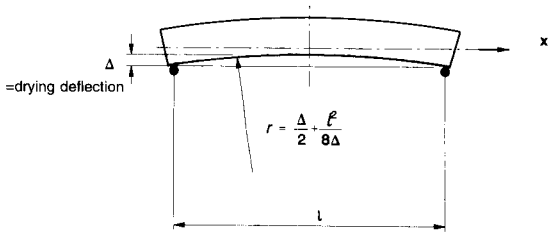

FIG. 2. Deflected shape of sample during drying.

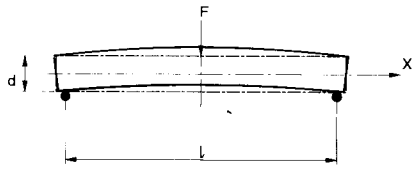

FIG. 3. Mid-span loading to determine the modulus of elasticity E of the sample.

Alexiou et al. (1990b) stated that direct measurement of internal stresses in wood is not possible; but drying stresses can be estimated by measuring the strains. Because information on the mechanical properties of blackbutt (*Eucalyptus pilularis*) across the grain is lacking, Alexiou et al. (1990b) could use instantaneous strain recovery only as an indicator of stress development. Also due to the highly variable magnitudes, the trends were not statistically significant. In addition, it is not possible to get the exact strain at the time of checking. Therefore, this slicing method can be used only during the first several days of drying. For these reasons, a new method needs to be developed to test and analyze drying stress.

EXPERIMENTAL AND ANALYTICAL METHOD

The main objective of this study was to develop a new method to determine the effect of presteaming on drying time and occurrence of drying stresses in wood. In order to accomplish the research objective, a coating and bending method was developed to replace the slicing method. Simplified assumptions for this method were: (1) water in wood between two opposite surfaces moves to the nearest surface, i.e., if a neutral plane is assumed between the two opposite surfaces, then water would not traverse the neutral plane; (2) drying stresses and strains vary linearly from the surface of the wood to the neutral plane; (3) strain and stress distributions are symmetrical with respect to the neutral plane; (4) slicing the wood into two halves along the neutral plane will not affect the moisture movement if the cut surface is coated. It is pertinent to point out that a sliced sample would develop a bend that is concave to the uncoated surface (Fig. 1) during the first phase of drying because the uncoated surface shrinks first.

As drying continues into the second phase, moisture close to the coated surface begins to shrink, and the bending will be convex with respect to the uncoated surface. The bending will release the drying stresses. If a force, F, is exerted on the sample (Fig. 2) to straighten it (bend backward), then the bending stress induced by this force is equal to the drying stress in the uncut sample. This force, F, can be obtained experimentally. Knowing F, the drying stress, σ, can be determined by elementary theory of bending as:

$$\sigma = \frac{M}{S} = \frac{Fl/4}{bd^2/6} = \frac{3}{2}\left(\frac{Fl}{bd^2}\right) \qquad (1)$$

where M is the mid-span moment due to F and equal to $Fl/4$, l is the distance between two supports (Fig. 2), S is section modulus of the cross section with respect to the x axis, d (Fig. 1) is the distance from the coated surface to the uncoated surface (i.e., depth of sample), and b is the width of the sample.

A potential problem with this procedure is that when the force is applied to the sample, the sample may crack before it straightens. If too small a force is used, the sample will not straighten completely. To solve this problem, it is possible to use another approach by first determining the modulus of elasticity, E, and then calculating the drying stress from elementary bending theory as follows:

$$\sigma = \frac{E(d/2)}{r} \qquad (2)$$

where r is the radius of curvature of the sample,

and equal to

$$\left(\frac{\Delta}{2} + \frac{l^2}{8\Delta}\right) \quad (3)$$

in which Δ is the midspan deflection of the sample after drying (Fig. 2).

The modulus of elasticity, E, of the sample can be determined from the relationship:

$$\delta = \frac{Fl^3}{48EI} \quad (4)$$

where δ is the deflection due to a concentrated load, F, applied at mid-span (Fig. 3), and $I = bd^3/12$ is the moment of inertia of the cross section with respect to the x-axis. Substituting the value of E into Eq. 2, yields the drying stress, σ. Because r/d > 10, the straight bar formula for maximum stress is used here (Timoshenko 1955).

MATERIALS

A green red oak (*Quercus* sp.) heartwood board was randomly selected for this study. The original moisture content (MC) of the board was 80%. The dimensions were 5 cm thick, 20 cm wide, and 240 cm long. Four clear blocks were randomly selected from the board (Fig. 4). In order to decrease the variance of the wood, each block was divided into two pairs, of which one was assigned to the control group and the other to the steaming group. Then each pair was split into two samples according to their structural positions with respect to the tree stem. The inner part that was nearer to the pith was labeled "inner," while the outer part that was nearer to the bark was called "outer" wood. The dimensions of each sample were about 20 mm in the radial (R) direction, 23 mm in the longitudinal (L) direction, and 140 mm in the tangential (T) direction. The sample was cut so that the rings were symmetrically oriented with respect to the center of the *l* dimension (T direction).

PROCEDURE

Block numbers were properly marked on the randomly selected board, indicating four randomly selected blocks. The blocks were cut as shown in Fig. 4. Then each block was cut into two pieces (a pair) (Figs. 1 and 4). The two pieces were randomly assigned to the control group and the steaming group. Each piece was marked by letters and numbers to identify its block, group, and positions-directions. Then each piece was cut into two samples of inner and outer positions.

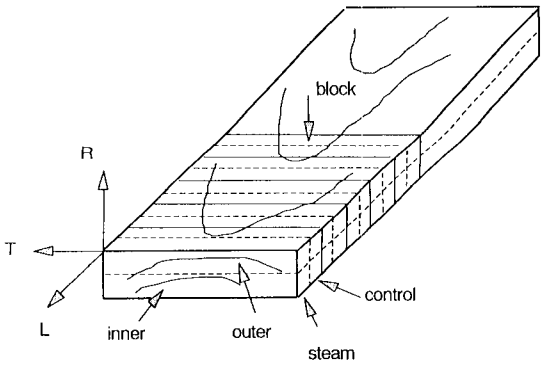

FIG. 4. Method of cutting sample blocks.

After cutting, the samples of the presteaming group were put inside a steamer for 2 h at atmospheric pressure and 100 C. Presteaming, however, causes some water to come out of the sample. In order for steamed samples to have the same moisture content as that in the control group, the presteamed samples were put into water in a flask, and the flask was vacuumed for 20 min every 6 h during 24 h. Then all the samples, in both control and presteaming groups, were coated as shown in Fig. 1. All the surfaces, except the top surface of the outer sample and the bottom surface of the inner sample, were coated with saran resin diluted in methyl ethyl ketone. Each sample was coated three times. Thus the inner and outer samples dried in the inward and outward direction, respectively.

In order to calculate the bending stress, the modulus of elasticity, E, was experimentally evaluated at 12 h and at the end of drying (about 800 h) on an Instron universal testing machine. All samples were placed inside a Blue M environmental chamber to dry, at a dry bulb

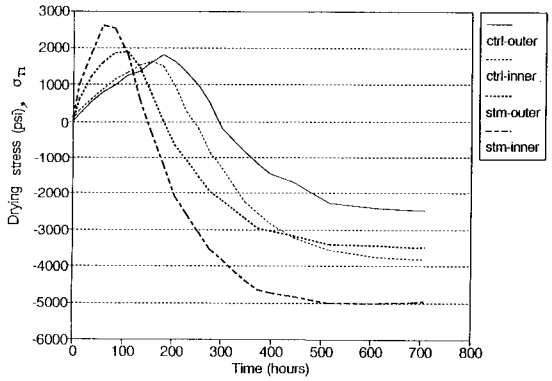

FIG. 5. Relationship between stress and drying time.

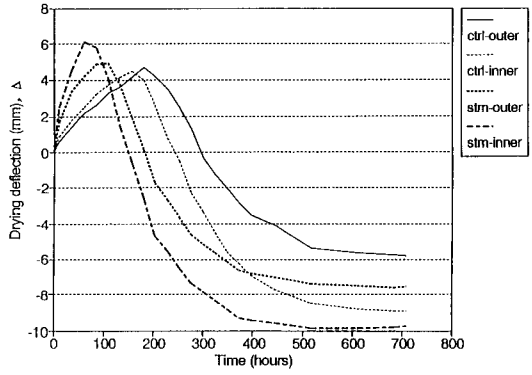

FIG. 6. Relationship between deflection and drying time.

temperature of 44 C, and a wet bulb temperature of 39.5 C (nominal 75% RH). The first measurement was made after 12 h, then subsequent measurements were made every 24 h. After 132 h, the measurement intervals were increased to 72 h or more. At each observation, five variables were measured: namely, the three dimensions of a sample, the weight, and the drying deflection. The drying deflection caused bending of the tangential (L-T) face (Fig. 1). The bending was assumed to be uniform for a sample, and the tangential face formed an arch. The chord length was measured and the radius of the arch was then calculated using the chord length, l, and the drying deflection, Δ (the height of the arch) in Eq. 3.

The MC profile was measured with extra samples in both the steaming and the control groups. One sample was cut into four slices along the tangential direction. The average MC of the slice was measured. These data were used to determine the MC at the mid-point of the slice. The four measuring points in the sample were at 2.5 mm, 7.5 mm, 12.5 mm, and 17.5 mm from the uncoated surface. Because of symmetry, these data were also used to estimate the MC of the paired sample.

From the data, the maximum stresses, the maximum deflections, the times corresponding to these stresses and deflections, and the times at MC of 30% and 16% were determined. In the first phase of drying, the surface layer

TABLE 1. *Summary of experimental results comparing treatment and control.*

Variable	Number of samples	Control		Steaming		F value	Pr > F
		Mean[1]	SD	Mean[1]	SD		
σ_{T_1} (psi)	8	1,748.5	178.9	2,321.3	549.6	19.74	0.0212
σ_{C_3} (psi)	8	−3,106.7	789.9	−4,212.5	1,171.1	33.92	0.0101
Δ_1 (in.)	8	0.184	0.019	0.222	0.035	28.74	0.0127
Δ_3 (in.)	8	−0.291	0.088	−0.345	0.061	9.21	0.0561
t_1 (h)	8	168.0	18.1	81.0	20.0	841.00	0.0001
Θ_{t1-2} (h)	8	98.6	22.2	83.6	8.7	4.66	0.1197
t_2 (h)	8	266.6	37.1	164.6	22.7	112.73	0.0018
Θ_{t2-3} (h)	8	333.4	57.0	345.4	49.7	0.28	0.6359
t_3 (h)	8	600.0	61.5	510.0	65.1	10.07	0.0503
t_4 (h)	8	596.8	127.1	490.5	44.3	8.35	0.0630
t_5 (h)	8	244.3	30.7	188.4	25.0	40.36	0.0079
E (psi)	8	80,757.4	11,975.3	86,403.9	11,010.1	0.97	0.3972
R (psi)	*6*	*1,713.0*	*143.8*	*1,721.3*	*116.0*	*0.02*	*0.9108*

[1] *Average of inner and outer samples.*

TABLE 2. *Summary of experimental results comparing directions of moisture movement.*

Variable	Number of samples	Inner		Outer		F value	Pr > F
		Mean[1]	SD	Mean[1]	SD		
σ_{T_1} (psi)	8	2,209.2	620.3	1,860.6	260.1	3.77	0.1002
σ_{C_3} (psi)	8	−4,354.0	789.9	−2,965.2	983.9	12.90	0.0115
Δ_1 (in.)	8	0.216	0.041	0.190	0.020	4.19	0.0867
Δ_3 (in.)	8	−0.372	0.032	−0.265	0.073	27.10	0.0020
t_1 (h)	8	111.0	50.4	138.0	45.8	22.09	0.0033
Θ_{t1-2} (h)	8	82.1	13.8	100.1	17.9	7.15	0.0369
t_2 (h)	8	193.1	53.5	238.1	61.8	19.04	0.0048
Θ_{t2-3} (h)	8	340.9	46.1	337.9	60.6	0.01	0.9187
t_3 (h)	8	534.0	80.9	576.0	71.4	1.43	0.2773
t_4 (h)	8	506.8	58.4	580.5	134.4	3.23	0.1225
t_5 (h)	8	199.0	30.6	233.6	41.5	10.04	0.0193
E (psi)	8	83,919.7	10,362.2	83,241.6	13,236.7	0.01	0.9126
R (psi)	6	1,740.2	111.9	1,694.0	142.8	0.36	0.5812

[1] Average of control and steaming samples.

(uncoated surface) was stretched, i.e., under maximum tension stress σ_{T_1}, and the core (coated surface) was under maximum compressive stress σ_{C_1}. Corresponding to σ_{T_1} are the drying deflection Δ_1, and time t_1 (Phase 1). At time t_2, the sample became straight, i.e., there was no drying deflection. Further drying (Phase 2) resulted in a reversal of curvature, and at time t_3, the maximum compressive stress σ_{C_3}, occurred on the uncoated surface and the corresponding drying deflection was Δ_3. Times t_4 and t_5 occurred when the average MC reached 30% and 16%, respectively. The time interval Θ_{t1-2} was the difference between t_2 and t_1; and Θ_{t2-3} was the difference between t_3 and t_2. The purpose of determining these two time intervals was to establish whether steaming had an affect on drying time at the maximum tension stress σ_{T_1}.

When the drying was completed, all samples were again tested on the Instron machine to determine the modulus of elasticity, E, followed by a bending strength test. Finally, all samples were oven-dried at 104 C for three days, and then weighed. The data were used to calculate the MC's during the drying period.

RESULTS

Maximum stresses

The maximum surface stresses differed significantly between the steamed and control samples. In the first phase, the maximum tension stress σ_{T_1} of the control group was about ¾ of that of the steaming group ($P = 0.02$). The difference between stresses due to directions was not significant ($P = 0.10$). If the blocks were divided into four parts, the stress for the inner direction in the steaming group was about 1.5 times as large as that of other groups (Figs. 5 and 6). Tension stress σ_{T_1} of the inner sample was less than that of the outer sample in the control group, but in the steaming group they were reversed.

Significant differences in compressive stress σ_{C_3} on the uncoated surface during the second drying phase were found for both methods (control and steaming) and directions (inner and outer wood), as shown in Tables 1 and 2. The steamed stress was about 4,213 psi and the unsteamed 3,107 psi, while the outer stress was 2,965 psi and the inner stress 4,354 psi.

Maximum deflections

The deflections Δ_1 for steaming and control, shown in Table 1, were significantly different ($P = 0.0127$) during the first phase; but in the second phase, the P value for Δ_3 was 0.0561 (Table 1), which was slightly over the critical value 0.05. From the SAS data, the steamed-inner Δ_1 (Fig. 6) was the highest, which indicated a trend similar to that observed for σ_{T_1}. The deflection of steamed-outer (Fig. 6) was

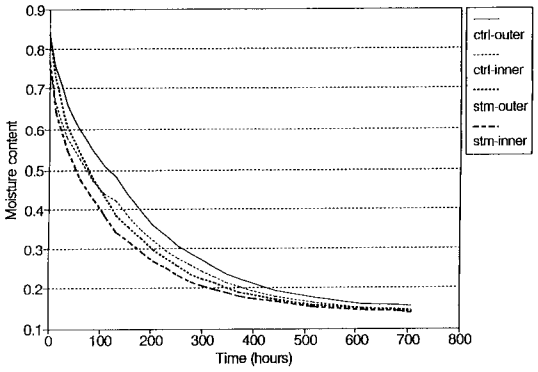

FIG. 7. Relationship between moisture content and drying time.

the second highest, while the outer and inner in the control group were almost the same in the first period.

Times and intervals

Time was recorded in hours from the beginning of the drying. Time t_1 was significantly different for both methods and directions (Tables 1 and 2). The steamed samples took 81 h, and the control samples 168 h to reach t_1. The inner samples took an average of 111 h, and outer samples 138 h. Time t_2 had the same trend as Time t_1. The steamed samples took 165 h, and the control samples 267 h; while the inner samples took 193 h, and the outer samples 238 h. Time t_3 for the control samples was approximately 20% higher than that for the steamed samples. However, the difference in t_3 between the inner and outer samples was only 8%.

The intervals Θ_{t1-2} and Θ_{t2-3} were not significant between steaming and control samples (Table 1). The interval, Θ_{t1-2}, was different for inner and outer samples but Θ_{t2-3} was not (Table 2). The Θ_{t1-2} for inner and outer samples was 82 h and 100 h, respectively, while Θ_{t2-3} for these samples was 341 h and 338 h, respectively.

The relationship between time and average MC is shown in Fig. 6. Time t_4, which was the time at which the average MC reached 30%, shows no significant difference between the control and steaming samples (Table 1), and between outer and inner samples (Table 2). However, time t_5, at which the average MC was 16%, shows a significant difference between steaming and control samples and between outer and inner samples.

Others

The modulus of elasticity and the bending strength showed no significant difference between the various types of samples, i.e., the test method and the sample location had no influence.

DISCUSSION

Steaming increased drying stress by up to 36%, while drying time decreased by 23% in red oak dried at 75% RH and 44 C from an average MC of 80% to 16%. Since moisture moved outward from the interior, the surface dried below the fiber saturation point (FSP), but was restrained from shrinking due to the adjacent interior which was still above FSP. As a result of this phenomenon, the wood on the surface layers was stretched, i.e., under tension, whereas the inner core was under compression. The moisture content of the steamed samples dropped faster than for the unsteamed samples; therefore the surface of the steamed samples shrank faster than the unsteamed. The greater the shrinkage difference between the surface and the interior of wood, the larger the stress. Casehardening occurs when the interior of the wood loses moisture as drying progresses, which begins to shrink when the moisture content gets below the FSP, causing a stress reversal if the surface layer has "set."

Normally, the maximum tension strength of southern red oak is about 480–510 psi (U.S. Forest Products Laboratory 1974). If the stress is greater than this amount, checks will occur. Figure 5 indicates that drying stresses of some samples were over 500 psi in the first 12 h, which was why some checks occurred on the surfaces of the samples.

The data show that casehardening occurred due to the loss of moisture on the surface of the wood. When a sample was placed inside

the drying chamber, its coated and uncoated surfaces were at the same temperature. Casehardening occurred only on the uncoated surfaces, due to drastic change in moisture below 30% MC. It occurred during the first interval (from the beginning to t_1), when the uncoated surface was under tension stress. During the second period, casehardening restrained the inner wood from shrinking, thus giving a tension stress to the inner wood. A higher tension stress on the surface caused greater casehardening, as a result of which tension stress developed in the inner wood. For this reason, the compressive stress was about 4,213 psi in the steamed wood and 3,107 psi in the unsteamed. The stress values obtained here should be somewhat less than the actual values. In fact, under constant stress, creep develops, which may decrease the stress. If stress is over a critical value (i.e., the maximum tensile strength perpendicular to the grain), the wood will crack. Therefore, the coating and bending method gives an indication that the wood may be destroyed if the value calculated from the data is large enough.

Bending stress is expressed in terms of E and r (Eq. 2). The statistical analysis indicated that there was a significant difference in drying deflection, but no significant difference in E between the control and the steaming groups. This means that the drying deflection can be used to indicate whether there is significant difference in drying stress. Figures 5 and 6 indicate parallel trends in the stress and deflection of the samples.

The two maximum stresses in the steamed samples occurred earlier than in the unsteamed samples. The first maximum stress of the inner direction occurred earlier than that of the outer. However, the time t_3 associated with the maximum compressive stress σ_{C3} was not significant. In addition, there was no difference for the interval Θ_{t1-2} and Θ_{t2-3} among the groups. This means that the time interval between the two maximum stresses was almost the same for the steamed and control samples, and for the inner and outer samples. The faster moisture loss at the beginning of the drying was a key factor for the development of drying stresses (Fig. 7).

This study shows that the coating and bending method may be used to study drying stresses. With this method, the effect of presteaming on drying stresses can be analyzed. Also, the drying stresses in inner and outer samples can be distinguished. Furthermore, this method can be used to analyze drying stresses at various drying conditions in different wood species. The advantages of the method presented here are: (1) the entire stress development within a sample can be observed and the drying stress can be determined whenever necessary; (2) the variances caused by cutting, which affect moisture distribution in the sample and result in deformation of the sample, can be eliminated; (3) the effect of environment in the testing room is avoided; and (4) measuring times are shortened. For further study, other methods may be used to determine the E values without requiring force application on the sample. The curved beam model may be used to determine the maximum stress during the first phase of the drying to obtain more accurate results. A method that utilizes image analysis to measure and analyze the drying checks and to relate checks to stresses may be used to improve this method.

CONCLUSIONS

Presteaming increased drying stress and decreased drying time in red oak when dried at 75% RH and 44 C from an average MC of 80% to 16%. The maximum drying stress of the steamed samples occurred earlier than that of the unsteamed samples due to faster moisture loss. Casehardening occurred on the surface due to a sharp change of moisture content when it was dried below the FSP. Steaming could be used to decrease drying time if drying stress, as well as the other accompanying defects such as checks, are of no consequence. Drying stresses were different in two directions (outer and inner), whether wood was steamed or not.

This study indicated that the coating and bending method was convenient to use for evaluating drying stresses in red oak. With this

method and a split-plot statistical model, the differences between steaming and control and between outer and inner two directions can be readily distinguished.

REFERENCES

ALEXIOU, P. N., A. P. WILKINS, AND J. HARTLEY. 1990a. Effect of pre-steaming on drying rate, wood anatomy and shrinkage of regrowth *Eucalyptus pilularis* SM. Wood Sci. Technol. 24:103–110.

———, J. F. MARCHANT, AND K. W. GROVES. 1990b. Effect of pre-steaming on moisture gradients, drying stresses and sets, and face checking in regrowth *Eucalyptus pilularis* SM. Wood Sci. Technol. 24:201–209.

CAMPBELL, G. S. 1961. The value of presteaming for drying some collapse-susceptible Eucalyptus. Forest Prod. J. 11(7):343–347.

CHOONG, E. T., AND S. ACHMADI. 1989. Effect of steaming and hot-water extractives on the longitudinal permeability of several Indonesian woods. J. Forest Res. Devel. 5(2):33–36. (Text in Indonesian, with English summary.)

FOGG, P. J. 1969. Longitudinal air permeability of four species of southern pine wood. Wood Sci. 2(1):35–43.

HASLETT, A. N., AND J. A. KININMONTH. 1986. Pretreatments to hasten the drying of *Nothofagus fusca*. N.Z. J. Forest Sci. 16:237–246.

KUBINSKY, D. 1971. Influence of steaming on the properties of *Quercus rubra* L. Wood. Holzforschung 23(1): 78–83.

KUEBLER, H. 1960. Drying stresses and stress relief in thin sections of wood. Rep. 2164, USDA Forest Prod. Lab., Madison, WI.

MCMILLEN, J. M. 1955. Drying stresses in red oak: Effect of temperature. Forest Prod. J. 5(4):230.

———. 1968. Transverse strains during drying of 2-inch ponderosa pine. USDA Forest Serv. Res. Paper FPL-83, Madison, WI.

RICE, R. W. 1988. Mass transfer, creep, and stress development during the drying of red oak. Ph.D. dissertation, Virginia Polytech. Inst. & State Univ., Blacksburg, VA.

SCHNIEWIND, A. P. 1960. On the nature of drying stresses in wood. Holzforschung. 12(6):161–168.

———. 1963. Mechanism of check formation. Forest Prod. J. 13(11):475–480.

SIAU, J. F. 1984. Transport processes in wood. Springer-Verlag, New York, NY. Pp. 98–100.

SIMPSON, W. T. 1975. Effect of steaming on the drying rate of several species of wood. Wood Sci. 7:247–255.

TIMOSHENKO, S. 1955. Strength of materials. Part I—Elementary theory and problems. D. Van Nostrand Company, Inc., New York, NY. Pp. 362–370.

U.S. FOREST PRODUCTS LABORATORY. 1974. Wood handbook—Wood as an engineering material, USDA Agric. Handb. 72, rev., Washington, DC.

YOUNGS, R. L., AND C. B. NORRIS. 1958. A method of calculating internal stresses in drying wood. Rep. 2133. USDA Forest Prod. Lab., Madison, WI.

———. 1959. New method of calculating internal stresses in drying wood. Forest Prod. J. 9(10):367–371.

ASSESSING INTERNAL HURRICANE DAMAGE TO STANDING PINE POLETIMBER

Timothy D. Faust
Associate Professor

Mark M. Fuller
Graduate Assistant

D. B. Warnell School of Forest Resources
University of Georgia
Athens, GA 30602

Robert H. McAlister
Forest Products Technologist

and

Stanley J. Zarnoch
Mathematical Statistician

U.S. Forest Service
Southeastern Forest Experiment Station
Forestry Sciences Laboratory
Athens, GA 30602

(Received May 1993)

ABSTRACT

Two test methods were used to assess type, location, and degree of internal stem damage to standing pine poletimber (5.0–8.9 in. diameter at breast height, DBH) caused by Hurricane Hugo. A total of sixty trees [15 from each of the four Forest Inventory Analysis (FIA) damage classes] were taken from three sites in the Francis Marion National Forest. Internal damage was expected in the form of ring shake and compression failure. Five stem sections (A through E) were taken from each tree at different heights. From each section, specimens were cut from four quadrants (Tension, Compression, Left, and Right) relative to the wind direction during the storm for toughness and tension perpendicular to the grain testing. A total of 2,147 toughness specimens were tested. A total of 273 specimens were tested in tension perpendicular to the grain. The dependent variables analyzed were toughness, tension strength, and specific gravity with FIA damage class as the whole plot factor.

Although there was an increasing trend in toughness from Damage Class 1 through 4, analysis of variance showed damage class not to be a significant effect on toughness. Stem section and quadrant were found to be significant on toughness. Much of the variation in toughness due to stem section may be attributed to the effects of juvenile wood differences with tree height. Also a high occurrence of reaction wood in Quadrant C (side of the tree away from the wind) would contribute to lower toughness strength. Similarly, specific gravity (SG) values showed an overall increase from Damage Class 1 through 4. Specific gravity of Damage Classes 1 and 4 was found to be significantly different. Statistical analysis showed no apparent relationship between damage class and tension strength perpendicular to the grain.

The lack of evidence for internal damage is relatively unimportant compared to the evidence of change in the wood properties from the formation of reaction wood. In leaning stems (FIA Damage Classes 2, 3, 4), reaction wood should continue to form. In straight trees, reaction wood formed in

Wood and Fiber Science, 26(4), 1994, pp. 536–545

the two growth seasons following the storm, but it is unclear whether it will continue to form. The results lead to the conclusion that stands with leaning stems should be harvested and replanted.

Keywords: Storm damage, poletimber, toughness, tension strength, FIA damage class.

INTRODUCTION

On September 22, 1989, Hurricane Hugo struck the South Carolina coast with sustained winds of 135 mph and gusts up to 175 mph. In the fall of 1989 the Forest Inventory and Analysis (FIA) Research Work Unit at the Southeastern Forest Experiment Station began a special inventory of the areas damaged by Hugo. A classification system was needed that would assign hurricane-damaged trees to discrete categories based on the amount of inflicted damage. The objective was to "provide a reasonable description of damage severity" and estimate the probability of mortality in the near future (Sheffield and Thompson 1992). The criteria for damage class were empirically derived, and a system of four damage classes emerged (Table 1).

Hugo caused extensive immediate damage to the Francis Marion National Forest with an estimated 75% of all marketable trees (DBH > 5.0) on the ground (Ehinger 1990). The FIA damage class system was devised and implemented in an effort to quantify the damage inflicted on the forest resource and to help foresters decide on the proper management strategies for the remaining stands. However, there were questions still unanswered. What possible long-range effects did Hugo have on the remaining 25%? In the case of poletimber (5.0–8.9 DBH), a question that naturally arose was "Should storm damaged poletimber be allowed to mature into sawtimber?" Internal damage to the stem in the form of ring shake and compression failures could reduce the utility of these trees for high-value products such as structural lumber. Such damage may not be evident until processing of the lumber is completed, adding further to the costs of utilizing these trees. Also, if stems with internal damage do enter the market, a significant liability risk

TABLE 1. *Summary of study variables.*

Variable	Levels
Wind Damage Class (FIA)	1—High risk of mortality in the near future. Tree lean is greater than 45°.
	2—Moderate risk of mortality, damage may degrade value for use as sawlogs or plylogs. Tree lean 15° to 44°.
	3—High probability of survival, risk of reduced growth and value degrade is minimal. Tree lean is less than 15°.
	4—No obvious wind damage. Tree is essentially straight.
Quadrant	T—Side of tree facing the wind during the storm (under tension stress).
	C—Side of tree opposite the wind direction (under compression stress).
	L—Left side of tree facing the wind (under shear stress).
	R—Right side of tree facing the wind (under shear stress).
Section (tree height)	A—Breast height
	B—3 feet below critical stress point
	C—Critical stress point (CSP)
	D—3 feet above critical stress point
	E—One foot below base of crown
Replicates	15 trees per damage class
Response variable	**Procedure**
Mechanical Testing	Toughness (ASTM D143-93)
	Tension perpendicular to the grain (ASTM D143-93)
Reaction Wood	Present or absent

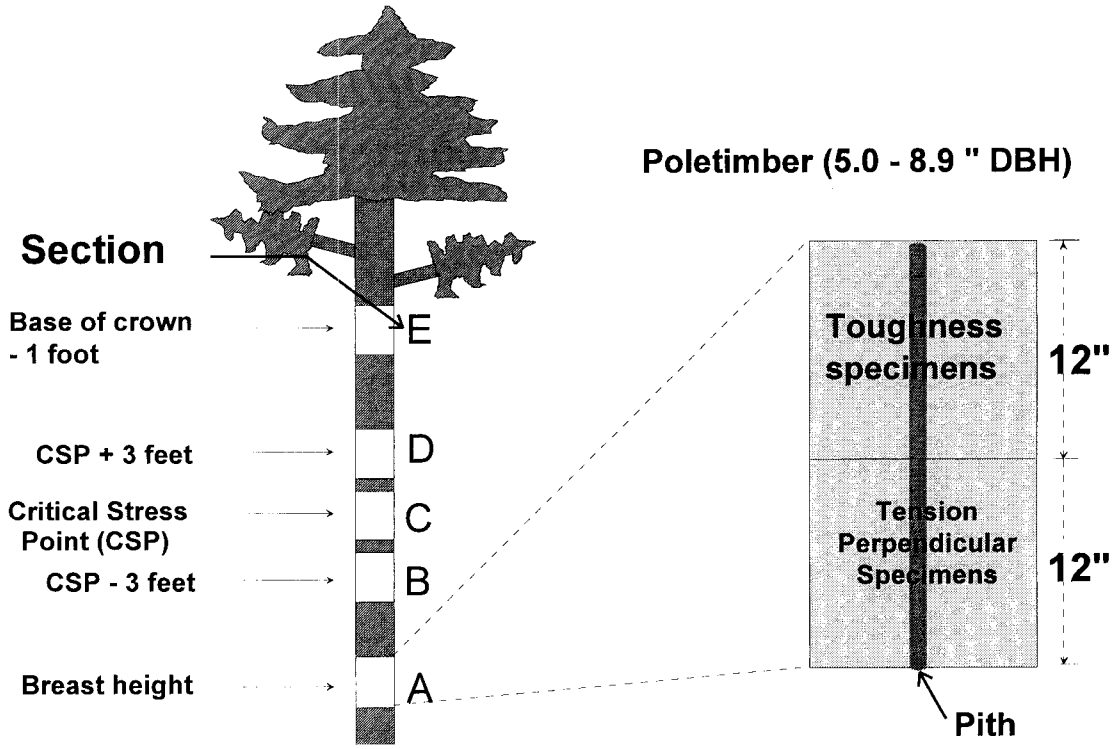

FIG. 1. Location of sections within the tree stem.

due to increased failure rates will occur. Thus, sawtimber from internally damaged stems should be sold for pulp chips, a lower value product.

Traditionally storm damage has been classified in terms of visual damage such as snapping of the trunk, uprooting, and bending (Webb 1988). Similarly, Mayer (1988) defined four types of storm damage as: stem breakage, stock (base of stem) breakage, root breakage, and tree throw. There have been other studies that differentiate only between tree throw and stem breakage. Although it is apparent that high winds could cause internal damage to tree stems, little information is available on the subject. The FIA damage class system that provides tree classification in terms of apparent storm damage and potential mortality allows only for conjecture as to the degree of internal stem damage. Although the FIA damage class system is only approximate, it is a very practical classification system, which brings us a step closer to understanding the nature of storm-damaged timber. What is needed is correlation between this visual damage classification system and actual internal damage as measured by mechanical testing and visual observation.

OBJECTIVE

The objective of this study was to assess type, location, and degree of internal stem damage to standing pine poletimber and to relate this damage to the FIA damage classes. Internal damage in the form of compression failures, ring shake, and reaction wood were examined by toughness tests, tension perpendicular to the grain tests, and visual observation of reaction wood formation, respectively. Wood specific gravity was measured at each location within the tree and analyzed with the mechanical properties. A summary of the study variables is presented in Table 1.

METHODS AND MATERIALS

A total of sixty poletimber-sized trees consisting of longleaf pine (*Pinus palustris,* Dim.) and loblolly pine (*Pinus taeda,* L.) was taken from natural stands in the Francis Marion National Forest near McClellanville, South Carolina, in August of 1991. To avoid the possibility of site bias, the trees were taken from three different sites. A member of the FIA research work unit helped to select the trees for the study, which consisted of 15 trees in each FIA damage class. Five stem sections were cut from each selected tree, as described below, and brought to the laboratory for further processing. In an attempt to obtain the best group of samples from each stem, it was first necessary to determine the point along the stem most likely to sustain wind damage—the critical stress point (CSP). Observations in the field were used to determine the critical stress point as the average height of broken poletimber-sized stems in close proximity to the sample tree. Using this value of critical stress point, the five 24-in. stem sections (Fig. 1) were cut on center at:

A— breast height
B— 3 feet below critical stress point
C— critical stress point (CSP)
D— 3 feet above critical stress point
E— one foot below base of crown

It was expected that internal damage to the trees was in the form of compression failures, ring shake, and reaction wood. Compression failures would be indicated by toughness testing as specified in ASTM D-143-93. Ring shake would be indicated by tension perpendicular to grain tests as specified in ASTM D-143-93, while the presence of reaction wood was determined by visual inspection of the outer 2 growth rings.

The five stem sections were cross-cut into two 12-in. sections. Toughness specimens were taken from one of these 12-in. sections and tension perpendicular specimens from the other. Toughness specimens were taken from the storm and the other 2 were consequently perpendicular to the wind direction. The quadrants parallel to the wind direction experienced the severest tension stress on the side of the tree facing the wind and severest compression stress on the side away from the wind. Toughness and tension perpendicular specimens were cut from each quadrant. Only straight-grained specimens free of knots were kept for testing. Reaction wood was present in many of the Position 1 (specimen closest to cambium and bark) toughness specimens. Care was taken during processing to remove as little wood from the bark side of the specimens as possible. Occurrence of reaction wood was visually observed in the outer 2 growth rings and recorded for each quadrant and section of each tree.

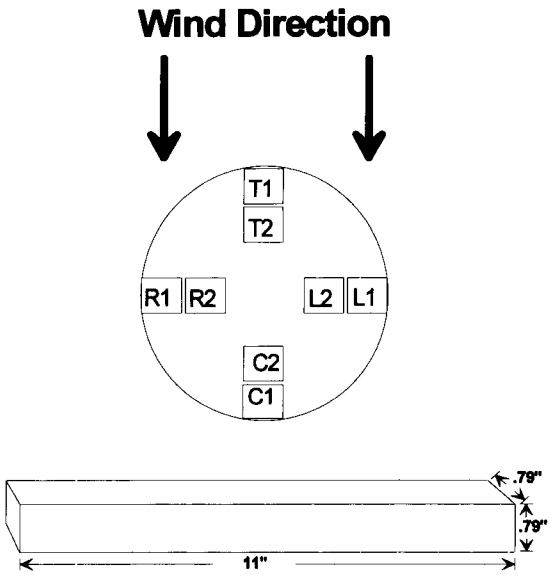

FIG. 2. Orientation of Toughness specimens in the tree stem.

Toughness specimens were taken from Position 1 and 2, except in the higher sections of some stems from smaller diameter trees, where it was not possible to obtain both specimens (see Fig. 2). The toughness testing was done on 1,821 samples with a Wiedemann-Baldwin Impact machine. Specific gravity was calcu-

To test for ring shake, it was necessary to stress the entire length of the tension perpendicular to the grain specimen since the location of the ring shake was unknown. The position and orientation of the specimens are shown in Fig. 3. Since the traditional throated tension perpendicular specimen described by ASTM D143 (ASTM 1993) does not stress the entire length of the specimen, the specimen was modified by using high strength epoxy to bond hard maple blocks to the bark and pith faces of the tension perpendicular to the grain specimens. Appropriate hardware was bolted to the maple blocks and tested as per ASTM standards. Only sections at DBH and critical stress point were tested since there was a higher probability of ring separation due to shear stress in these specimens. The tension perpendicular testing was done on 273 specimens with a Tinius Olsen 5000 universal testing machine.

EXPERIMENTAL DESIGN

This study was analyzed as a split-plot design where the whole-plot factor was the four tree damage classes each represented by a subsample of trees. Whole-plot replication was by means of blocks defined as the three sites. The subplot factor was a factorial combination of the five tree sections by four quadrants of each tree. The design was unbalanced, which led to a complicated analysis. At the whole-plot level, there were no trees in one damage class for one of the sites. This resulted in a missing cell and, hence, only 5 degrees of freedom for the site by damage class effect instead of the typical $2 \times 3 = 6$. In addition, the number of trees sub-sampled in each site by damage class was unequal. At the subplot level, there were several missing observations at various section by quadrant treatment combinations. Due to the unbalanced nature of this study, approximate F-tests were performed in the typical split-plot design fashion using the whole-plot and subplot error terms. The expected mean squares obtained from SAS (SAS Institute Inc. 1988) indicated that these tests were close to those in the typical balanced situation. Mean separation tests were performed on the main factor effects with Tukey's test. General mean comparisons were not performed since they would require synthesized error terms using Satterthwaite's procedure, which was not attempted because of the complexity of the design.

RESULTS AND DISCUSSION

Toughness and specific gravity analysis

Results from the analysis of variance on toughness and specific gravity are shown in Table 2, while treatment means and Tukey's multiple comparisons for all main effects are shown in Table 3. The analysis was performed on the Position 1 and Position 2 specimens both separately and combined.

The effect of juvenile wood is evidenced by the lower values of toughness and specific gravity of the Position 2 specimens as compared to the Position 1 specimens. The Position 2 specimens should exhibit more juvenile properties of lower toughness and specific gravity because of their closer proximity to the pith.

FIA damage class effects.—The damage class factor was not quite significant for toughness ($P = 0.07$). Generally, toughness decreased with increasing damage (i.e., highly damaged trees had lower toughness). Similarly, Tukey's comparison tests showed a trend of decreasing specific gravity with increasing degree of damage. Damage class effects on specific gravity were significant at the 0.05 level. This trend supports the conclusion that trees with higher specific gravity and hence higher strength were better able to survive the effects of the storm. Perhaps this trend is due to the development of root systems. A better root system provides better support for the tree stem and is important in resisting windthrow and root upheaval. It seems logical that they develop denser wood tissue, since better developed root systems provide more nutrient and moisture uptake.

The interaction of damage class quadrant and also had a significant effect on toughness ($P = 0.02$). Figure 4 illustrates this interaction. The highest toughness values are concentrated

TABLE 2. *Results from the analysis of variance (P-values)*[1] *based on a split-plot design.*

Source	Positions 1 and 2			Position 1			Position 2		
	df[2]	Toughness	SG	df	Toughness	SG	df	Toughness	SG
Site	2	—[3]	—	2	—	—	2	—	—
Damage Class (DC)	3	0.07	0.05	3	0.08	0.07	3	0.17	0.14
Site × DC	5	—	—	5	—	—	5	—	—
Tree (Site × DC)	49	—	—	49	—	—	49	—	—
Sect	4	0.00	0.00	4	0.00	0.00	3	0.00	0.00
Quad	3	0.00	0.00	3	0.00	0.00	3	0.00	0.26
Sect × Quad	12	0.42	0.06	12	0.07	0.66	9	0.06	0.95
DC × Sect	12	0.55	0.31	12	0.11	0.00	9	0.78	0.77
DC × Quad	9	0.02	0.59	9	0.00	0.11	9	0.98	0.04
DC × Sect × Quad	36	0.90	0.93	36	0.88	0.57	27	0.80	0.94
Error (b)	1,015	—	—	1,011	—	—	554	—	—
Total (corrected)	1,150			1,146			673		

[1] Probability that main effect or interaction has no effect on the measured response.
[2] Degrees of freedom.
[3] —Not of interest or cannot be calculated.

near the tension (T) quadrant, the lowest values near the compression quadrant, and intermediate values are predominantly associated with the left and right quadrants. The trend is increasing toughness from Damage Class 1 to 4. The tension quadrant at Damage Class 4 caused the interaction effect by not having higher toughness than the other quadrants. This may be explained by the low occurrence of reaction wood and higher specific gravity in this combination of damage class and quadrant.

The purpose of the toughness test was to detect compression failures occurring on the transverse axis of the wood. While a trend in toughness with damage class was observed, it was probably due to the significant trend in specific gravity rather than the detection of internal damage. Compression failures were observed in several samples that were tested. However, these compression failures were extremely localized and their effects lost in the large sample of specimens.

Section and quadrant effects.—The section

TABLE 3. *Means for toughness and specific gravity with Tukey's mean separation.*[1]

Factor		Positions 1 and 2		Position 1		Position 2	
		Toughness (in-lb)	SG	Toughness (in-lb)	SG	Toughness (in-lb)	SG
Damage Class	1	278a	0.526b	295a	0.556b	246a	0.471a
	2	313a	0.557ab	322a	0.582ab	296a	0.518a
	3	306a	0.560ab	322a	0.586ab	286a	0.517a
	4	321a	0.589a	329a	0.605a	307a	0.565a
Section	A	347a	0.599a	358a	0.630a	331a	0.551a
	B	305b	0.574b	323b	0.604b	280b	0.524b
	C	301bc	0.558c	314bc	0.588c	275b	0.507c
	D	284cd	0.537d	304c	0.566d	242c	0.485d
	E	283d	0.516e	283d	0.516e	—	—
Quadrant	T	354a	0.547c	383a	0.577c	315a	0.512b
	L	308b	0.569a	314b	0.584ab	296ab	0.531a
	R	296b	0.562b	301b	0.579bc	281b	0.526a
	C	261c	0.556b	270c	0.590a	251c	0.515b

[1] Means in the same Factor for a given variable not followed by the same letter are significantly different at the $\alpha = 0.05$ level using Tukey's test.

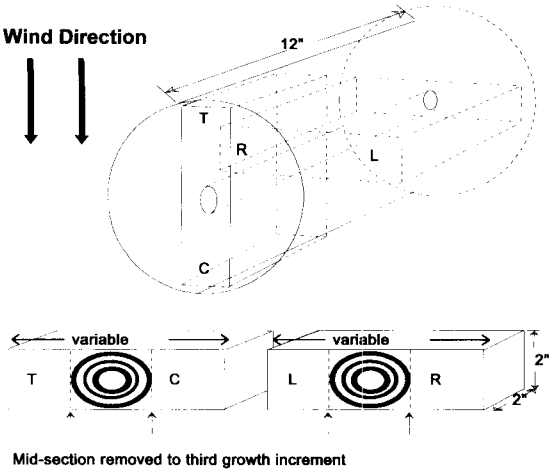

FIG. 3. Orientation of tension perpendicular specimens in the tree stem.

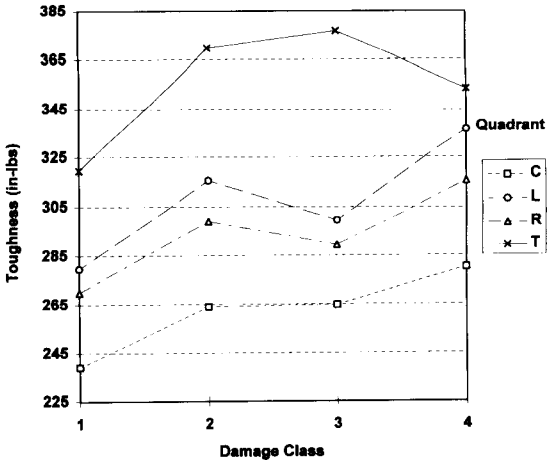

FIG. 4. Interaction of Damage Class and Quadrant.

variable reflects tree height and shows significant effects on toughness as expected (P = 0.00). The lower toughness associated with juvenile wood is evidenced by decreasing toughness with increasing section height. Toughness specimens become closer to the pith and tree crown higher up the stem. These specimens have wood tissue with more juvenile characteristics. The trend is identical for specific gravity, which is a primary measure of juvenility.

Quadrant had a significant effect on toughness and specific gravity (P = 0.00). Quadrant indicates the location of the specimen around the tree stem relative to the wind direction during the storm. The windward side of the stem (T) shows the highest toughness, while the side of the stem undergoing compression (C) showed the lowest toughness. The L and R quadrants were always intermediate in toughness and closest in actual value. This observation is logical since the L and R quadrants experienced similar stresses. The trends are more complex for specific gravity with quadrant. It would be logical that specific gravity would be constant around the tree stem at a specific tree height. Therefore, we would not expect the quadrant to have a significant effect on specific gravity. The T quadrant of the section was significantly lower in specific gravity than the other quadrants at Position 1 and 2. This is contrary to accepted relationships between wood strength and specific gravity. However the occurrence of reaction wood offers some explanation of why this trend occurs. Reaction wood has higher specific gravity but lower strength.

Occurrence of reaction wood

Low average toughness values of the compression side specimens may be attributed to the high occurrence of reaction wood. Figure 5 illustrates the frequency of reaction wood occurrence in damage class by quadrant. The C quadrant had highest occurrence of reaction wood as would be expected. However, extensive reaction wood was occurring on Damage Class 4 trees, which were standing straight. Residual stress from the storm must have triggered reaction wood formation in the following growing season. Considering toughness values with quadrant as a factor, compression side toughness values were considerably lower than all others due to partial rings of reaction wood, which in many cases had been growing since the storm. In some cases reaction wood extended into the left and right quadrants. The overall effect of reaction wood in the left and right quadrants, however, was less pronounced for two reasons. There were fewer occurrences of reaction wood in these quadrants since the

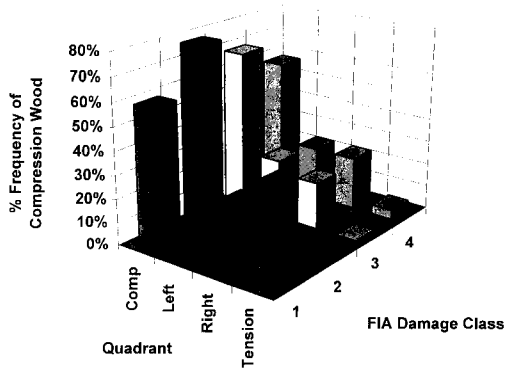

FIG. 5. Reaction wood frequency for quadrant by damage class.

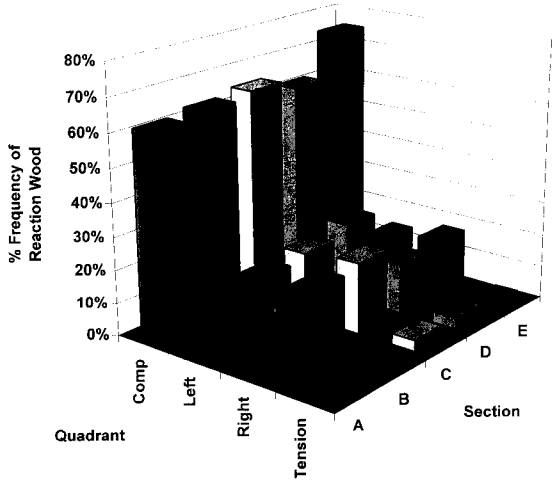

FIG. 6. Reaction wood frequency for quadrant by stem section.

reaction wood bands did not always extend into the left and right quadrants. Secondly, the reaction wood bands generally became thinner as they proceeded away from the compression quadrant, so the strength reduction due to the reaction wood band was diminished in the left and right quadrants.

Perhaps more importantly, reaction wood was observed in trees of all four damage classes. This is significant since even trees appearing to have no wind damage (i.e., not leaning), those of Damage Class 4, have a frequency of reaction wood as high as Damage Class 1. Stress from the wind has caused formation of reaction wood in the two growing seasons after the storm even in trees that are straight and have no visible damage. The formation of reaction wood in leaning stems should continue until harvesting; however it is unknown how long reaction wood will continue to form in Damage Class 4 trees that are essentially straight. The formation of reaction wood occurred almost uniformly over all tree heights as shown in Fig. 6.

Evidence of ring shake

Observations of failures in tension perpendicular to the grain showed no evidence of ring shake, which was confirmed by the test results of tension strength perpendicular to the grain. There were no significant differences found in tension strength for damage class or quadrant. The section variable was significant with Section A significantly higher in tensile strength than Section C (see Table 4). This trend is consistent with observations of decreasing toughness with tree height. Table 5 shows tension strength means for damage class by quadrant. It is noted that these average tension strength values are consistent with the literature (Wood Handbook 1987).

TABLE 4. *Mean tension strength values for Damage Class by stem section.*

Damage class	Section		Damage class means[1]
	A	C	
1	500.9	480.6	488.8
2	518.4	514.9	516.3
3	519.9	457.4	485.4
4	504.5	490.8	496.8
Section means[2]	511.5	485.5	496.5

[1] Damage class means were not significantly different at the 0.05 level.
[2] Section means were significantly different at the 0.05 level.

TABLE 5. *Mean tension strength values for Damage Class by Quadrant.*

Damage class	Quadrant				Damage class means
	C	T	L	R	
1	505.9	509.9	487.7	456.3	488.8
2	491.7	503.4	557.0	511.8	516.3
3	471.2	499.2	488.0	483.3	485.4
4	499.4	490.3	517.4	486.5	496.8
Quadrant means[1]	490.7	500.2	512.1	483.1	496.5

[1] Quadrant means were not significantly different at the 0.05 level.

SUMMARY AND CONCLUSIONS

The results of the study offer inconclusive evidence that the FIA damage classes are indicative of internal damage to storm-stressed trees. It was expected that compression failures and micro-fractures would be found to have a varying effect on toughness and that ring shake would have a similar effect on tension perpendicular to the grain in a manner consistent with the FIA damage classes; but this relationship was marginally significant for toughness strength and nonexistent for tension strength perpendicular to the grain. Several interesting patterns did arise however. Specific gravity was a factor in determining the extent of damage. The specific gravity measurements made on the toughness specimens do offer some explanation as to the nature of wind damage. In particular, with damage class as the whole plot factor, the specific gravity values of Position 1 specimens fall into a pattern. Here again we consider only the Position 1 specimens to avoid the highly variable juvenile wood present in most Position 2 specimens. Moving from Damage Class 1 to 4 specific gravity shows an increasing trend and significantly different means between Damage Classes 1 and 4 at the 0.05 level using Tukey's test. The trees most resistant to wind damage, those classified in Damage Class 4, were found to have the highest average specific gravity. Thus there is a negative relationship between wind damage, as defined by the FIA damage class system, and wood density. Other studies (Foster 1988 and Studholme 1989 for instance) have shown this negative relationship between sustained wind damage and specific gravity. The variation of toughness and specific gravity could be explained in part by the occurrence and extent of reaction wood observed. The relatively higher specific gravity and lower strength of reaction wood will impact the utilization of these trees.

In conclusion, with dwindling timber resources, it will become more important to correctly determine the short-term as well as long-term effects of catastrophic storms on our timber resources. While the FIA visual damage classification system was developed to predict risk of mortality, it has been shown not to be an indicator of internal damage as measured by loss of mechanical properties. FIA damage class was a good indicator of the wood quality in the tree as measured by specific gravity.

The high occurrence of reaction wood as measured in this study indicates that residual stress from the storm caused reaction wood in all damage classes. It is likely that reaction wood formation will continue in leaning stems (Damage Classes 1 to 3). Further study is needed to determine if non-leaning trees will continue reaction wood formation. The formation of reaction wood appears to be the major damage to trees still standing after the storm.

ACKNOWLEDGMENTS

Support for this study was provided by the Southeastern Forest Experiment Station, USDA Forest Service, Asheville, NC. Gratitude is expressed to Michael Thompson (Forester, Forest Inventory and Analysis, Asheville, NC) for evaluation of the standing poletimber in the Francis Marion National Forest.

REFERENCES

AMERICAN SOCIETY FOR TESTING MATERIALS. STANDARD D143-93. 1993. Toughness and tension perpendicular to the grain procedures. Philadelphia, PA.

EHINGER, L. H. 1990. Hurricane Hugo damage. Annual Conference of the International Society of Arboriculture, August 1990, in Toronto, Ontario.

FOSTER, D. R. 1988. Species and stand response to catastrophic wind in central New England, USA. J. Ecology 76:135–151.

MAYER, H. 1988. Windthrow. Philosophical Transactions of the Royal Society of London. Series B, Biological Sciences. 1989, 324:1223, 267–281.

SHEFFIELD, R. M., AND M. T. THOMPSON. 1992. Hurricane Hugo—Effects on South Carolina's forest resource. Southeastern Forest Experiment Station Research Paper SE-284.

STUDHOLME, W. P. 1989. Windthrow on the Canterbury Plains. Workshop on wind damage in New Zealand exotic forests. FRI bulletin 146. Forest Research Institute, Ministry of Forestry, PV 3020, Rotorua, New Zealand.

SAS INSTITUTE, INC. 1988. SAS/Stat Users Guide, Release 6.03 Edition, Cary, NC: SAS Institute, Inc. 1,028 pp.

USDA FOREST PRODUCTS LABORATORY. 1987. Wood handbook: Wood as an engineering material. Agric. Handbk. 72, Washington, D.C. 466 pp.

WEBB, S. L. 1988. Windstorm damage and microsite colonization in two Minnesota forests. University of Minnesota, Department of Ecology and Behavioral Biology, Minneapolis, MN.

THE EFFECT OF LOG ROTATION ON VALUE RECOVERY IN CHIP AND SAW SAWMILLS

Thomas C. Maness
Assistant Professor

and

W. Stuart Donald
Graduate Research Assistant

Department of Wood Science
Faculty of Forestry
University of British Columbia
Vancouver, BC V6T 1Z4

(Received April 1993)

ABSTRACT

Advances in three-dimensional scanning techniques and computer optimization permit real time solution and implementation of optimal log rotation before it is fed into the chipper heads. A random sample of 834 S-P-F logs from the interior of British Columbia were examined using simulation to determine the effects of log rotation strategies on value recovery for a small log Chip and Saw. Both log sweep and cross-sectional eccentricity are shown to cause significant reductions in value recovery. Eight rotation placements from 0° to 315° were studied to determine if a single rotational placement could be found that performs best. On average, the "horns up" position (0° rotation) was found to significantly outperform all others in maximizing value recovery. The ability to rotate each log into the optimal position produced significant benefits. The benefits were more highly related to the degree of cross-sectional eccentricity present in the log rather than the degree of sweep present in the log.

Keywords: Sawmilling, sawing optimization, lumber manufacturing, computer-aided manufacturing.

INTRODUCTION

Loss of value recovery in sawlog conversion to lumber can be attributed to several geometric factors. Diameter, log roundness, sweep and crook, taper and length all play an important part in determining the positioning of the log in relation to the saws to obtain the highest value recovery. Modern setworks with double-length infeeds in Chip and Saw (CNS) sawmills are capable of scanning the logs, determining the optimal set position, and executing the optimal decision in seconds. In the past, sawing optimization systems have set the log in relation to the saws without regard to rotating the log into the optimal position. This paper explores the costs and benefits from determining and setting the correct rotation position in a small log CNS mill.

BACKGROUND

Early sawing optimization systems focused solely on log diameter, length, and taper as principal components in determining the log set (Hallock and Lewis 1971; Shi et al. 1990). The main assumptions in this type of analysis are that the shape of the log cross section is the same at all points along the log (and usually circular), and that the log exhibits no sweep, or deviation from a straight line along the log's length. When these assumptions are made, the rotation of the log can have no effect on the yield whatsoever. Steele et al. (1987) found that when using these assumptions, the complex three-dimension analysis can be replaced by a much simpler and faster method that predicts the optimal Best Opening Face position well.

Wood and Fiber Science, 26(4), 1994, pp. 546–555

However, it is well known in the sawmill that the sweep of the log and its cross-sectional shape play a very important part in determining the optimal set position. It is also known that these factors have a particularly important negative impact on value recovery with smaller diameter logs (Wang et al. 1992). Simplified methods that predict the optimal BOF position may not perform well in the sawmill, particularly with decreasing log size.

Currently there are three methods for dealing with log sweep at a CNS. The most technologically advanced method involves curve sawing, in which a two-sided cant is sawn parallel to curve in the log (Hasenwinkle et al. 1987; Lindstrom 1979). Curve sawn logs are generally sawn "horns down" to produce a two-sided cant, and then the cant is sawn with a variable curve linebar.

A second, less expensive method, involves choosing a rotation position in which, on average, the highest value yield can be obtained from sweepy logs. While opinions differ on this ideal position, generally the log is sawn either "horns up" (concave-up or 0 degree rotation), "horns down" (180°) or "horns up 45" (45°). For illustration, Fig. 1 shows a side view of both "horns up" and "horns down" cant sawing. Of these positions, machinery designers favor the "horns down" position as the most accurate and simplest mechanism to hold the log in place as it is being sawn. Once the ideal position is chosen, all logs are rotated at the infeed of the machine to this position prior to sawing.

Both of the above methods select the rotational position based primarily on sweep rather than the cross-sectional eccentricity of the log. A third sawing method would involve optimizing setworks that calculate the correct rotation for each log and automatically set it into this position as it is being sawn. The advantage of this setworks system is that both sweep and cross-sectional eccentricity can be taken into account when determining the sawing position. This method is now possible due to two new technological advances in the sawmilling industry: 1) the availability of real shape scanning devices at the headsaw; and, 2) the enormous increases in computer power that enable real time solution of complex real-shape logs.

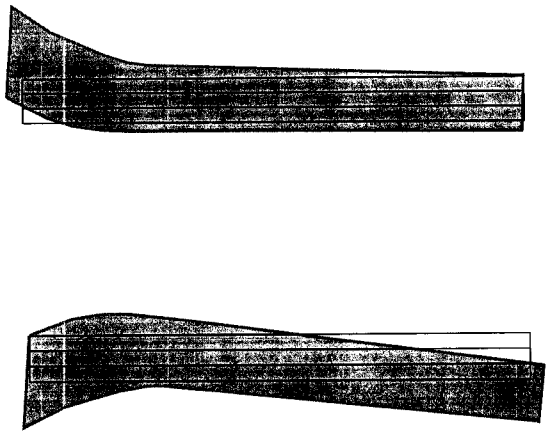

FIG. 1. "Horns up" (top) and "horns down" (bottom) sawing position for log with asymmetrical sweep pattern.

The majority of lumber production from CNS mills is sawn using method 2. The technology currently exists to implement method 3, but uncertainty concerning the economic benefits of such a system may impede its widespread implementation. Therefore, objectives of this study are:

1. determine if an ideal rotation position exists which on average maximizes the value recovery from a population of small diameter logs from a typical CNS sawmill; and,
2. estimate the economic benefits from calculating the optimal rotation and setting the log accordingly prior to sawing.

METHODOLOGY

Sawing simulation

To determine the actual optimal rotation for a sawlog it would be necessary to saw the log in many different rotations and calculate the value recovery from each position. Since this is impossible, another solution is to use computer simulation to saw the log. To satisfy the objectives of this study, the simulation package used must be able to look at the three-dimensional geometry of actual scanned logs,

TABLE 1. *Summary statistics on the 834 logs used in the study.*

Variable	Minimum	Maximum	Mean	SD
Dia—Small end diameter	3.40	12.95	8.40	2.49
Len—Log length	8.20	20.60	15.46	3.55
Tpr—Log taper	0.02	4.17	1.11	0.61
Swp—Log sweep	0.15	2.03	0.56	0.34
Ecc—Log eccentricity	0.01	5.70	0.48	0.62

perform sawing cuts with realistic constraints imposed by the CNS sawing system, and allow carefully controlled positioning of the log in relation to the saws. For these reasons, the sawing simulator SAWSIM was chosen to determine the value recovery from each set position.

The logs used in this study were randomly chosen from a log database maintained at the University of British Columbia containing two-axis scan data from thousands of logs taken in interior British Columbia (BC) small log sawmills. Two-axis scanning is the scanning method used when logs are modeled as elliptical in cross section. Although it is understood that this type of log modeling results in inaccuracies (Mongeau et al. 1993), it was the best method of modeling applied in the industry available to provide data for the purpose of this study. The sampling procedure was stratified to cover log diameters in the range of 3 in. sed (small end diameter) to 13 in. sed, and log lengths from 8 ft to 20 ft. The sample was not stratified with respect to taper and sweep. Summary statistics for the 834 logs used in the study are shown in Table 1.

A set of cross-sectional cant profiles was created to mimic the possible set of profiles available to a four-side chipping profiling machine without band saws (no side boards) for the purpose of producing dimension lumber. It was assumed that the system would use a 0.5- by 1-in. "multispline" combination to guide the log through the machine center. This assumption reflects the trend towards this practice as opposed to the use of a 2 × 4 spline board.

Each profile represents a stack of lumber separated by saw kerfs. Profile widths ranged from 4 to 12 in. nominally. Profile heights start with the combination of the heights of one 2-in. board up to the height of seven 2-in. boards, with the top board of each profile alternating between a 1-in. and a 2-in. board as the profile heights increase. It was assumed that 1-in. boards would be recovered in 4- and 6-in. widths only.

Up to eight possible profile patterns were created for each of four log diameter ranges. Table 2 lists the diameter ranges used and their assigned profiles. The profile codes are interpreted as follows: the rightmost digit if equal to 1 represents the existence of a 1-in. top board in the stack, a zero indicates all 2-in. boards in the stack; the second rightmost digit represents the number of 2-in. boards in the stack; the remaining digits to the left indicate the nominal width of the profile; cns is the name given to the simulated machine center.

TABLE 2. *Log diameter ranges and assigned profiles.*

Diameter Range 1	Assigned profiles	Diameter Range 2	Assigned profiles	Diameter Range 3	Assigned profiles	Diameter Range 3	Assigned profiles
	cns-411		cns-621		cns-831		cns-1051
	cns-420		cns-630		cns-840		cns-1060
3.40″	cns-421	6.50″	cns-640	8.50″	cns-841	11.50″	cns-1061
to	cns-430	to	cns-830	to	cns-1041	to	cns-1250
6.49″	cns-621	8.49″	cns-831	11.49″	cns-1050	12.95″	cns-1251
	cns-630		cns-840		cns-1051		cns-1260
	cns-640		cns-841		cns-1060		cns-1261
					cns-1061		cns-1270

Profile codes are interpreted as follows: the right most digit if equal to one indicates the presence of a 1-in. top board in the stack, a zero indicates all 2-in. boards in the stack; the second rightmost digit represents the number of 2 in. boards in the stack; the remaining digits to the left indicate the nominal width of the profile; cns is the name given to the simulated machine center.

The schematic in Fig. 2 illustrates an applied profile, the CNS-831 profile. The dark shaded region is the profile; the light shaded areas within it are the sawing pattern. Below the cant profile is the profile of the "multispline." The profile has one 1-in.-thick board and three 2-in.-thick boards.

Sawing simulation was used to determine which of the possible profiles was optimal for each log in the study when rotated to each of the angles of the set of rotation angles. To accomplish this, the sample logs were first oriented to the same starting rotation angle of 0°—"horns up." The possible cant profiles respective of each log's profile-group/diameter range were applied, and the resulting sawing pattern was determined. The sawing pattern that yielded the greatest value for each log was recorded as the optimal sawing pattern. The simulations were repeated for rotation increments of 45° until simulations for all the possible rotation angles were complete. This resulted in an optimal sawing pattern for each rotation angle and log combination.

Each log was sawn using the method known as split taper log–full taper cant (Williston 1981), as shown in Fig. 2. The sawing patterns were determined by finding the best combination of horizontal and vertical placements for the log with respect to the saws and chipping heads for each profile. The optimal combination of horizontal and vertical placement was found by exhaustive search iteration. Horizontal placements of the log were considered using 0.25-in. offsets from the center sawn position for both sides of center for a total of 10 offsets. For each horizontal placement of the log, the best vertical placement was determined by simulating a gang edger with a variable linebar. We assume that all boards from the sawing pattern except the innermost board can be edged to remove wane. This ensures that the cant made in the simulation would have two parallel planer faces, a requirement assumed necessary for the proposed real machinery to firmly hold the log while processing. Optimal board skewing at the edger was determined by choosing from two possible skewing angles for each board. Gang sawing and subsequent edging processes were iterated with the linebar shifting left of the saws on 0.5-in. increments for a total of 10 iterations. The combination of profile and horizontal and vertical placements resulting in the greatest value was considered the optimal sawing pattern.

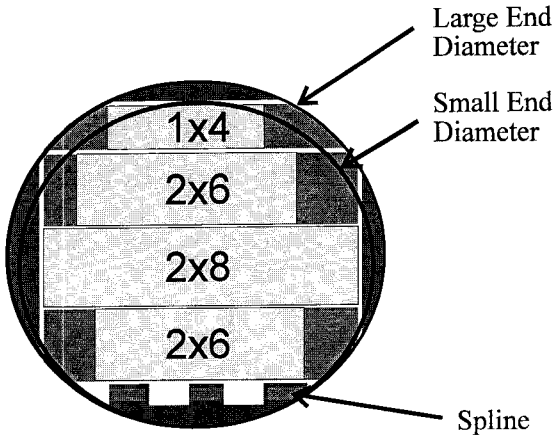

FIG. 2. The CNS-831 profile with a likely sawing pattern.

The horizontal and vertical placement increments and rotation angle increments were chosen to optimize a trade-off between simulation accuracy in finding an optimal solution, simulation processing time, and the volume of resulting data. Horizontal and vertical placements were in increments of 0.25 and 0.5 inches respectively for 10 increments each. This resulted in a trial of 100 placement positions, an acceptable total. The increment for horizontal placement was twice that of vertical placement because the starting references for each placement are different. For the vertical placement, the cant is aligned with the simulated gang-saw's linebar and the point of reference is the linebar. The 0.5 in. was necessary to cover the worst possible sweep situation. These increments provided enough profile coverage for 5 in. of sweep. In the case of the horizontal placement, the point of reference is the horizontal geometric center of the log. As a result, there was less horizontal distance for necessary profile coverage, which allowed the finer increment. The 45° rotation increment was chosen as small enough for accuracy and

falls among those angles that are commonly used in industry, namely: 0°, 45° and 180°.

The product values used for the simulation are shown in Table 3. These reflect average dimension lumber prices of early 1992, and were taken from the publication Random Lengths (Anon. 1992). Two-in. products were assumed to be kiln-dried "Western Spruce-Pine-Fir," either Std.&Btr. Light Framing (2 × 4) or #2&Btr. Structural Light Framing (2 × 6, 2 × 8, 2 × 10, 2 × 12). The one-in. boards were assumed to be kiln-dried "Engelmann Spruce," #3 Common.

TABLE 3. *Product prices using in the sawing simulation.*

Product	Prices by product length						
	8	10	12	14	16	18	20
1 × 4	215	215	215	215	215	215	215
1 × 6	235	235	235	235	235	235	235
2 × 4	185	211	172	178	223	210	210
2 × 6	188	206	174	170	196	225	222
2 × 8	190	172	187	173	204	240	240
2 × 10	190	190	256	268	250	235	235
2 × 12	190	190	256	268	250	235	235

Chip prices ($/ton)		
Low	Medium	High
25	50	75

RESULTS AND DISCUSSION

Determination of ideal rotation

First, we wish to determine the effect of the different log rotation classes on value recovery. To accomplish this, we use the regression approach, analysis of covariance procedure (Neter et al. 1990). In this procedure, we employ seven indicator variables taking on the values of 1, −1, or 0 to represent the eight rotation classes according to the following rule:

$$Rot_1 = \begin{cases} 1 \text{ if from rotation class 1 (0°)} \\ -1 \text{ if from rotation class 8 (315°)} \\ 0 \text{ otherwise} \end{cases}$$

. .
. .
. .

$$Rot_7 = \begin{cases} 1 \text{ if from rotation class 7 (270°)} \\ -1 \text{ if from rotation class 8 (315°)} \\ 0 \text{ otherwise} \end{cases}$$

Thus there are seven treatment variables.[1] The covariance model is expressed as:

$$Vrc = \beta_0 + \beta_1 Dsq + \beta_2 Len + \beta_3 Tpr + \beta_4 Swp + \beta_5 Chp + \beta_6 Ecc + \beta_7 Rot_1 + \beta_8 Rot_2 + \ldots + \beta_{13} Rot_7 + \epsilon \quad (2)$$

where

Vrc = value recovery of the log in $/cubic meter (gross)
Dsq = square of the average small end diameter of log in inches
Ecc = measure of maximum log cross section eccentricity: max(dia axis 1 − dia axis 2)^2/Dsq
Len = log length in feet
Tpr = log taper (expressed in percent)
Swp = log sweep (expressed in percent)
Chp = chip price indicator:
1 high prices
0 moderate prices
−1 low prices

Equation (2) was estimated using the statistical analysis system (SAS 1991) with all terms and interaction terms for $\beta_1 - \beta_6$. Model coefficients were eliminated using the partial F-test procedure with an alpha value of 0.05 to remain in the model. Only one variable was eliminated at each step. Once a variable was eliminated, it was not considered for re-entry into the model. Regression results showing remaining coefficients in the full model are presented in Table 4. All remaining variables in the model are highly significant. All treatment effects (Rot) are left in the full model as these are the variables of interest.

The signs of the primary coefficients in Table 4 agree with intuition. Both diameter and length have positive effect on value recovery. Increasing taper has a positive effect on value recovery. This is because diameters are measured from the small end, and logs with larger taper

[1] Only seven coefficients are estimated in the model. The value of the coefficient for the eight rotation groups (315°) is obtained as $\beta_{13} = -\beta_6 - \beta_7 - \ldots - \beta_{12}$. See Neter et al. (1990) Chapter 23 for a full discussion.

TABLE 4. *Statistical estimation of full model and Duncan's Multiple Range Test on treatments.*

Source of variation	Linear regression results				
	df	SS	MS	*F*	*P*-value
Model	802,306.9	2	53,487.1	1,182.0	0.0
Error	301.185.0	665	45.2		
Total	1,103,491.9	667			
R-square	0.727				

Source of variation	Estimate	*t*	*P*-value	SE of estimate
Intercept	38.929	42.6	0.0000	0.9125
Dsq	0.046	4.3	0.0001	0.0105
Len	0.050	9.8	0.0001	0.0506
Tpr	1.479	5.6	0.0001	0.2613
Swp	−9.691	−35.9	0.0001	0.2693
Ecc	−1.035	−7.2	0.0001	0.1427
ChipPrc	3.224	31.9	0.0001	0.1009
Dsq·Len	0.011	19.7	0.0001	0.0006
Dsq·Tpr	−0.035	−12.6	0.0001	0.0028
0	1.222	5.6	0.0001	0.2179
45	0.705	3.2	0.0012	0.2179
90	−1.617	−7.4	0.0001	0.2179
135	0.155	.07	0.4740	0.2179
180	−1.159	−5.3	0.0001	0.2179
225	0.108	0.5	0.6173	0.2179
270	0.024	0.1	0.9102	0.2179

Duncan's Multiple Range Test

Duncan grouping	Mean	Rotation
A	58.140	0
B A	57.624	45
B	57.478	315
B	57.074	135
B	57.027	225
B	56.943	270
C	55.748	180
C	55.300	90

Means with the same letter are not sigr ificantly different.

have more volume. Sweep and cross-section eccentricity have a negative impact on value recovery. Increasing chip prices has a large positive effect on value recovery.

The signs of the interaction terms in the model are insightful. *Dsq·Len* (diameter squared times length), a well-known predictor of log volume, is positively correlated with value recovery. The negative sign on *Dsq·Tpr* (diameter squared times taper) indicates that high log taper will tend to reduce the expected increase due to larger logs. This indicates that value recovery would be higher on larger diameter logs with low taper than the reverse.

The primary statistical test with this model is whether or not the rotation class has any effect in the model, and if so, which of the various classes has the most beneficial effect. The other variables are included in the model only to account for the known effects of diameter, length, and so on and reduce the error variability. This test is similar to the fixed treatment effects of analysis of variance models. The test hypothesis is:

$$\text{Ho: } \beta_7 = \beta_8 = \ldots = \beta_{13} = 0$$
$$\text{Ha: Not Ho} \qquad (3)$$

The test is carried out using the general linear model test approach fitting full and reduced

TABLE 5. *Statistical estimation of reduced model and Duncan's Multiple Range Test on treatments.*

Source of variation	Linear regression results SS	df	MS	*F*	*P*-value
Model	797,049.3	1	99,631.1	2,166.2	0.0
Error	306,442.6	665	45.9		
Total	1,103,491.9	667			
R-square	0.722				

Source of variation	Estimate	*t*	*P*-value	SE of estimate
Intercept	38.929	42.3	0.0000	0.9199
Dsq	0.046	4.3	0.0001	0.0106
Len	0.050	9.8	0.0001	0.0511
Tpr	1.479	5.6	0.0001	0.2634
Swp	−9.691	−35.6	0.0001	0.2714
Ecc	−1.035	−7.2	0.0001	0.1439
ChipPrc	3.224	31.7	0.0001	0.1016
Dsq·Len	0.011	19.5	0.0001	.0006
Dsq·Tpr	−0.035	−12.5	0.0001	0.0028

models. The full model is that presented in Table 4. The reduced model is that of Table 5 with $\beta_7, \beta_8, \ldots, \beta_{13}$ removed. The appropriate test statistic is:

$$F^* = \frac{MSR(X_7, \ldots, X_{13} \mid X_1, \ldots, X_6)}{MSE(Full)} = \frac{SSE(Reduced) - SSE(Full)}{p - q} \div MSE(Full) =$$

$$= \frac{306{,}442.65 - 301{,}185.07}{7} \Big/ 45.25 = 16.60 \quad (4)$$

F^* is significant at the 0.001 level. The null hypothesis is rejected. We conclude that log rotation has a significant effect on value recovery.

Since treatment effects are found in the model, we next determine which, if any, log rota-

TABLE 6. *Statistical estimation of model with zero and optimal rotation.*

Source of variation	Linear regression results SS	df	MS	*F*	*P*-value
Model	188,684.5		209,264.9	463.5	0.0
Error	74,986.5	165	45.2		
Total	263,671.0	166			
R-square	0.715				

Source of variation	Estimate	*t*	*P*-value	SE of estimate
Intercept	42.749	44.3	0.0000	0.9645
Len	0.393	6.5	0.0001	0.0600
Tpr	1.47	3.0	0.0021	0.4787
Swp	−8.732	−16.2	0.0001	0.5369
Ecc	−0.457	−4.7	0.0001	0.0970
ChipPrc	3.051	15.1	0.0001	0.2017
Dsq·Len	0.013	30.8	0.0001	0.0004
Dsq·Tpr	−0.036	−7.2	0.0001	0.0050
Opt	1.458	3.0	.0005	0.4167
Opt•Ecc	0.289	2.1	0.0298	0.1331

tions perform superior to the others. This is determined using Duncan's Multiple Comparison procedure for treatment means for the eight rotation classes. The results of this procedure, shown in Table 4, show clearly that the "horns up" (0° rotation) position can be distinguished from all other rotations except the 45° position. However, the 45° rotation itself cannot be statistically distinguished from the large group of other middle performing rotations (grouping B). The "horns down" (180°) and 90° positions are clearly sub-performers (grouping C). Thus, the evidence supports the adoption of the "horns up" position as performing best, on average, on the test group of logs. The reason that "horns up" performs better than "horns down" can be seen in Fig. 1. Often sweep is more pronounced in the butt end of the log (as in Fig. 1) rather than uniform and symmetrical throughout the log. Recovery is much higher in the "horns up" case when saw lines are placed through such a log.

Value of optimal rotation setting

Next, we wish to determine the effect of implementing the optimal rotation for each log as it is being sawn in the CNS. To accomplish this, we again use the regression approach analysis of covariance procedure. In this case we employ a single dummy variable, which indicates the sawing position, as follows:

$$Opt = \begin{cases} 1 \text{ if log is rotated to optimal position before sawing} \\ 0 \text{ if log is sawn at the "horns up" position} \end{cases} \quad (5)$$

The model to be estimated is:

$$\begin{aligned} Vrc = {} & \beta_0 + \beta_1 Dsq + \beta_2 Len + \beta_3 Tpr + \\ & + \beta_4 Swp + \beta_5 Chp + \beta_6 Ecc + \\ & + \beta_7 Opt + \beta_8 Opt \cdot Swp + \\ & + \beta_9 Opt \cdot Ecc + \epsilon \end{aligned} \quad (6)$$

We calculate the model coefficients using all 834 logs sawn in the optimal rotation (the experimental group) and the same 834 logs sawn in the "horns up" position (the control group). The "horns up" position is chosen as the control group since this position was found to be the "ideal log rotation" in the preceding section.

Equation (6) was estimated using the statistical analysis system (SAS 1991) with all terms and interaction terms for $\beta_1 - \beta_9$ included. Model coefficients were eliminated using the same procedure as that described above. Regression results showing the model statistics are presented in Table 6. Signs on all model coefficients are the same as the model discussed above. The major difference between the estimation of Eq. 1 and Eq. 6 is that the variable *Dsq* dropped out of Eq. 6.

A significant benefit to optimally rotating logs prior to sawing would be indicated if the coefficient for *Opt* is statistically significant. The hypothesis is:

$$\begin{aligned} &\text{Ho: } \beta_7 = 0 \\ &\text{Ha: } \beta_7 \neq 0 \end{aligned} \quad (7)$$

Confidence limits around β_7 at the $\alpha = 0.05$ level are:

$$\begin{aligned} \beta_7 - \text{std. err.} \cdot t_{\alpha/2,df} \leq \beta_7 \leq \\ \leq \beta_7 + \text{std. err.} \cdot t_{\alpha/2,df} \\ 1.459 - 0.4167 \cdot 1.961 \leq \beta_7 \leq \\ \leq 1.459 + \\ + 0.4167 \cdot 1.961 \\ 0.6413 \leq \beta_7 \leq \\ \leq 2.2759 \end{aligned} \quad (8)$$

Thus, β_7 is concluded to be statistically different from zero since the 0.05 level confidence interval does not contain zero.

To determine of rotation optimization significantly mitigates the negative effects of sweep and cross-sectional eccentricity, we examine coefficients β_8 and β_9. Both coefficients have positive signs indicating that benefits are obtained from rotational optimization. However, the coefficient on $Opt \cdot Swp$ (β_8) was not significantly different from zero using a partial F-test (P-value = 0.76) and was dropped from the final model. However, the coefficient on $Opt \cdot Ecc$ (β_9) is significant with a P-value of 0.0298. Thus, indications are that the beneficial effect of optimally rotating logs is more related to cross-sectional eccentricity than to sweep.

Using the same method as above, confidence limits around β_9 are:

$$0.0284 \leq \beta_9 \leq 0.5506 \quad (9)$$

Therefore, we conclude that estimated benefits increase slightly with increasing eccentricity.

We use the confidence limits around β_7 and β_9 to determine the benefits from optimal rotation. Assuming a CNS line sawing 200,000 cubic meters annually and an average eccentricity of 0.48 (which we found in this study) we obtain the following confidence limits on the benefits to optimal rotation:

$$\$320{,}000 \pm \$189{,}000 \quad (10)$$

The cost of implementing an automated log turning device in a CNS is estimated to be between $300,000 and $1 million.[2] Assuming the highest implementation cost and the lowest benefits, the internal rate of return for automated rotation equipment with a ten year lifespan would be approximately 5%. The mid-range scenario gives an IRR of 48%. The best case (lowest costs and highest benefits) IRR is 169%. The reader should note that these IRR estimates do not take maintenance costs into account.

SUMMARY AND CONCLUSIONS

Advances in three-dimensional scanning techniques and computer optimization permit real time solution and implementation of optimal log rotation before it is fed into the chipper heads. This study examined 834 S-P-F logs obtained from the interior of BC using SAWSIM to determine the effects of log rotation strategies on value recovery for a small log CNS. Results show that log rotation plays an important role in determining value recovery. Both log sweep and cross-sectional eccentricity are shown to cause significant reductions in value recovery.

Eight rotation placements from 0° to 315° were studied to determine if a single rotational placement could be found that performs best when the optimal log rotation cannot be implemented. On average, the "horns up" position (0° rotation) was found to significantly outperform all others in maximizing value recovery.

When compared to the "horns up" position, the ability to rotate the log into the optimal position produced significant benefits. These benefits were found to be related to the degree of cross-sectional eccentricity present in the log more so than the degree of sweep present in the log. Internal rate of return estimates for the installation of automatic log turner systems range from a low of 5% to a high of 169%. The mid-range estimate was found to be 48%.

More research is required prior to concluding that automatic log rotation setting should be implemented on a mass scale. This research should include the study of installed equipment at test sites and should concentrate on the following factors:

1. The degree of accuracy in rotational placement required to obtain the maximum financial return. This study demonstrates benefits using only 45° intervals. The benefits could be much larger when a higher accuracy in log placement is used.
2. The effect of full shape scanning information. This study used information collected from two-axis log scanning and assumes the log cross-sectional shape is elliptical.

ACKNOWLEDGMENTS

This research was partially funded by the Natural Sciences and Engineering Research Council of Canada (NSERC).

REFERENCES

ANONYMOUS. 1992. Random lengths—Lumber price guide. 10 January, 1992. Random Lengths Publications, Eugene, OR.

HALLOCK, H., AND D. W. LEWIS. 1971. Increasing softwood dimension yield from small logs—Best opening face. USDA Forest Serv. Res. Paper FPL 166. Madison, WI.

HASENWINKLE, E. D., F. WISLOCKER, AND C. BLICKENDERFER. 1987. Variable curve linebar. U.S. Patent, 4,633,924. U.S. Patent Office, Washington, D.C.

H. A. LEACH AND COMPANY LTD. 1990. SAWSIM. Users guide. Howard A. Leach, Ltd., Vancouver, BC.

LINDSTROM, N. E. 1979. Apparatus for curved sawing of timber. U.S. Patent 4,144,782. U.S. Patent Office, Washington, D.C.

MONGEAU, J. P., R. BEAUREGARD, AND T. E. G. HARLESS. 1993. Softwood log shape modeling with shadow scanners. Wood Fiber Sci. 25(3):261–277.

NETER, J., W. WASSERMAN, AND M. H. KUTNER. 1990. Applied linear statistical models: Regression, analysis

[2] Based on personal communication with Bob Chapman, President, Optimil Machinery, Ltd.

of variance, and experimental design. Richard D. Irwin, Inc., Boston, MA.

SAS INSTITUTE. 1991. User's guide: Statistics. SAS Institute, Cary, NC.

SHI, R., P. H. STEELE, AND F. G. WAGNER. 1990. Influence of log length and taper on estimation of hardwood BOF position. Wood Fiber Sci. 22(2):142–148.

STEELE, P. H., E. M. WENGERT, AND K. LITTLE. 1987. Simplified procedure for computing best opening face position. Forest Prod. J. 37(5):44–48.

WANG, S. J., B. D. MUNRO, D. R. GILES, AND D. M. WRIGHT. 1992. Curve sawing performance evaluation. Forest Prod. J. 42(1):15–20.

WILLISTON, E. M. 1981. Small log sawmills. Miller-Freeman Publications, Inc., San Francisco, CA.

THE EFFECT OF MOISTURE CYCLING ON CREEP OF SMALL GLUED LAMINATED BEAMS

Robert J. Hoyle, Jr.
Professor Emeritus

Rafik Y. Itani
Professor

and

Jill Teresa Anderson
Former Graduate Student

Civil and Environmental Engineering
Washington State University
Pullman, WA 99164-2910

(Received February 1993)

ABSTRACT

Creep information for sawn lumber exposed to constant and cyclic humidity environments previously published by the authors is supplemented by this study using glued laminated material of about the same size, tested on the same apparatus, and using the same general procedure.

For both sawn and glued laminated material, the relative creep was measured at about 55% of their average ultimate strength. Relative creep was measured for specimens matched with respect to modulus of elasticity (MOE) and exposed to a constant relative humidity (65 F and 65% RH) for about 1,000 hours, and a cyclic relative humidity (65 F and 90% RH for 82 hours followed by 65 F and 40% RH for 82 hours). This 164-hour cycle was repeated six times for about 1,000 hours of cyclic exposure. This is a more severe change in equilibrium moisture content of the environment than is likely to occur in building structures.

The result showed relative creep of the glued laminated material increased by 40% to 72% as a result of cycling. One very low MOE pair showed an increase of 167%. The increase for solid sawn lumber previously reported was 200% to 400% due to cycling. Results also showed that the ratio of relative creep for cycled to constant humidity exposure did not change appreciably as time under load was increased. These differences are attributed to permeability differences between glued laminated wood and sawn lumber. The gluelines are believed to retard water vapor movement and reduce the moisture change rate and extremes of wood moisture content in any given cycle.

Keywords: Douglas fir, glued laminated, creep, humidity, cycled.

INTRODUCTION

Research results on the creep behavior of nominal 4- by 4-inch Douglas fir beams from two studies conducted at Washington State University's Department of Civil and Environmental Engineering have been published in this journal (Hoyle et al. 1985, 1986). The species was Interior North Douglas fir (*Pseudotsuga menziesii*) and the grade was No. 2 and Better (Western Wood Products Association).

The first results (1985) were for exposure to a constant relative humidity environment of 70 F and 65% RH for 400 hours. The second results (1986) were obtained in cyclic humidity environments, one of which was 70 F and 90% RH for 84 hours, then at 70 F and 40% RH for 84 hours; the 168-hour cycle repeated for 1,250 hours.

This paper reports test results for glued laminated beams of the same species and of similar

Wood and Fiber Science, 26(4), 1994, pp. 556–562

TABLE 1. *Regression models.*

Beam	Constant RH A	B	C 10^{-3}	R^2	Beam	Cycled RH A	B	C 10^{-3}	R^2
				Model 1: $\delta_R = A(1 - e^{-BT})$					
1A	0.2101	0.05009	*	0.977	2B	0.3796	0.00761	*	0.994
3A	0.1954	0.02263	*	0.980	3B	0.3552	0.01008	*	0.992
4A	0.2383	0.02565	*	0.975	4B	0.4903	0.00839	*	0.992
5A	0.1729	0.09492	*	0.988	5B	0.4348	0.01077	*	0.992
6A	0.1908	0.03921	*	0.980	6B	0.3125	0.01050	*	0.994
Group A	0.2002	0.03912	*	0.968	Group B	0.3940	0.00932	*	0.970
				Model 2: $\delta_R = A(1 - e^{-BT}) + Ct$					
1A	0.1660	0.1369	0.131	0.991	2B	0.2631	0.01549	0.185	0.998
3A	0.1495	0.0452	0.126	0.994	3B	0.2659	0.01864	0.154	0.997
4A	0.1722	0.0777	0.174	0.994	4B	0.3367	0.01837	0.253	0.998
5A	0.1518	0.1477	0.072	0.996	5B	0.3262	0.02047	0.191	0.997
6A	0.1488	0.0904	0.122	0.995	6B	0.2340	0.01946	0.138	0.999
Group A	0.1557	0.0992	0.128	0.998	Group B	0.2843	0.01862	0.186	0.975
				Model 3: $\delta_R = At^B$					
1A	0.07716	0.1813	*	0.9997	2B	0.04349	0.3402	*	0.9969
3A	0.04656	0.2481	*	0.9999	3B	0.05305	0.3033	*	0.9940
4A	0.06159	0.2362	*	0.9998	4B	0.06153	0.3279	*	0.9963
5A	0.08051	0.1421	*	0.9978	5B	0.06873	0.2953	*	0.9940
6A	0.06115	0.2031	*	0.9992	6B	0.04614	0.3061	*	0.9938
Group A	0.06465	0.2017	*	0.9992	Group B	0.05446	0.3144	*	0.9723

* Not applicable.

size (3- by 3.75-inch versus 3.5- by 3.5-inch) subjected to the same humidity cycle at 65 F, and loaded to approximately the same stress level. Each glued laminated beam consisted of five ¾-inch laminations with gluelines arranged horizontally.

The object of this study was to compare the creep behavior of glued laminated and solid sawn beams under very similar conditions of cyclic humidity environments.

LITERATURE REVIEW

The papers previously published provide a discussion of the literature on creep. Those discussions of the mathematical models for creep will be of interest, since we have employed the same models (see Table 1) in the analysis of results for the glued laminated beams. Anderson's thesis (1985) contains tables of relative creep for all the readings taken in this study and may possibly be useful to readers who wish to examine creep with a view of testing other mathematical models.

MATERIAL TESTED

Six 12-foot-long glued laminated beams were obtained from a laminator. Each beam consisted of five laminations of nominal 1- by 8-inch Douglas fir lumber. The finished size of the beams was 3.75 by 6.75 inches. All laminations were visually graded to Western Wood Products Association (WWPA) Rules 81 (1981) for Stress Rated Boards (SRB). (Stress Rated Boards of nominal 1 by 8 size are graded by the same rules as Structural Joists and Planks.) The outside laminations were No. 1 SRB (F_b = 1,350 psi), and the three interior laminations were No. 2 SRB (F_b = 875 psi). These grades were selected so the lumber quality would be similar to that of the previously tested No. 2 and Better solid sawn beams. The adhesive used in their manufacture was phenol-resor-

TABLE 2. *Relative creep for cycled and uncycled Douglas fir glulam beams.**

Beam	Elastic modulus (ksi)	Time under load (hours) 400	600	800	1,000
5A	1,590	0.1837 (0.1884)	0.1937 (0.1996)	0.1943 (0.2079)	0.2088 (0.2146)
4B	1,580	0.4037 (0.4337)	0.4854 (0.4885)	0.5348 (0.5391)	0.5580 (0.5897)
4B/5A		2.19 (2.30)	2.51 (2.45)	2.75 (2.59)	2.67 (2.75)
1A	1,740	0.2297 (0.2286)	0.2425 (0.2461)	0.2512 (0.2593)	0.2592 (0.2700)
3B	1,730	0.3192 (0.3275)	0.3519 (0.3583)	0.3840 (0.3893)	0.3974 (0.4202)
3B/1A		1.39 (1.43)	1.45 (1.46)	1.53 (1.50)	1.53 (1.56)
4A	1,730	0.2531 (0.2536)	0.2798 (0.2791)	0.2813 (0.2987)	0.3106 (0.3148)
5B	1,720	0.4226 (0.4025)	0.4562 (0.4409)	0.4568 (0.4791)	0.4840 (0.5173)
5B/4A		1.67 (1.58)	1.63 (1.58)	1.62 (1.60)	1.56 (1.64)
3A	1,820	0.2073 (0.2059)	0.2237 (0.2276)	0.2337 (0.2445)	0.2420 (0.2584)
2B	1,860	0.3432 (0.3356)	0.3753 (0.3730)	0.3940 (0.4100)	0.4171 (0.4476)
2B/3A		1.66 (1.63)	1.68 (1.64)	1.69 (1.68)	1.72 (1.73)
6A	2,300	0.1998 (0.2065)	0.2214 (0.2242)	0.2324 (0.2377)	0.2497 (0.2487)
6B	2,400	0.2894 (0.2891)	0.3158 (0.3168)	0.3403 (0.3444)	0.3506 (0.3720)
6B/6A		1.45 (1.40)	1.43 (1.41)	1.46 (1.45)	1.40 (1.50)

* Numbers in parentheses are from regression. Other numbers are from actual measured relative creep.

cinol resin, a common laminating adhesive for glued laminated beams.

Each of the six beams was sawed longitudinally, and the sawn edges were surfaced to form two 3-inch-wide by 3.75-inch-deep pieces, which were marked 1 through 6, A and B, it being assumed that the A and B pieces would be reasonably well matched in terms of modulus of elasticity (MOE). This did not prove to be the case when the pieces were statically tested, so they were matched on the basis of MOE into pairs, one for constant humidity exposure (A); and the other for cyclic humidity exposure (B). The MOE values of the specimens as paired are given in Table 2. Two beams were omitted in the reporting of test results because the pins driven into those beams to support the deflection measuring bridge were accidentally disturbed during the creep tests, creating errors that could not be reliably corrected. Thus the test material consisted of five pairs of beams, well matched on the basis of MOE.

METHOD OF TESTING

Test material was stored at 65 F and 65% RH for over 30 days prior to testing. This material had been seasoned to 12% moisture content prior to laminating, and the storage conditions were to maintain this moisture level.

The applied load was chosen to cause a bending stress high enough to produce measurable creep in a reasonable time, but below a level that would cause rapid creep to failure. Past experience has suggested that stress below 55% of the ultimate strength of the specimens would not cause tertiary creep (i.e., deflection at an accelerating rate, culminating in failure). The ultimate strength of the material was determined by reversing the procedure of deriving allowable stresses for design. Recognizing the actual size and moisture content of the glued laminated material and using the allowable bending stresses for the outer laminations (1,350 psi), it was determined that 2,600 psi would be about 53% of the average ultimate strength of the glued laminated material. (This glued laminated material is of a lower quality and strength than that customarily used in the manufacture of commercial glued laminated beams). In this study, we purposely used a quality level to match the solid sawn 4 by 4s in the earlier creep studies.

All beams were loaded to the 2,600 psi stress

level. Loads were applied at three equally spaced locations along the 140-inch simple span. The beams were supported on a knife edge at one end and a roller at the other. The loads were at midspan and quarter-points.

Previous experience showed that upon initial loading there will be a period of rapid dial gage motion during the first minute or two after loading, which ceases within 2 minutes. It was our practice to take as the initial deflection the reading when that motion stopped, always in less than 2 minutes after the last of the three loads was in place. The room conditions during this loading period were 65 F and 65% RH. We allowed the loaded beam to remain at this condition for 7 hours before beginning the exposure regimes for constant humidity and for cyclic humidity. The reason for this may be of interest. It takes about 1 hour to load six beams, and we wished to have the six beams in a given set to have about equal time under load before starting the test exposure. This technique made the preliminary period 7 hours, to 7 hours and 50 minutes, rather than zero minute to 50 minutes had we started the test exposure immediately after the sixth beam was loaded. There was probably very little moisture absorption or desorption during this period.

Following the 7-hour period, the relative humidity was continued at 65% for the "A" specimens, requiring about 10 minutes, and continued at this relative humidity and 65 F for the entire period of 989 additional hours.

Following the 7-hour period, the relative humidity for the "B" specimens was raised to 90% for 82 hours and then changed to 40% for another 82 hours, all at 65 F. The equilibrium moisture contents for these conditions were 21% and 8%, although, of course, the specimens did not come to these moisture contents during the 82-hour periods. (We had targeted these periods to be 84 hours, but did not actually expose them exactly that long). The cycle of 164 hours was repeated six times for a total exposure of 993 hours, including the initial 7-hour period at 65 F and 65% RH. The time required to reduce humidity was about 2 hours.

RESULTS

Deflection data were used to compute the relative creep for each reading taken on each beam. Relative creep is the ratio of the constant load deflection at any given reading time to the initial deflection taken at 2 minutes after the three loads had been applied to each beam. Thus, 0.25 relative creep means that creep was 25% of the initial elastic deflection.

Three regression models for relative creep versus time (hours) were fitted to the data. These models are given in Table 1. We had selected these models from the creep literature and had gained experience with them in the studies mentioned in the introduction. Consistent with those studies, we employed the same models for this one. We believe the creep fundamentals do not change for the glued laminated specimens, although the rates would be expected to differ for sawn versus glued laminated material, and the cycling would increase the breaking of hydrogen bonds that is supposed to aggravate creep. The regressions for each of the three models were performed by SAS NLIN (Statistical Analysis System NonLinear) program using the D.U.D. method (Council and Helwig 1979). The fitted equations are given in Table 1.

Table 2 lists creep at periods of 400, 600, 800, and approximately 1,000 hours (actually 996 and 993 hours), actual measured values and values from regression in parentheses. Ratios of relative creep, cycled to constant relative humidity, are also tabulated for specimens matched according to MOE. While the original intent was to physically match specimens cut from the same 3.75- by 6.75-inch beam, it was found that there were great differences in the MOE of members of these pairs. In retrospect, we believe this is due to the fact that dividing a graded member does not result in two members of equal grade, a principle well recognized by the grading agencies. The halves no longer contain the same growth characteristics. Modulus of elasticity was measured on all specimens before creep testing, so it was possible

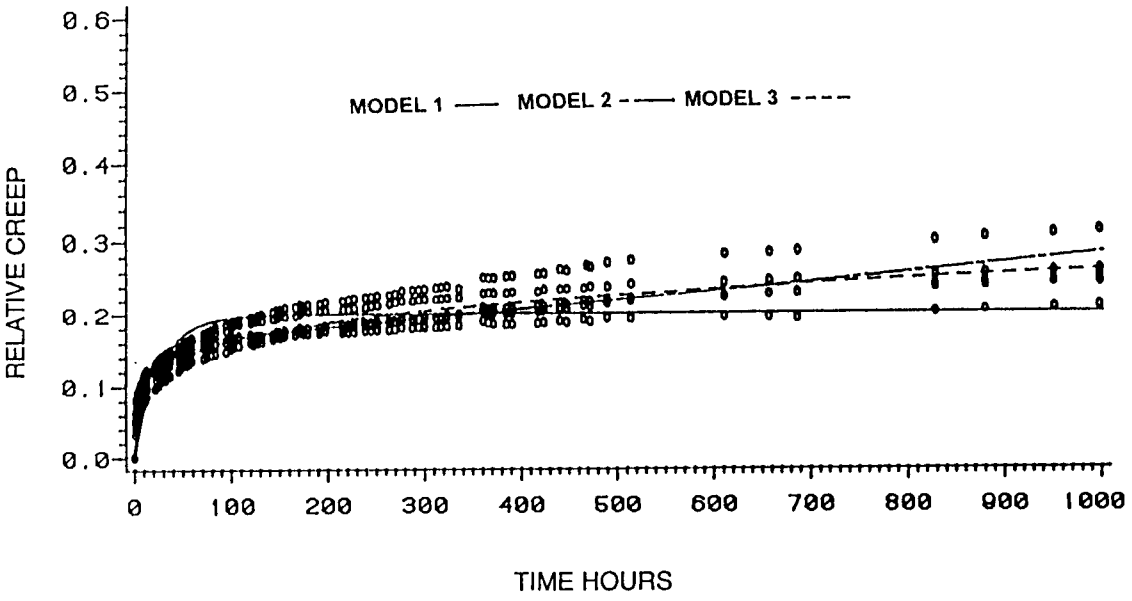

FIG. 1. Beams tested in constant humidity.

to identify and match A and B specimens based on elastic modulus.

DISCUSSION AND CONCLUSIONS

Table 1 lists the regression coefficients and the squares of the correlation coefficients. The values of R^2 are nearly unity for all models and specimens, which indicates that the variation in relative creep is due almost entirely to time and humidity. The models all fit well by this procedure. The graphical presentations in Figs. 1 and 2 make us prefer model 3 for

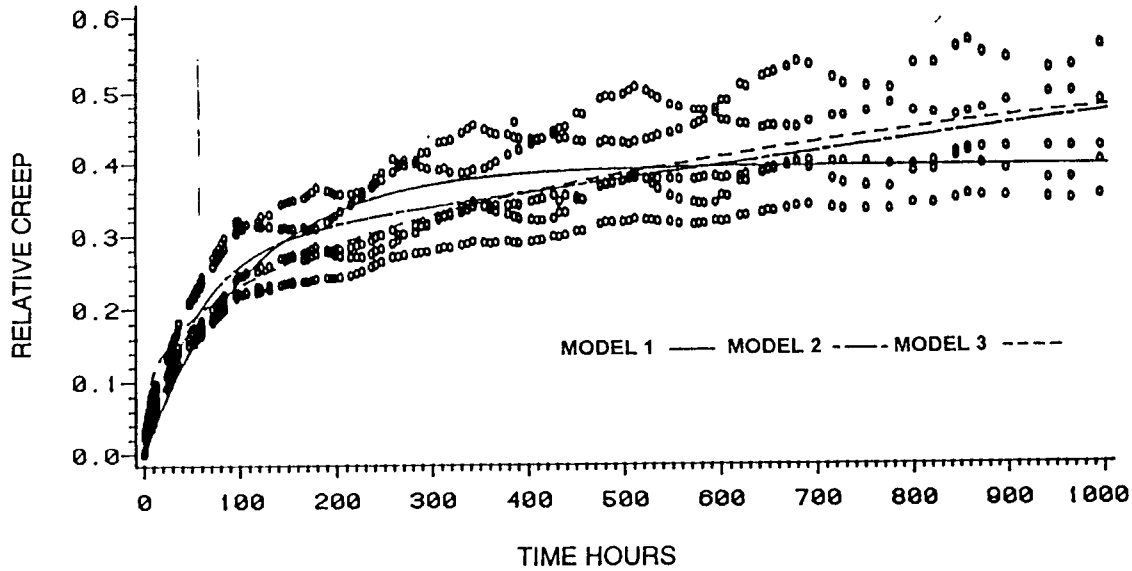

FIG. 2. Beams tested in cyclic humidity.

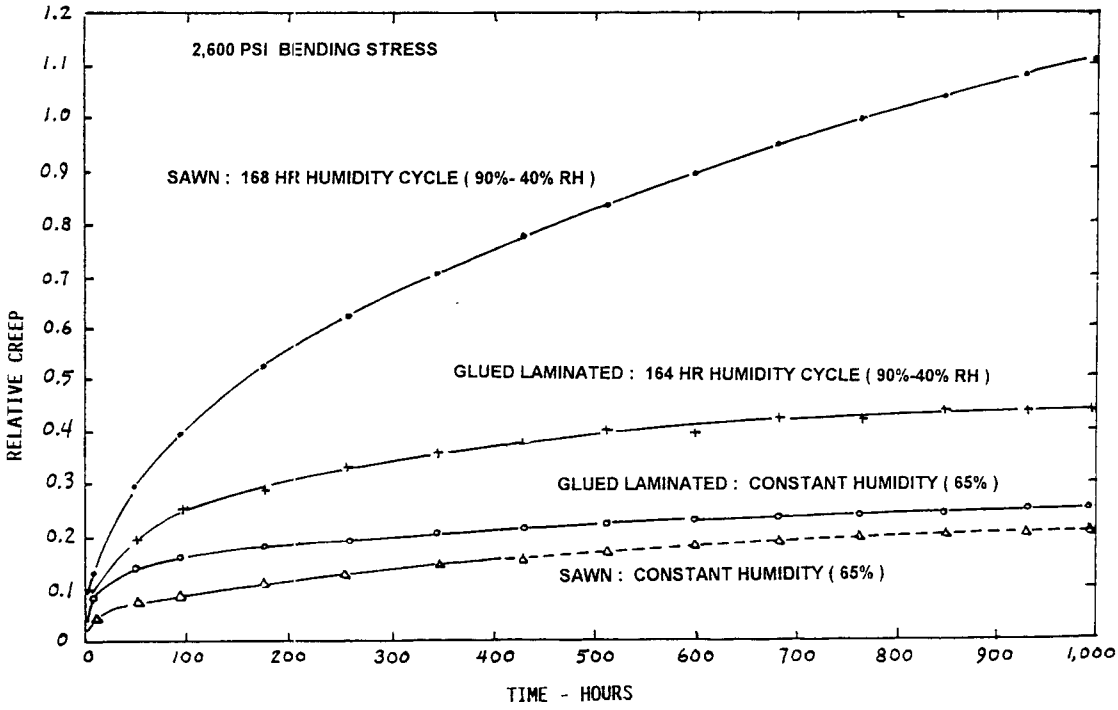

FIG. 3. Relative creep vs. time for sawn and glued laminated wood beams.

the constant humidity data, with little difference between models 2 and 3 for the cyclic humidity data. Model 1 is a poorer fit in all cases.

The information in Table 2 permits observing relative creep in terms of time and MOE. This experiment was not designed to detect the influence of MOE on creep and there is not a sufficient range of MOE to permit any conclusions about its influence. The creep in the low MOE specimens was more affected by humidity variation than in the case of the higher MOE beams. To learn more about the MOE influences, it would be good to have more replications of beams at each of a wider range of MOE levels. This noticeably different behavior of the low MOE specimen could be just a random variation in creep behavior.

The particular finding that is of interest is the ratio of relative creep of cycled (B) beams to constant humidity beams (A). It seems clear that cycling increases relative creep, a result we had expected from the prior work on sawn lumber beams. This ratio does not appear to increase or decrease very much with increasing time under load.

The effect of cyclic humidity on the glued laminated material was not as great as had been seen for the solid sawn material. To compare the creep of glued laminated wood and sawn wood of the same general size, quality, and at the same stress level, Fig. 3 is presented using data from this study for the glued laminated wood; for sawn wood at constant humidity from the Hoyle et al. (1985) paper; and for sawn wood in a cyclic humidity environment from the Hoyle et al. (1986) study.

The curves for the glued laminated wood are the average relative creep for five specimens each for the constant and cycled humidity conditions at approximately 84-hour intervals. Each plotted point is the average of five (A) specimens for the constant humidity condition and five (B) specimens for the cyclic humidity conditions.

The regression relative creep values at the

same times are plotted for the sawn wood studies, using Model 3 regression equations. The portion of the constant humidity curve for the sawn wood shown as a dashed line is the part at times exceeding 400 hours, and since that study had a maximum duration of 400 hours, this is an extrapolation.

All of the curves in Fig. 3 were for a constant applied stress of 2,600 psi, with very similar temperature and humidity conditions.

The cyclic fluctuation of relative creep is not as evident as it actually was, because the regressions were not fitted to a model that would show these fluctuations, in the case of the sawn material. For the glued laminated material, there is a small fluctuation of points plotted for the cycled glued laminated material. But the important feature of Fig. 3 is the relative position of the curves for the several conditions, showing the large effect of the cyclic humidity on solid sawn as opposed to the much smaller effect on glued laminated material.

Laminated members benefit by the dispersion of growth characteristics and by seasoning prior to gluing. This makes them more uniform in moisture content and less susceptible to the development of drying stresses. The grain deviation around knots is often supported by straighter grained adjacent laminations, which would reinforce the areas of distorted grain and reduce creep. The action of gluelines to impede moisture migration in the glued laminated material would be expected to restrain the development of creep, since internal moisture changes and creep are related directly. Thus we believe the relative position of the curves is logical, and the figure provides evidence of the magnitude of this difference.

REFERENCES

ANDERSON, J. T. 1985. The effect of moisture cycling on the creep of glulam beams. M.S. thesis, Department of Civil and Environmental Engineering, Washington State University, Pullman, WA.

COUNCIL, K. A., AND J. T. HELWIG, eds. 1979. SAS/GRAPH user's guide, 1971 ed. SAS Institute Inc., Cary, NC.

HOYLE, R. J., JR., M. C. GRIFFITH, AND R. Y. ITANI. 1985. Primary creep in Douglas-fir beams of commercial size and quality. Wood Fiber Sci. 17(3):300–314.

———, R. Y. ITANI, AND J. J. ECKARD. 1986. Creep of Douglas-fir beams due to cyclic humidity fluctuations. Wood Fiber Sci. 18(3):468–477.

SAS INSTITUTE. 1979. SAS user's guide. Statistical Analysis Systems, Cary, NC.

WESTERN WOOD PRODUCTS ASSOCIATION. 1981. Western lumber grading rules 81, Portland, OR.

SWST DISTINGUISHED SERVICE AWARD

The SWST Distinguished Service Award is given in recognition of extraordinary contributions to wood science and technology. Such service may have been made in an educational, technological, industrial, or scientific area in furtherance of the objectives of the Society of Wood Science and Technology, as outlined in its Constitution and By-Laws.

Past recipients of the award have been as follows:

1966—Harry Tieman
1968—Alfred Stamm
1980—Jim Bethel
1981—George Garratt
1982—Alexis Panshin
1983—Fred Dickinson
—Fred Wangaard
—Frank Kaufert
—Herbert Fleischer
—Herbert McKean
—Alfred Stamm
1984—George Marra
1985—John Haygreen
1986—Christen Skaar
1987—Peter Koch
1988—Stanley Suddarth
1989—Robert Youngs
1990—Wilfred Côté
1991—Charles Berolzheimer
1992—Stephen Preston
1993—Robert Kennedy

Dr. William T. Nearn is the recipient of the award for 1994. Bill's illustrious career has included a lifetime of service to both academia and to industry. He served as SWST President in 1967–68, and at that time, along with Ben Jayne and Bob Hoyle, established *Wood and Fiber,* the forerunner of this journal.

Bill's academic background includes a B.S. from New York State College of Forestry in 1943 and an M.F. and D. For. from Yale University School of Forestry, with the last two completed after 3 years' service in the U.S. Army.

He then joined Pennsylvania State University for 13 years, finally leaving as an Associate Professor to accept a position at the Weyerhaeuser Company. There his tenure spanned 24 years and included time spent as a Senior Scientist in the Pioneer Research Group, followed by a series of management assignments in Wood Science and Morphology, Scientific Services, and Control Technology Research.

In 1984, Bill retired from Weyerhaeuser and returned to academia as Associate Director of the Mississippi Forest Products Laboratory and Head of the Department of Wood Science and Technology. In 1987, he returned to the Pacific Northwest, where he has been engaged as a consultant in Bellevue, Washington.

The SWST Distinguished Service Award was presented to him at the annual meeting of SWST in Portland, Maine, on June 26, 1994, by the 1993–94 President, Paul Blankenhorn. Bill then addressed the membership with thoughts on the past and future pathway of SWST. A written text of his remarks follows.

Wood and Fiber Science, 26(4), 1994, p. 563

THANKS AND THOUGHTS

William T. Nearn

Consultant
1725 128th St SE
Bellevue, WA 98005-3911

It is difficult to convert what was said at the annual SWST meeting into text and come close to preserving the soul of the moment. In accepting The Distinguished Service Award, I wanted first to thank my peers and friends for this much-appreciated recognition and second, to use the opportunity to express some thoughts on the past and future pathway of SWST.

As a warm-up for the latter, I shared my view of the "Double Helix," James Watson's account of the discovery of the structure of DNA, one of the more far-reaching scientific feats of the 20th century.

Although not intended as such, the "Double Helix" is a case study of what can be accomplished by a group of diverse and, at times, adversarial scientists who had in hand parts of the puzzle, but were bogged down in detail or other more mundane interests.

Watson was the required catalyst. He wanted to work on "something of value" and believed that understanding gene replication was necessary for further progress in genetics. Neither chemist nor physicist, he was convinced that the role of DNA had been neglected and that building a molecular model was the key to understanding its role in gene replication. Crick, a physicist, "gadfly," and laboratory colleague, was finally persuaded to join the search, followed by Wilkins, whose lab specialized in X-ray diffraction and who had an earlier but suppressed interest in DNA. As the model grew, crashed, and was revised, others joined in the effort.

The results of the team were announced in *Nature,* summed up in two brilliant understatements.

> "We wish to suggest a structure for DNA, this structure has novel features which are of considerable biological interest."—"It has not escaped our notice that the specific pairing we have postulated immediately suggests a possible copying mechanism for the genetic material."

Watson, Crick, and Wilkins were awarded a Nobel prize; and you are all aware of the new vistas that were opened up.

SWST AND THE FUTURE

Lately, I've come to the conclusion that SWST as an organization spends too much quality time examining its own navel. Over the past 25 years, the membership has done a remarkable job in moving from a suspect organization with shaky finances to a respected professional group and publisher of a world-class journal with a comfortable bank account. Today and in the recent past, the more frequently discussed issues have included:

- zero growth in membership;
- a rapid decline in the numbers of students who choose wood science as a career and the demise of wood science programs;
- a failure to develop a position on various issues that are perceived as concerns to the profession.

These discussions occur within the same paradigm that existed 25 years ago. At the time, a major objective was to introduce more "rigor" into training of wood scientists. It was driven to some extent by those things that some of the founders wished they had learned, by individuals who believed clones of themselves to be the ideal, by cavalier comments from industry that it would be nice to have a chemist, physicist, engineer, wood anatomist etc. in one package, and by a subliminal need to le-

Wood and Fiber Science, 26(4), 1994, pp. 564–565

gitimize wood science as a profession. Our focus was inward.

In order to survive and prosper in the short and long term, the forest products industry at a minimum must:

- learn to operate synergistically with the needs of the environment;
- learn to manufacture a quality product at competitive prices with an acceptable rate of return using the forest raw material available from plantations that are in the ground and reaching rotation age on shore and abroad;
- learn to target quality, function, and service to meet customers' needs at home and abroad.

While these statements may seem hackneyed, they are a formidable challenge. The corporations, government agencies, and individuals who will participate, survive, and succeed in meeting these challenges are those who are comfortable and effective working in multidisciplined teams.

SWST will contribute and prosper if it fosters an environment that encourages the membership to focus on these needs. Once it begins to apply its energies in this fashion, other issues such as increased enrollment and membership will become more tractable.

The most robust paths to new concepts or solutions to current problems are based on first principles. It may seem an oxymoron to suggest that first principles exist on more than one level. Nevertheless, within any profession, there is a body of knowledge that has been elucidated, challenged, monitored, and modified to a level that can be applied as "first principles" in addressing problems within a given field. It goes without saying that these "first principles" do not violate the laws of thermodynamics etc. Wood science, at its best, is a subset of "first principles." My vision of the path of SWST toward survival and growth through the 90s and beyond is to maintain a professional focus that will:

- Evolve a new paradigm whose goal is to identify places within the forest products industry where wood scientists can make a *substantial difference.* Team within and outside the community to do so.
- Evolve a network to communicate the linkages between "the first principles" of wood science and the financial health of the forest products industry, conservation of the forest resource, and end user satisfaction. Provide information in a form that is interactive and reaches management and manufacturing as well as R&D.
- Establish strong working alliances with other professional and semiprofessional organizations that have tangent and overlapping interests in technology transfer, science, materials, natural resources, and public policy germane to these areas.
- Focus more time and resources toward making a *difference* rather than nourishing the profession per se. Let the quality of the product speak for itself. Flogging the terms *scientist* and *basic research* won't do the job.

It is easier to pontificate than operate. I hope that these thoughts will stimulate a dialogue that is of value in helping SWST to grow, rather than dribble, into the year 2000.

GEORGE MARRA AWARD

The George Marra Award is given in memory of George Marra by the Marra family in recognition of George's devotion to excellence in writing. Every article in each issue of the most recent volume of *Wood and Fiber Science* is read and judged by a three-person committee—one each from academia, government, and industry.

The first place winners of this year's George Marra Award are Chungping Dai and Paul Steiner for their paper "Compressive behavior of randomly formed wood flake mats," which appeared in the October 1993 issue of *Wood and Fiber Science.*

The second place winners are Jerrold Winandy and Jeffrey Morrell for their paper "Relationship between incipient decay, strength, and chemical composition of Douglas-fir heartwood," which was published in the July 1993 issue of *Wood and Fiber Science.*

Honorable mention is awarded to David Ritter, Robert Kroll, and Roland Gertjejansen for their paper "Zones of gelatinous fibers in *Populus balsamifera* L.," which was published in the April 1993 issue of *Wood and Fiber Science.*

Previous winners of the award are:

1986—Kirk C. Nadler, Elvin T. Choong, and David M. Wetzel for "Mathematical modeling of the diffusion of water in wood during drying."

1987—Michael B. Thurmond, Frank E. Woeste, and David W. Green for "Floor loads for reliability analysis of lumber properties data."

1988—Leslie Groom and Anton Polensek for "Nondestructive prediction of load-deflection relations for lumber."

1989—Terrance E. Conners and Thomas E. McLain for "Modeling moisture gradient effects on bending properties."

1990—First place: Philip E. Humphrey and Larry J. Ostman for "Bolted timber connections. Part I. A wafer technique to model wood deformation around bolts." Second place: Irving B. Sachs, Gary F. Leatham, and Gary C. Myers for "Biomechanical pulping of aspen chips by *Phanerochaete chrysosporium*: Fungal growth pattern and effects on wood cell walls."

1991—First place: M. P. Wolcott, F. A. Kamke, and D. A. Dillard for "Fundamentals of flakeboard manufacture: Viscoelastic behavior of the wood component." Second place: William T. Simpson and Yi-Fu Tang for "Empirical model to correlate press drying time of lumber to process and material variables."

1992—First place: David W. Green and David E. Kretschmann for "Lumber property relationships for engineering design standards." Second place: Steven E. Taylor and Donald A. Bender for "Stochastic model of localized tensile strength and modulus of elasticity in lumber." Honorable mention: Michael L. Hoag and Robert L. Krahmer for "Polychromatic X-ray attenuation characteristics and wood density applications."

1993—First place: David E. Kretschmann and B. Alan Bendtsen for "Ultimate tensile stress and modulus of elasticity of fast-grown plantation loblolly pine lumber." Second place: Charles B. Vick and Thomas A. Kuster for "Mechanical interlocking of adhesive bonds to CCA-treated southern pine—A scanning electron microscopic study." Honorable mention: Kelly La Fare and Rafik Y. Itani for "Comprehensive load distribution model for wood truss root assemblies."

Wood and Fiber Science, 26(4), 1994, pp. 566–567

GUIDELINES AND PROCEDURES FOR GEORGE MARRA AWARD

1. Award recognizes excellence in research and writing.
2. Papers considered are those published in the four quarterly issues of one volume of *Wood and Fiber Science.*
3. The first place award consists of the following:
   a. $1000 to the author(s) (provided by the Marra family)
   b. A plaque to the sponsoring firm or institution
   c. Certificate(s) and plaque(s) to the author(s)

   The second place award, if warranted, will consist of certificate(s) and plaque(s) to the author(s) and a plaque to the sponsoring firm or institution. Up to two other papers may be selected for honorable mention, for which the certificate(s) will be awarded.
4. Presentation of the awards will take place at the annual meeting.
5. The selection committee will be appointed by the President.
6. The selection committee will consist of at least three members, one of which will be designated the chair by the President. One member will be selected from each of the areas of the private sector, industry, government, and academia. A committee member may not have a paper considered for an award.
7. Committee responsibilities are as follows:
   a. Individually "score" all papers in the volume using George Marra's judging criteria.
      1) Research quality (30 points)
         Complexity of the problem
         Originality
         Impact on present knowledge of the subject
      2) Clarity and completeness of the introductory section (30 points)
         Objective
         Introduction
         General procedures
      3) Conclusion, recognition and literature (20 points)
         Conclusion that speaks to objective
         Recognition of important assistance received
         Command of the literature
      4) Clarity of exposition; i.e., understandable to those in other specialties (20 points)
   b. Committee chair will rank papers based on average score obtained from combining each member's scores.
   c. Each member re-review and rank the four papers with the highest combined scores.
   d. Combine reviews and select the first and second (if warranted) place papers and those for honorable mention (if any).
8. The chair will report the selection of the winning paper(s) to the President by 90 days prior to the SWST Annual Meeting.

SWST ACCREDITATION

SWST began accrediting schools for their Wood Science and Technology programs in 1984. The following is a list of schools accredited thus far:

Program Reviewed	*Year Accredited*
North Carolina State University, Raleigh	1984
University of Massachusetts, Amherst	1985
University of Washington, Seattle	1985
University of Minnesota, St. Paul	1985
Virginia Polytechnic Institute and State University, Blacksburg	1985
Mississippi State University, Mississippi State	1987
West Virginia State University, Morgantown	1989
Oregon State University, Corvallis	1991
Clemson University, Clemson	1992
Pennsylvania State University, University Park	1992
North Carolina State University, Raleigh	1994

INDEX TO WOOD AND FIBER

Wood and Fiber Science, 26(4), 1994, pp. 569–577

D

E

F

G

H

I

J

K

L

M

N

O

P

R

S

T

U

V

W

X

Y

AUTHOR INDEX

WOOD and FIBER SCIENCE

VOLUME 26

1994

PUBLISHED QUARTERLY BY

THE SOCIETY OF WOOD SCIENCE and TECHNOLOGY

SOCIETY OF WOOD SCIENCE AND TECHNOLOGY

1994–1995 Officers of the Society

President: HOWARD ROSEN, 341 Soapstone Lane, Silver Spring, MD 20905

Past President: PAUL BLANKENHORN, Forest Resources Laboratory, Pennsylvania State University, University Park, PA 16802

President-Elect: GEZA IFJU, Department of Wood Science and Forest Products, Virginia Tech, Blacksburg, VA 24061-0323

Vice President: DUANE LYON, Forest Products Laboratory, Mississippi State University, P.O. Drawer FP, Mississippi State, MS 39762-5724

Executive Director: VICKI L. HERIAN, Society of Wood Science and Technology, One Gifford Pinchot Drive, Madison, WI 53705

Directors:

W. RAMSAY SMITH, Louisiana Forest Products Laboratory, Louisiana State University, Baton Rouge, LA 70803

H. MICHAEL BARNES, Forest Products Laboratory, Mississippi State University, P.O. Drawer FP, Mississippi State, MS 39762-5724

BARRY S. GOODELL, University of Maine, 5755 Nutting Hall, Orono, ME 04469

MICHAEL HOAG, National Particleboard Association, 18928 Premiere Court, Gaithersburg, MD 20879-1569

WOOD AND FIBER SCIENCE

WOOD AND FIBER SCIENCE is published quarterly in January, April, July, and October by the Society of Wood Science and Technology, One Gifford Pinchot Dr., Madison, WI 53705, in cooperation with the Forest Products Society.

Editor

JOHN F. SIAU

Editorial Assistant

CAROL B. OVENS

Newsletter Editor

DOUGLAS D. STOKKE

There are three classes of membership in the Society: Members—dues $50.00; Associate Members—dues $50.00; Retired Members—dues $20.00; Student Members—dues $15.00. Applications for membership and information about the Society may be obtained from the Executive Director, Society of Wood Science and Technology, One Gifford Pinchot Dr., Madison, WI 53705.

Institutions and individuals may subscribe to WOOD AND FIBER SCIENCE at $110.00 per volume (four issues). New subscriptions begin with the first issue of a new volume. Single issues are $28.00 each. Back issues may be purchased for $10.00 each, except for 1993 and later years, which are full price. All subscriptions are to be ordered through the Executive Director. Make checks for subscriptions and membership payable to the Society of Wood Science and Technology.

The Executive Director, at the Business Office shown below, should be notified 30 days in advance of a change in address. Copies undeliverable because of address change will be destroyed. Issues lost in the mail will be replaced free if notice is received within one month of date of issue of the succeeding number.

Printing Office: Allen Press, Inc., P.O. Box 368, Lawrence, KS 66044, USA

Business Office: Society of Wood Science & Technology, One Gifford Pinchot Dr., Madison, WI 53705.

Editorial Office: John F. Siau, Department of Wood Science and Forest Products, Brooks Forest Products Center, Virginia Tech, Blacksburg, VA 24060-0503.

Second-class postage paid at Madison, Wisconsin 53705, USA, and at additional mailing offices.

CONTENTS TO VOLUME 26

NUMBER 1, JANUARY 1994

NUMBER 2, APRIL 1994

Editorial

Articles

Books

NUMBER 3, JULY 1994

Editorial

Articles

NUMBER 4, OCTOBER 1994